Supporting Information

Lipid Droplets Specific BODIPY based Rotors with Viscosity Sensitivity to Distinguish Normal and Cancer Cells: Impact of Molecular Conformation

Charutha Kalarikkal[a], Anjali[#b], Sarbani Bhattacharjee[#b], Koyeli Mapa[b]*, and Chinna Ayya Swamy P[a]*

[a]Main group Organometallics Optoelectronic Materials and Catalysis lab, Department of Chemistry, National Institute of Technology, Calicut, India-673601.

[b]Department of Life Sciences, School of Natural Sciences, Shiv Nadar University, Greater Noida, Gautam Buddha Nagar, Uttar Pradesh 201314, India.

Corresponding author : swamy@nitc.ac.in

[#]Equal contribution

Table of Contents

1. General Information

1.1 Materials and Measurements

All the commercially available chemicals and solvents were purchased and used as received. Toluene was dried over sodium, freshly distilled, and then used. The chlorinated solvents were dried over CaH_2 and subsequently stored over 4 Å molecular sieves. All the heating reactions were performed in a reaction block on a magnetic stirrer using a temperature-controlled probe. Moisture sensitive reactions were performed under a nitrogen atmosphere. The 500 MHz ^{1}H NMR, 126 MHz ^{13}C NMR, 471 MHz ^{19}F NMR and 160.4 MHz ^{11}B NMR spectra were recorded on a JEOL JNM-ECZ-500R/M1, 500 MHz NMR spectrometer. All solution ^{1}H and ^{13}C spectra were referenced internally to the solvent signal [TMS ($\delta = 0$)]. ^{11}B and ^{11}F spectra were referenced externally to $BF_3 \cdot Et_2O$ ($\delta = 0$) in C_6D_6. All the chemical shifts were reported in δ ppm, and the coupling constants (J) were given in Hertz (Hz). The HRMS was performed on a Waters Synapt XS spectrometer in the positive ion mode using acetonitrile as the solvent. The UV−Vis absorption spectra were measured using a UV-Vis spectrophotometer SHIMADZU-2600 with a slit width of 2. Fluorescence measurements were carried out on a PerkinElmer 6500 fluorescence spectrometer.

Fluorescence Quantum Yield

The fluorescence quantum yields of compounds **5a-c** and **6a-c** in solution were evaluated by using quinine sulfate as a reference (0.1 M in H_2SO_4, $\Phi_F = 57.7$ %). The quantum yield Φ is calculated using the formula:

$$\Phi = \Phi_F \times (I/I_R) \times (A_R/A) \times (\eta/\eta_R)^2$$

where Φ = quantum yield of the compound, I = integral area of the emission peak, A = absorbance at λ_{ex}, η = refractive index of the solvent.

Determination of viscosity

Viscosity for the mixture of solvents (DMSO and glycerol in different propositions) was calculated using the following equation:

$$\ln (\eta_{mix}) = \sum_i w_i \times \ln (\eta_i)$$

where η_{mix} is the viscosity of the mixture, η_i is the viscosity of each component, and w_i is the weighting factor ($0<w<1$) of each component. At 25 °C, glycerol has viscosity (η) of 934 cP, and DMSO has 2 cP.

Cell based studies

HeLa and HEK293T cells were maintained in a 100 mm dish to about 80-90% confluency. The cells were grown in complete media (DMEM, 10% FBS (Gibco), 1% Penicillin-Streptomycin antibiotic) at 37 °C, in a 5% CO_2 incubator. For fluorescence detection, Cells were seeded on glass bottom 35 mm confocal dishes, which were then maintained in a CO_2 incubator at 37 °C for 24 h, then cells were incubated with 500 nM of probes along with 200 nM of Nile Red (Sigma Aldrich), 200 nM of Mitotracker^{TM} (Invitrogen), 200 nM of Lysotracker (Invitrogen) and 200 nM of Hoechst 33342 (Invitrogen) for 30 minutes in three separate setups of experiments. After incubation cells were washed thrice with 1X PBS followed with the addition of 1mL complete media and finally cells were observed under confocal microscope.

MTT assay

$5x10^3$ cells/well were seeded in 96 well plate, after 24 h Hela cells are treated with probes in different concentrations, and incubated for 24 h at 37 °C, CO_2-5% and humidity-controlled conditions. Following incubation, the cells were washed with 1X PBS, thrice. Then cells were treated with 0.5 mg/mL of MTT for 2 h and absorbance was measured at 590 nm.

Statistical Analyses

All the MTT data was acquired for three independent experiments and presented as the mean of three individual observations with the standard deviation. IC_{50} values were calculated using the AAT Bioquest IC_{50} calculator.

Live Cell Imaging and Image analysis

Confocal imaging was carried out using Nikon A1R MP + Ti-E confocal microscope. Images were acquired using Apochormat 100X 1.4 NA oil immersion-based objective lens. Imaging was performed at temperatures 37 °C, CO_2-5% and humidity-controlled conditions. 405 nm, 488 nm, 560 nm and 640 nm lasers were used to excite the signals from Probes, Nile Red, Lysotracker and MitoTracker Far Red and Hoechst 33342 respectively, the emission signals were detected by an automated du4 detector. The visible puncta of the lipid droplets in HeLa and HEK293T cells were quantified by drawing manual ROI (Region of Interest) on individual cells using Nikon NIS Essentials analysis software. The Mean Fluorescent Intensity plots were

plotted with the help of GraphPad Prism. The co-localization studies of the Probe and Nile Red were quantified by drawing manual ROI (Region of Interest) on individual cells using Nikon NIS Essentials analysis software. The average for Pearson's co-efficient were plotted with the help of GraphPad Prism.

Statistical Analyses

All statistical analyses were performed by using GraphPad Prism on the dataset of n≥25, of three independent individual experiment. An unpaired t-test was performed to compare the dataset of the two groups. All error bars indicate mean ± SEM. The significance values were depicted in the figures using the following key legend: *: p <0.05, **: p <0.01, ***: p <0.001, ****: p<0.000.1.

Photostability

HeLa were maintained in a 100 mm dish to about 80-90% confluency. The cells were grown in complete media (DMEM, 10% FBS(Gibco), 1% Penicillin-Streptomycin antibiotic) at 37 °C, in a 5% CO_2 incubator. For fluorescence detection, Cells were seeded on glass bottom 35 mm confocal dishes, which were then maintained in a CO_2 incubator at 37 °C for 24 h, then cells were incubated with 500 nM of probes along with 200 nM of Nile Red. For the photostability test, cells incubated with the different probes were continuously irradiated with lasers (488 nm). The images were captured at 2-minute time intervals.

2. Synthetic procedure for the precursors and target molecules

Synthesis of 2, 3-diphenylacrylonitrile derivatives (1 a-c)

Benzyl cyanide or para-substituted benzyl cyanides (13 mmol) and sodium hydroxide (1.7 g, 43.25 mmol) were added to 4-bromobenzaldehyde (2 g, 10.81 mmol) in 40 mL methanol and stirred the reaction mixture at 40 °C for 4 h. The reaction progress was monitored using thin layer chromatography (TLC) and the complete consumption of reactant was observed. The reaction mixture was then allowed to cool to room temperature, and the solid product was isolated by filtration. The crude solid product was washed multiple times with methanol and dried under vacuum. The pure product was obtained as white powder with moderately good yields. The characterisation data of synthesised compounds matched the literature reports.[1,2,3]

*(Z)-3-(4-bromophenyl)-2-(4-methoxyphenyl)acrylonitrile (**1a**):* White solid powder (3.2 g, 95 %). ^{1}H NMR (500 MHz, $CDCl_3$) δ: 7.71 (d, *J* = 9.3 Hz, 2H), 7.59 (d, *J* = 9.0 Hz, 2H), 7.57 (d, *J* = 8.7 Hz, 2H), 7.34 (s, 1H), 6.96 (d, *J* = 9.0 Hz, 2H), 3.85 (s, 3H).

*(Z)-3-(4-bromophenyl)-2-phenylacrylonitrile (**1b**):* White solid powder (3.0 g, 98 %). ^{1}H NMR (500 MHz, $CDCl_3$) δ: 7.75 (d, *J* = 8.0 Hz, 2H), 7.67 (d, *J* = 7.1 Hz, 2H), 7.59 (d, *J* = 8.7 Hz, 2H), 7.48 – 7.39 (m, 4H).

*(Z)-3-(4-bromophenyl)-2-(4-chlorophenyl)acrylonitrile (**1c**):* White solid powder (3.4 g, 99 %). ^{1}H NMR (500 MHz, $CDCl_3$) δ: 7.75 (d, *J* = 8.2 Hz, 2H), 7.61 (m, 4H), 7.44 (s, 1H), 7.43 (d, *J* = 8.8 Hz, 2H). $^{13}C\{^{1}H\}$ NMR (126 MHz, $CDCl_3$) δ: 141.5, 136.0, 133.1, 132.8, 131.1, 129.9, 127.7, 125.7, 117.9, 111.7.

Synthesis of (Z)-2-(4-methoxyphenyl)-3-(4-(4,4,5,5-tetramethyl-1,3,2-dioxaborolan-2-yl)phenyl) acrylonitrile (2a)

100 mL oven dried Schlenk flask was charged with compound **1a** (1 g, 3.18 mmol), bis(pinacolato)diboron (1.0 g, 4 mmol), potassium acetate (0.9 g, 9.54 mmol), triphenylphosphine (33.5 mg, 0.13 mmol), and purged with N_2. The reactants were dissolved in 50 mL of dry toluene and degassed the reaction mixture thoroughly with N_2 for 30 minutes. The dichlorobis(triphenylphosphine)palladium(II) (45 mg, 0.06 mmol) catalyst was added and the reaction mixture was refluxed at 110 °C for 24 h. The volatiles were removed under reduced pressure, the crude product was extracted with ethyl acetate (50 mL for 3 to 4 times) and washed thoroughly with brine solution. The organic fraction was dried over anhydrous sodium sulphate (Na_2SO_4) and was evaporated under reduced pressure, resulting in a brown color solid as the crude product. It was then purified by silica gel column chromatography with hexane/ethylacetate (95:5) as the eluents. The pure product was obtained as a white solid.[4,5] (1.03 g, 90 %). ^{1}H NMR (500 MHz, $CDCl_3$) δ: 7.90 – 7.82 (m, 4H), 7.62 (d, *J* = 8.9 Hz, 2H), 7.44 (s, 1H), 6.96 (d, *J* = 9.0 Hz, 2H), 3.86 (s, 3H), 1.36 (s, 12H). $^{13}C\{^{1}H\}$ NMR (126 MHz, $CDCl_3$) δ: 161.0, 140.3, 136.8, 135.6, 128.6, 127.8, 127.3, 118.4, 114.9, 112.5, 84.5, 83.9, 55.9, 25.3. HRMS (ESI) m/z: $[M + H]^+$ calcd for $C_{22}H_{24}BNO_3$, 362.1927; found, 362.1927.

The synthesis of **2b** and **2c** was similar procedure of **2a** and data as follows:

*(Z)-2-phenyl-3-(4-(4,4,5,5-tetramethyl-1,3,2-dioxaborolan-2-yl)phenyl)acrylonitrile (**2b**):* The compound **2b** was synthesized using compound **1b** (1 g, 3.51 mmol), bis(pinacolato)diboron (1.1 g, 4.41 mmol), potassium acetate (1.0 g, 10.6 mmol), triphenylphosphine (37 mg, 0.14 mmol), and dichlorobis(triphenylphosphine)palladium(II) (50 mg, 0.07 mmol). The pure product was obtained as white solid (1 g, 86 %). The NMR data matches well with the literature reported values.[4] ^{1}H NMR (500 MHz, $CDCl_3$) δ: 7.89 (q, *J* = 8.3 Hz, 4H), 7.69 (d, *J* = 7.1 Hz, 2H), 7.55 (s, 1H), 7.48 – 7.38 (m, 3H), 1.37 (s, 12H).

*(Z)-2-(4-chlorophenyl)-3-(4-(4,4,5,5-tetramethyl-1,3,2-dioxaborolan-2-yl)phenyl) acrylonitrile (**2c**):* The compound **2c** was synthesized using compound **1c** (1 g, 3.13 mmol), bis(pinacolato)diboron (1 g, 3.93 mmol), potassium acetate (0.9 g, 9.41 mmol), triphenylphosphine (33.0 mg, 0.12 mmol), and dichlorobis(triphenylphosphine)palladium(II) (45 mg, 0.06 mmol). The pure product was obtained as white solid (1 g, 88 %). ^{1}H NMR (500 MHz, $CDCl_3$) δ: 7.92 – 7.84 (m, 4H), 7.62 (d, *J* = 8.8 Hz, 2H), 7.52 (s, 1H), 7.42 (d, *J* = 8.8 Hz, 2H), 1.36 (s, 12H). $^{13}C\{^{1}H\}$ NMR (126 MHz, $CDCl_3$) δ: 142.9, 136.2, 135.8, 135.7, 133.4, 129.7, 128.9, 127.7, 118.0, 111.7, 84.6, 25.3. HRMS (ESI) m/z: $[M + H]^+$ calcd for $C_{21}H_{21}BClNO_2$, 366.1432; found, 366.1435.

Synthesis of 8-(4-Bromophenyl)-4,4-difluoro-4-bora-3a,4a-diaza-*s*-indacene (3):

4-bromobenzaldehyde (1 g, 5.40 mmol) was added to an excess of freshly distilled pyrrole (9.4 mL, 135 mmol), stirred at room temperature under a N_2 atmosphere. The reaction mixture was degassed using N_2, followed by the addition of a catalytic amount of trifluoroacetic acid (41 µL, 0.50 mmol). The crude reaction mixture was stirred at room temperature until 4-bromobenzaldehyde was consumed completely (monitored by thin layer chromatography). The reaction mixture was extracted with ethylacetate and water, and the organic fraction was dried over anhydrous Na_2SO_4 and was evaporated under reduced pressure to obtain the crude product. The crude product was purified by silica gel column chromatography using hexane/ethylacetate (9:1) as the eluents. The pure product (dipyrromethane) was obtained as a brown solid (0.93 g, 57 %). The resultant dipyrromethane (0.93 g, 3 mmol) was added to freshly distilled DCM (350 mL), stirred at room temperature under a N_2 atmosphere. After degassing the reaction mixture thoroughly using N_2 gas, DDQ (0.80 g, 3.55 mmol) was added and was stirred for 5 h at room temperature. Triethylamine (4.3 mL, 30.90 mmol), and $BF_3{\cdot}Et_2O$ (3.81 mL, 30.90 mmol) were then added subsequently to the resultant product and stirred at room temperature for overnight. The crude was purified by silica gel column chromatography (hexane/ethylacetate = 95:5) and yielded pure product as a green solid (290 mg, 27 %). The NMR data matches well with the reported literature values.[6] ^{1}H NMR (500 MHz, $CDCl_3$) *δ*: 7.95 (s, 2H), 7.69 (d, *J* = 8.5 Hz, 2H), 7.45 (d, *J* = 8.5 Hz, 2H), 6.91 (d, *J* = 4 Hz, 2H), 6.56 (d, *J* = 4 Hz, 2H).

Synthesis of 8-(4-Bromophenyl)-4,4-difluoro-1,3,5,7-tetramethyl-4-bora-3a,4a-diaza-*s*-indacene (4):

4-bromobenzaldehyde (1 g, 5.40 mmol) and 2, 4 dimethyl pyrrole (1.3 mL, 13 mmol) were added to freshly distilled DCM (350 mL), stirred at room temperature under a N_2

atmosphere. The reaction mixture was thoroughly degassed using N_2 for at least 30 minutes, followed by the addition of a catalytic amount of trifluoroacetic acid (41.4 µL, 0.50 mmol). After 1 h, DDQ (1.41 g, 6.2 mmol) was added to the reaction mixture and was stirred for 5 h at room temperature. Triethylamine (7.53 mL, 54 mmol), and $BF_3{\cdot}Et_2O$ (6.67 mL, 54 mmol) were then added to the resultant product and stirred at room temperature for overnight. The crude was purified by silica gel column chromatography (hexane/ethylacetate = 95:5) and yielded as an orange crystalline solid (0.58 g, 27 %). The NMR data matches well with the literature reported values.[7] ^{1}H NMR (500 MHz, $CDCl_3$) δ: 7.64 (d, *J* = 8.5 Hz, 2H), 7.18 (d, *J* = 8.4 Hz, 2H), 5.99 (s, 2H), 2.55 (s, 6H), 1.41 (s, 6H).

Synthesis of Compounds 5a-c:

Compound **3** (300 mg, 0.86 mmol), respective phenylacrylonitrile boronic acid pinacol ester **2 (a-c)** (0.95 mmol), and potassium carbonate (2 M, 5 mL) were added to a 100 mL Schlenk flask. The reactants were dissolved in 30 mL of THF, and thoroughly degassed the reaction mixture using N_2 gas for 30 minutes. After degassing, tetrakis(triphenylphosphine) palladium (0) $Pd(PPh_3)_4$ (0.05 mmol) catalyst was added to the reaction mixture and refluxed for 24 h under N_2 atmosphere. The volatiles were evaporated under reduced pressure and the crude product was extracted using ethylacetate and brine solution. The organic layer was dried over anhydrous Na_2SO_4 and was evaporated under reduced pressure. The crude was further purified by silica gel column chromatography (hexane/ethylacetate = 9:1). The pure products were obtained as a red solid powder in moderate yield.

Synthesis of Compound 5a:

Red solid powder (220 mg, 51 %). ^{1}H NMR (500 MHz, $CDCl_3$) δ: 7.99 (d, *J* = 8.5 Hz, 2H), 7.77 (d, *J* = 8.5 Hz, 2H), 7.72 (d, *J* = 8.4 Hz, 2H), 7.70 – 7.63 (m, 4H), 7.60 (d, *J* = 8.2 Hz, 2H), 7.48 (s, 1H), 6.98 (d, *J* = 8.9 Hz, 2H), 6.69 (d, *J* = 4.2 Hz, 2H), 6.43 (dd, *J* = 4.2, 1.5 Hz, 2H), 3.87 (s, 3H). ^{13}C{^{1}H} NMR (126 MHz, $CDCl_3$) δ: 160.9, 144.2, 142.3, 142.0, 141.2, 139.9, 137.4, 133.8, 132.0, 131.7, 130.2, 129.3, 127.9, 127.8, 127.5, 126.7, 118.7, 118.2, 115.0, 111.7, 55.9. ^{11}B{^{1}H} NMR (160.4 MHz, $CDCl_3$) δ: -0.64 (t, *J* = 28.9 Hz). ^{19}F{^{1}H} NMR (471 MHz, $CDCl_3$) δ: -144.75 (q, *J* = 28.9 Hz). HRMS (ESI) m/z: $[M - BF_2 + H]^+$ calcd for $C_{32}H_{23}BF_2N_3O$, 454.1919; found, 454.1946.

Synthesis of Compound 5b:

Red solid powder (239 mg, 59 %). ^{1}H NMR (500 MHz, $CDCl_3$) δ: 8.04 (d, *J* = 8.4 Hz, 2H), 7.97 (s, 2H), 7.82 – 7.76 (m, 4H), 7.73 – 7.67 (m, 4H), 7.60 (s, 1H), 7.51 – 7.41 (m, 3H), 7.01 (d, *J* = 4.3 Hz, 2H), 6.58 (dd, *J* = 4.3, 2.0 Hz, 2H). ^{13}C{^{1}H} NMR (126 MHz, $CDCl_3$) δ: 147.2,

144.7, 142.9, 142.02, 141.8, 135.3, 134.8, 134.0, 133.9, 132.0, 131.7, 130.5, 129.9, 129.6, 128.1, 127.6, 126.5, 119.1, 118.5, 118.2, 112.5. $^{11}B\{^1H\}$ NMR (160.4 MHz, $CDCl_3$) δ: -0.65 (t, *J* = 28.9 Hz). $^{19}F\{^1H\}$ NMR (471 MHz, $CDCl_3$) δ: -144.82 (q, *J* = 28.8 Hz). HRMS (ESI) m/z: $[M - BF_2 + H]^+$ calcd for $C_{30}H_{20}BF_2N_3$, 424.1813; found, 424.1842.

Synthesis of Compound 5c

Red solid powder (250 mg, 57 %). ^1H NMR (500 MHz, $CDCl_3$) δ: 8.03 (d, *J* = 8.4 Hz, 2H), 7.96 (s, 2H), 7.79 (t, *J* = 8.7 Hz, 4H), 7.67 (d, *J* = 8.4 Hz, 2H), 7.64 (d, *J* = 8.7 Hz, 2H), 7.57 (s, 1H), 7.44 (d, *J* = 8.7 Hz, 2H), 7.00 (d, *J* = 4.3 Hz, 2H), 6.57 (dd, *J* = 4.4, 2.0 Hz, 2H). $^{13}C\{^1H\}$ NMR (126 MHz, $CDCl_3$) δ: 147.2, 144.7, 142.8, 142.2, 142.1, 135.9, 135.3, 133.9, 133.7, 133.3, 132.0, 131.7, 130.6, 129.8, 128.1, 127.7, 127.5, 119.1, 118.2, 111.3. $^{11}B\{^1H\}$ NMR (160.4 MHz, $CDCl_3$) δ: -0.65 (t, *J* = 28.8 Hz). $^{19}F\{^1H\}$ NMR (471 MHz, $CDCl_3$) δ: -144.76 (q, *J* = 28.7 Hz). HRMS (ESI) m/z: $[M - BF_2 + H]^+$ calcd for $C_{30}H_{19}BClF_2N_3$, 458.1424; found, 458.1420.

Synthesis of Compounds 6a-c:

Compound **4** (200 mg, 0.50 mmol), respective phenylacrylonitrile boronic acid pinacol ester **2 (a-c)** (0.55 mmol), and potassium carbonate (2 M, 5 mL) were added to a 100 mL Schlenk flask. The reactants were dissolved in 30 mL of THF, and thoroughly degassed the reaction mixture using N_2 gas for 30 minutes. After degassing, tetrakis(triphenylphosphine) palladium (0) $Pd(PPh_3)_4$ (0.03 mmol) catalyst was added to the reaction mixture and refluxed for 24 h under N_2 atmosphere. Later, the solvent THF was evaporated under reduced pressure and the crude product was extracted using ethylacetate and brine solution. The organic layer was dried over anhydrous Na_2SO_4 and was evaporated under reduced pressure. The crude was further purified by silica gel column chromatography (hexane/ethylacetate = 9:1). The pure products were obtained as a red solid powder in moderate yield.

Synthesis of Compound 6a:

Red solid powder (168 mg, 53 %). ^1H NMR (500 MHz, $CDCl_3$) δ: 7.98 (d, *J* = 8.5 Hz, 2H), 7.79 (t, *J* = 8.5 Hz, 4H), 7.65 (d, *J* = 8.9 Hz, 2H), 7.48 (s, 1H), 7.39 (d, *J* = 8.3 Hz, 2H), 6.98 (d, *J* = 8.9 Hz, 2H), 6.00 (s, 2H), 3.87 (s, 3H), 2.57 (s, 6H), 1.46 (s, 6H). $^{13}C\{^1H\}$ NMR (126 MHz, $CDCl_3$) δ: 161.1, 156.1, 143.6, 141.9, 141.7, 141.0, 139.8, 137.0, 135.1, 134.0, 131.9, 130.2, 129.2, 127.9, 127.4, 121.8, 118.7, 115.1, 114.9, 112.0, 56.0, 15.1. $^{11}B\{^1H\}$ NMR (160.4 MHz, $CDCl_3$) δ: -0.16 (t, *J* = 33.1 Hz). $^{19}F\{^1H\}$ NMR (471 MHz, $CDCl_3$) δ: -146.07 (q, *J* = 33.0 Hz). HRMS (ESI) m/z: $[M + H]^+$ calcd for $C_{35}H_{30}BF_2N_3O$, 558.2528; found, 558.2532.

Synthesis of Compound 6b:

Red solid powder (130 mg, 50 %). ^{1}H NMR (500 MHz, $CDCl_3$) δ: 8.02 (d, *J* = 8.4 Hz, 2H), 7.80 (dd, *J* = 8.4, 2.8 Hz, 4H), 7.72 (d, *J* = 7.1 Hz, 2H), 7.60 (s, 1H), 7.50 – 7.41 (m, 3H), 7.39 (d, *J* = 8.4 Hz, 2H), 6.00 (s, 2H), 2.57 (s, 6H), 1.46 (s, 6H). ^{13}C{^{1}H} NMR (126 MHz, $CDCl_3$) δ: 156.1, 143.6, 142.3, 141.9, 141.6, 140.9, 135.2, 134.9, 133.7, 131.9, 130.4, 129.8, 129.6, 129.2, 128.1, 128.0, 126.5, 121.8, 118.5, 112.3, 15.1. ^{11}B{^{1}H} NMR (160.4 MHz, $CDCl_3$) δ: -0.16 (t, *J* = 33.1 Hz). ^{19}F{^{1}H} NMR (471 MHz, $CDCl_3$) δ: -146.07 (q, *J* = 33.0 Hz). HRMS (ESI) m/z: $[M + H]^+$ calcd for $C_{34}H_{28}BF_2N_3$, 528.2422; found, 528.2407.

Synthesis of Compound 6c:

Red solid powder (165 mg, 59 %). ^{1}H NMR (500 MHz, $CDCl_3$) δ: 8.01 (d, *J* = 8.5 Hz, 2H), 7.80 (d, *J* = 8.5 Hz, 4H), 7.65 (d, *J* = 8.7 Hz, 2H), 7.57 (s, 1H), 7.44 (d, *J* = 8.7 Hz, 2H), 7.40 (d, *J* = 8.4 Hz, 2H), 6.00 (s, 2H), 2.57 (s, 6H), 1.45 (s, 6H). ^{13}C{^{1}H} NMR (126 MHz, $CDCl_3$) δ: 156.2, 143.5, 142.6, 142.2, 141.6, 140.9, 135.9, 135.3, 133.4, 131.9, 130.5, 129.8, 129.3, 128.1, 128.0, 127.7, 121.8, 118.2, 111.2, 15.1. ^{11}B{^{1}H} NMR (160.4 MHz, $CDCl_3$) δ: -0.16 (t, *J* = 33.1 Hz). ^{19}F{^{1}H} NMR (471 MHz, $CDCl_3$) δ: -146.11 (q, *J* = 32.8 Hz). HRMS (ESI) m/z: $[M + H]^+$ calcd for $C_{34}H_{27}BClF_2N_3$, 562.2033; found, 562.2028.

3. NMR and HRMS Spectra of the precursors and target molecules

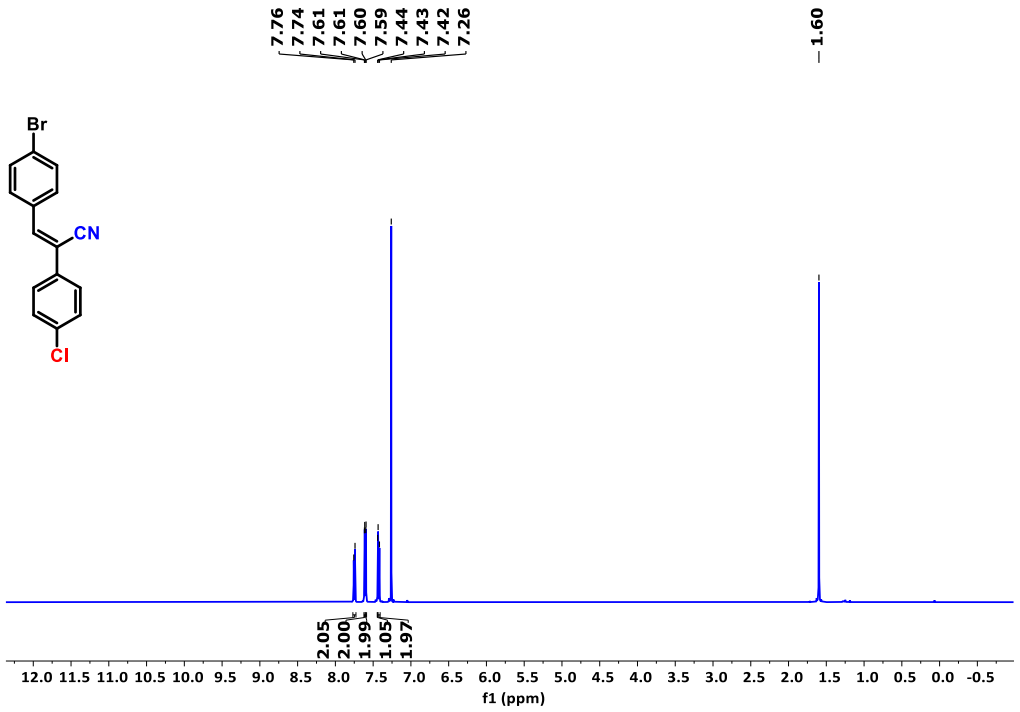

Figure S1. ^{1}H NMR spectrum (500 MHz, RT) of compound **1c** in $CDCl_3$.

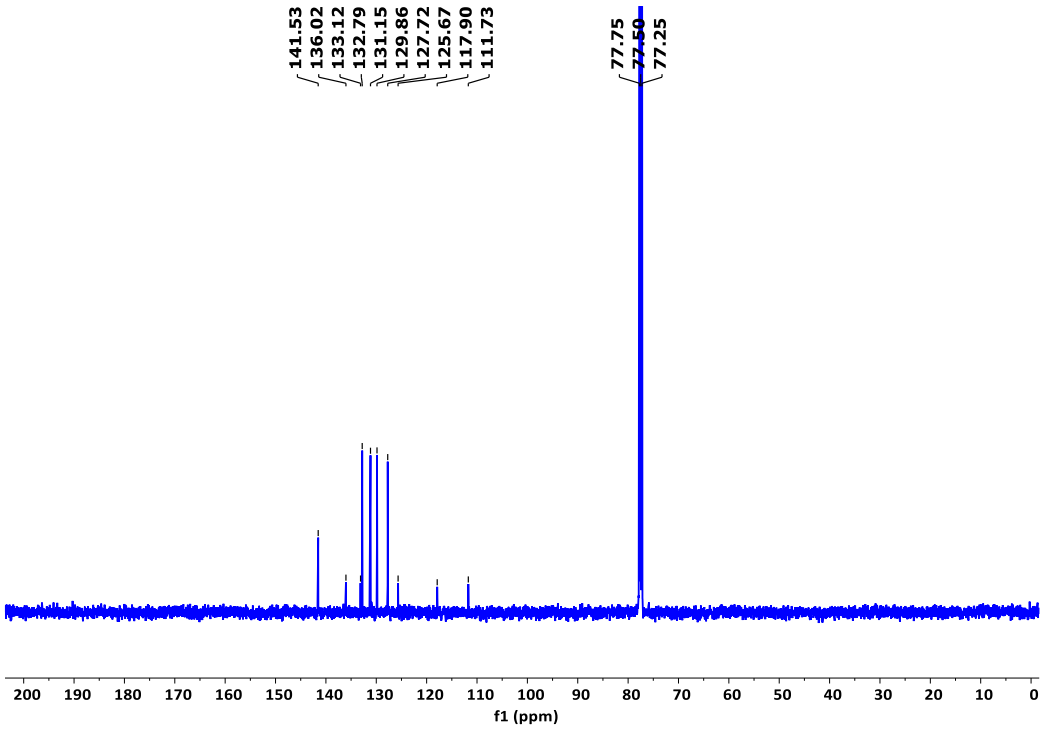

Figure S2. $^{13}C\{^{1}H\}$ NMR spectrum (126 MHz, RT) of compound **1c** in $CDCl_3$.

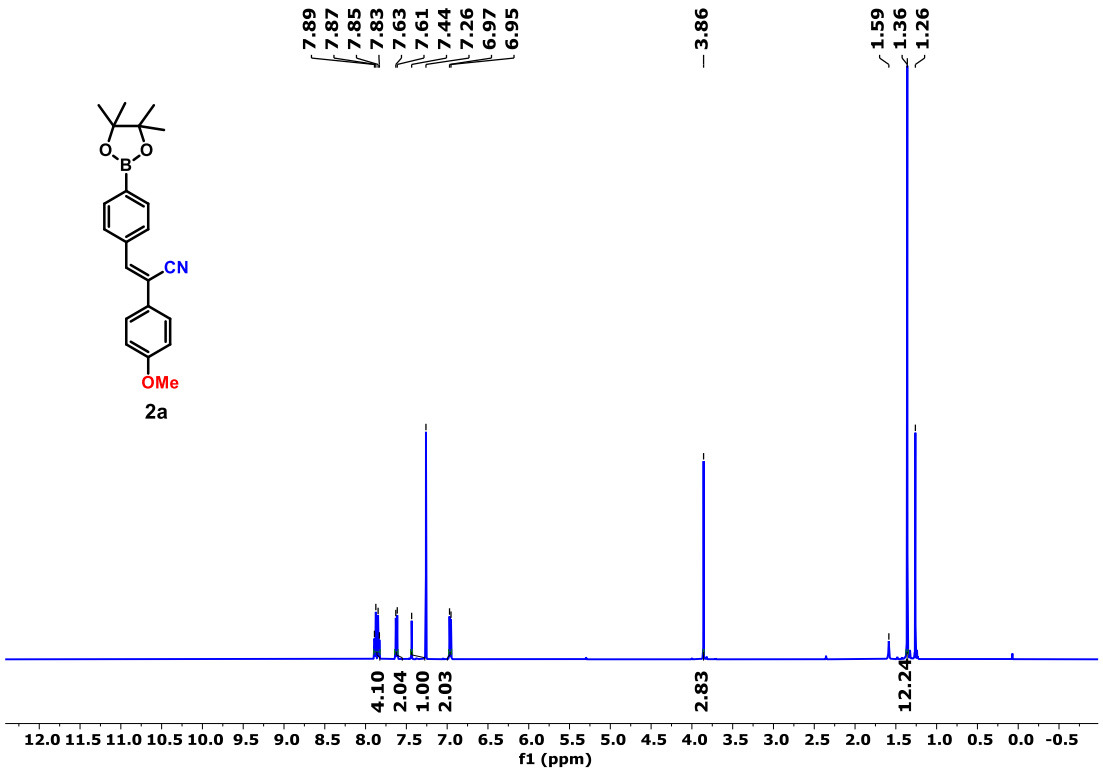

Figure S3. ^{1}H NMR spectrum (500 MHz, RT) of compound **2a** in $CDCl_3$.

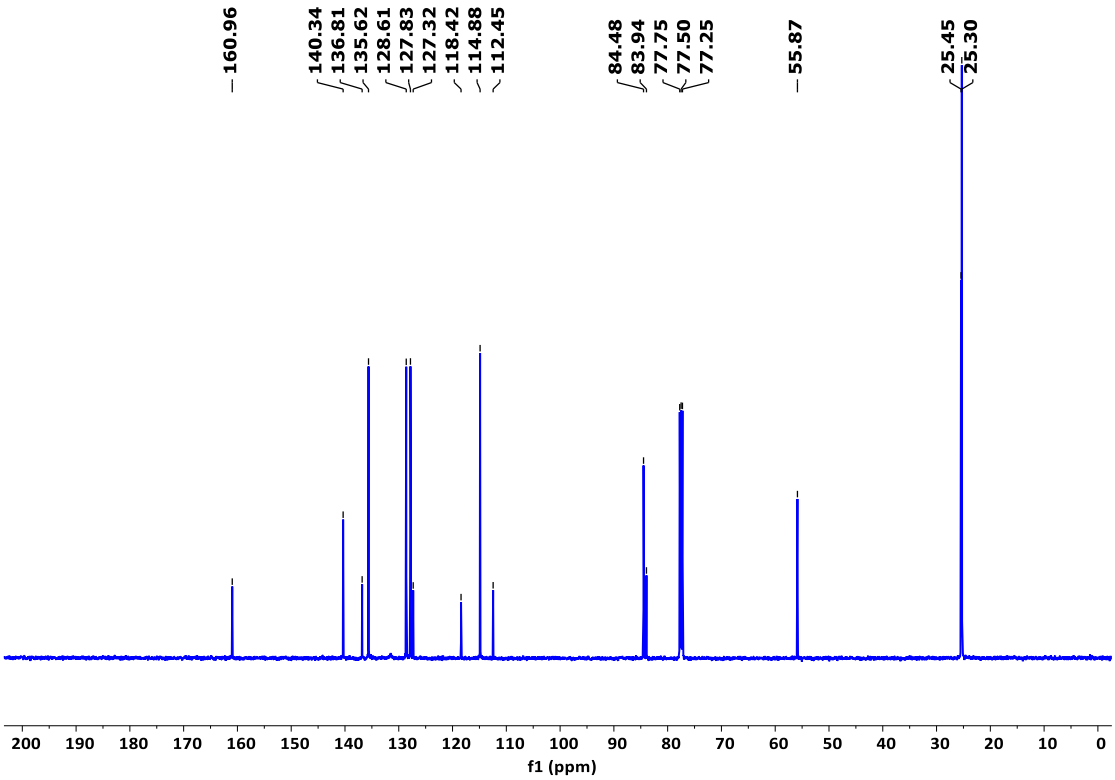

Figure S4. $^{13}C\{^{1}H\}$ NMR spectrum (126 MHz, RT) of compound **2a** in $CDCl_3$.

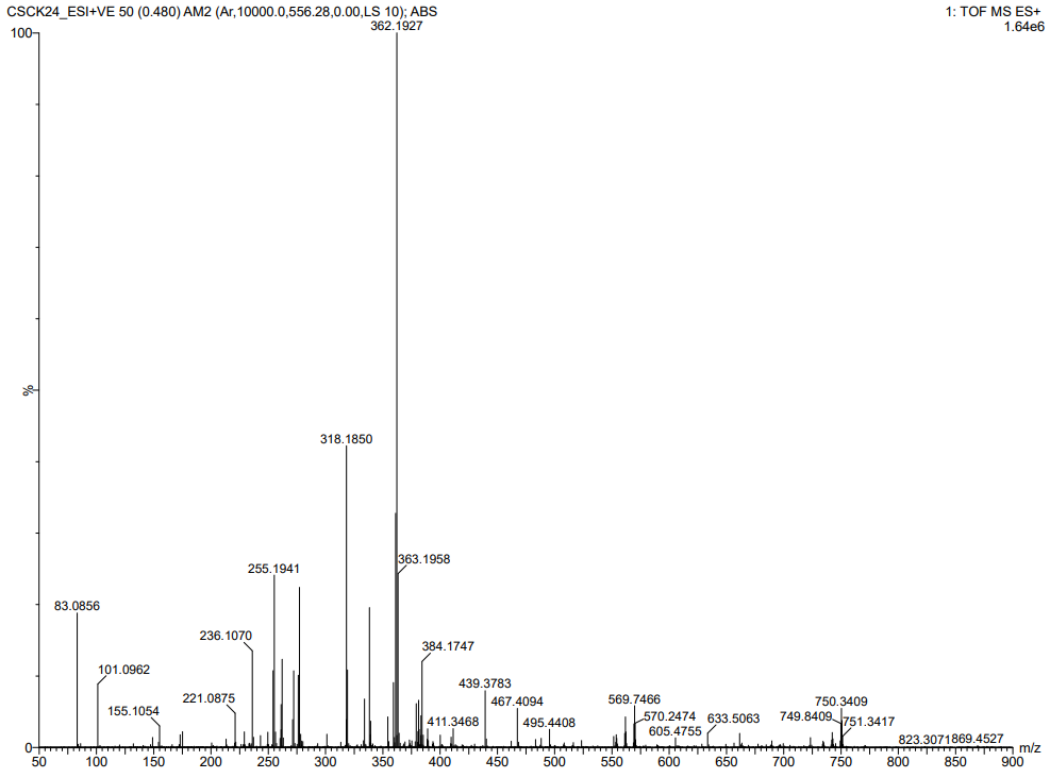

Figure S5. HRMS spectrum of compound **2a**.

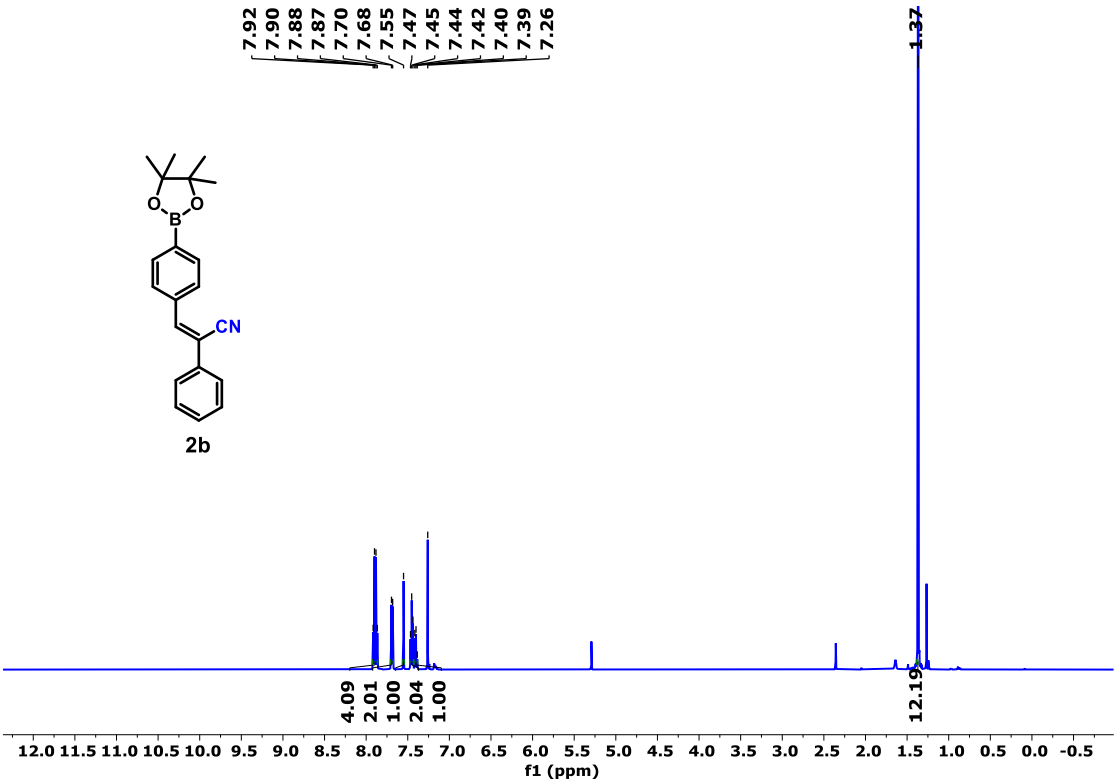

Figure S6. ^{1}H NMR spectrum (500 MHz, RT) of compound **2b** in $CDCl_3$.

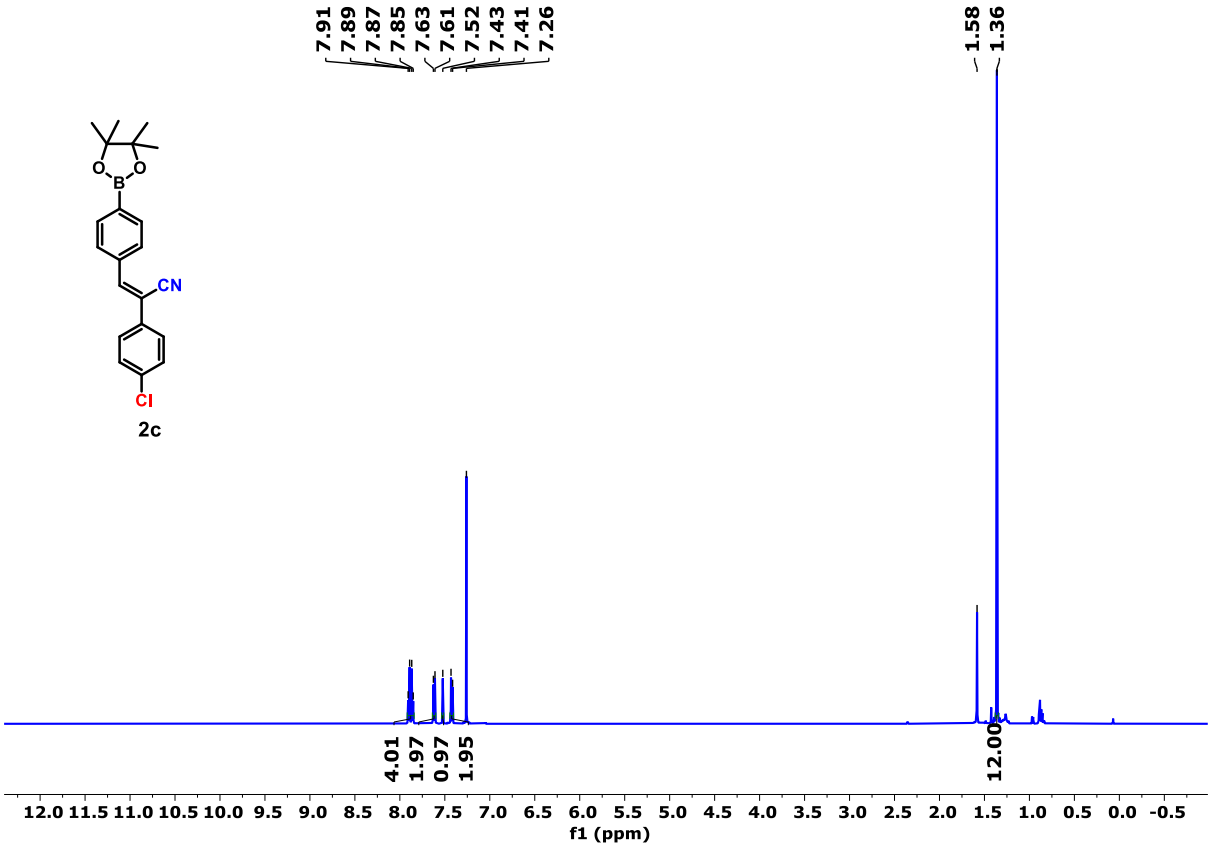

Figure S7. ^{1}H NMR spectrum (500 MHz, RT) of compound **2c** in $CDCl_3$.

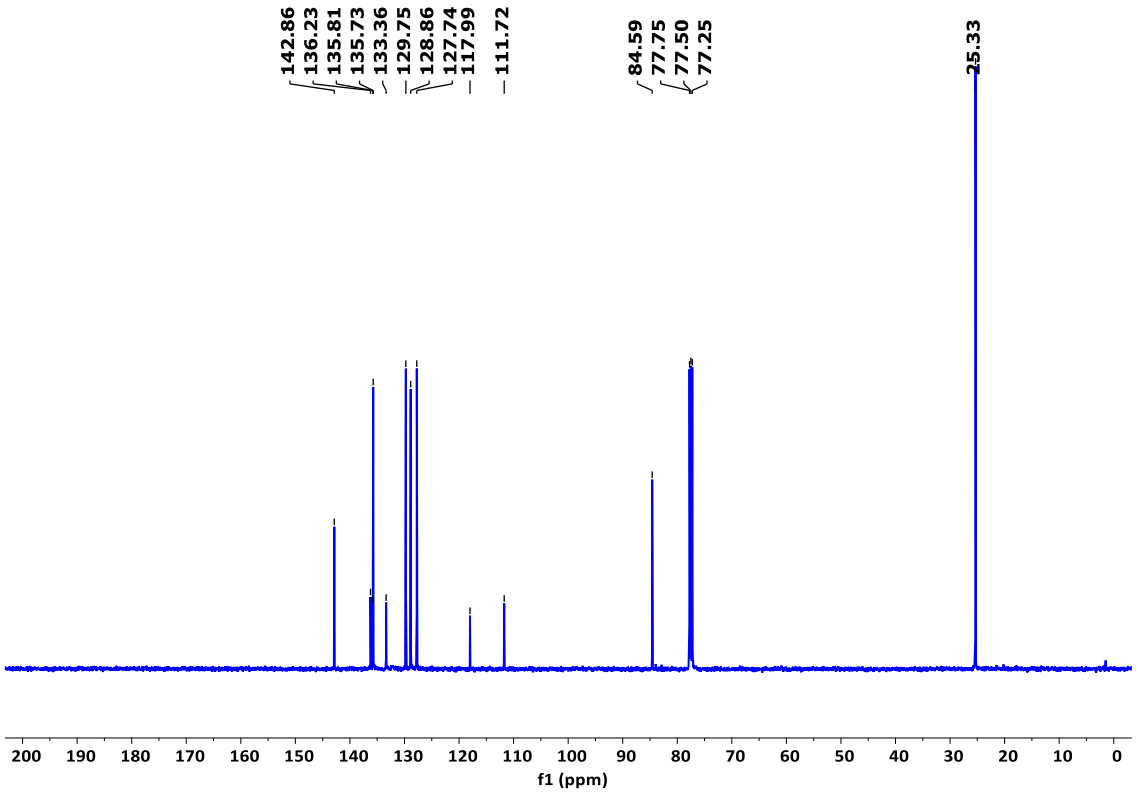

Figure S8. $^{13}C\{^{1}H\}$ NMR spectrum (126 MHz, RT) of compound **2c** in $CDCl_3$.

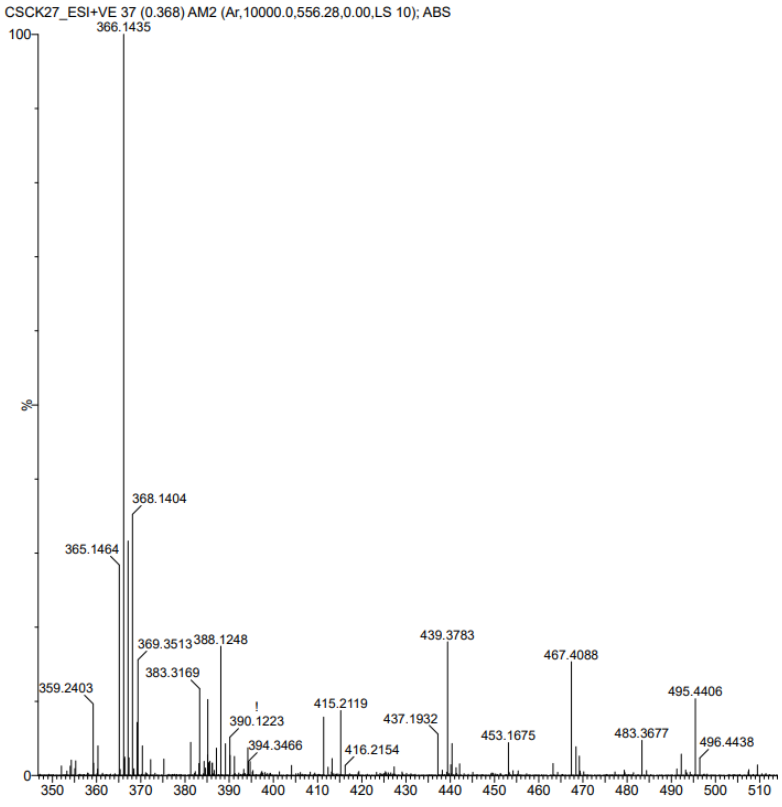

Figure S9. HRMS spectrum of compound **2c**.

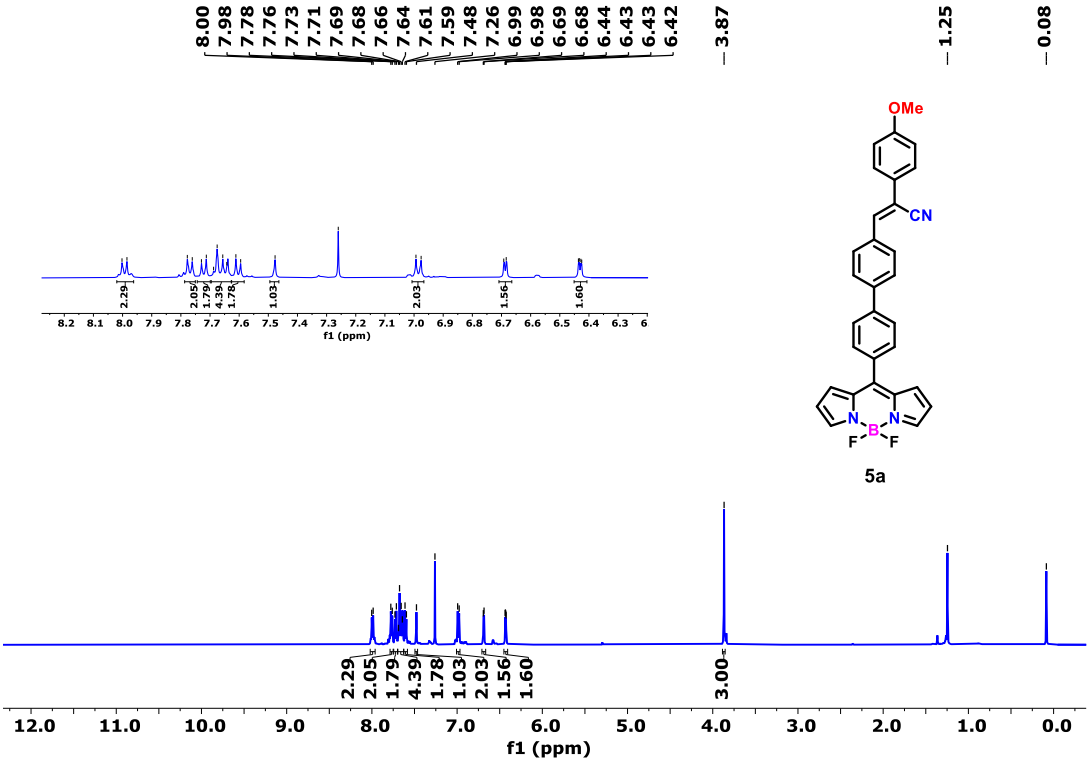

Figure S10. ^{1}H NMR spectrum (500 MHz, RT) of compound **5a** in $CDCl_3$.

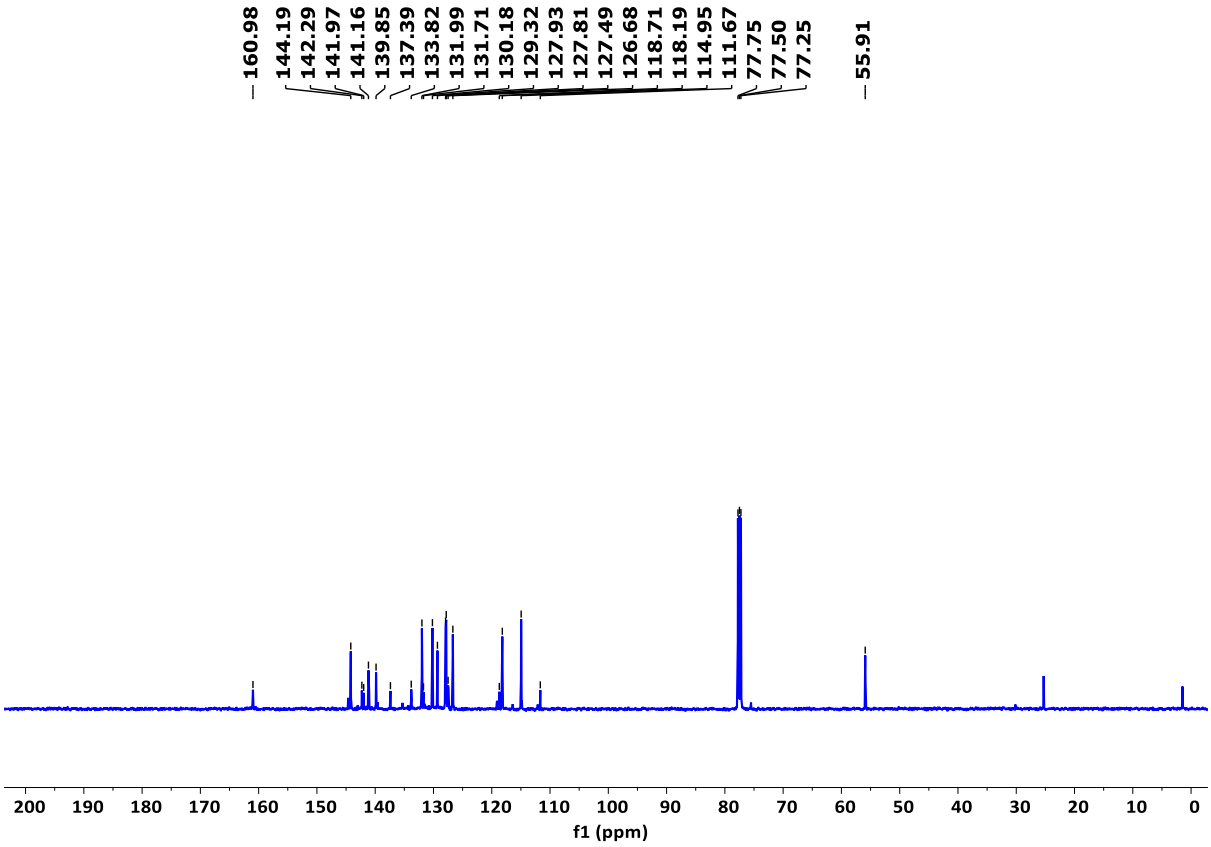

Figure S11. $^{13}C\{^{1}H\}$ NMR spectrum (126 MHz, RT) of compound **5a** in $CDCl_3$.

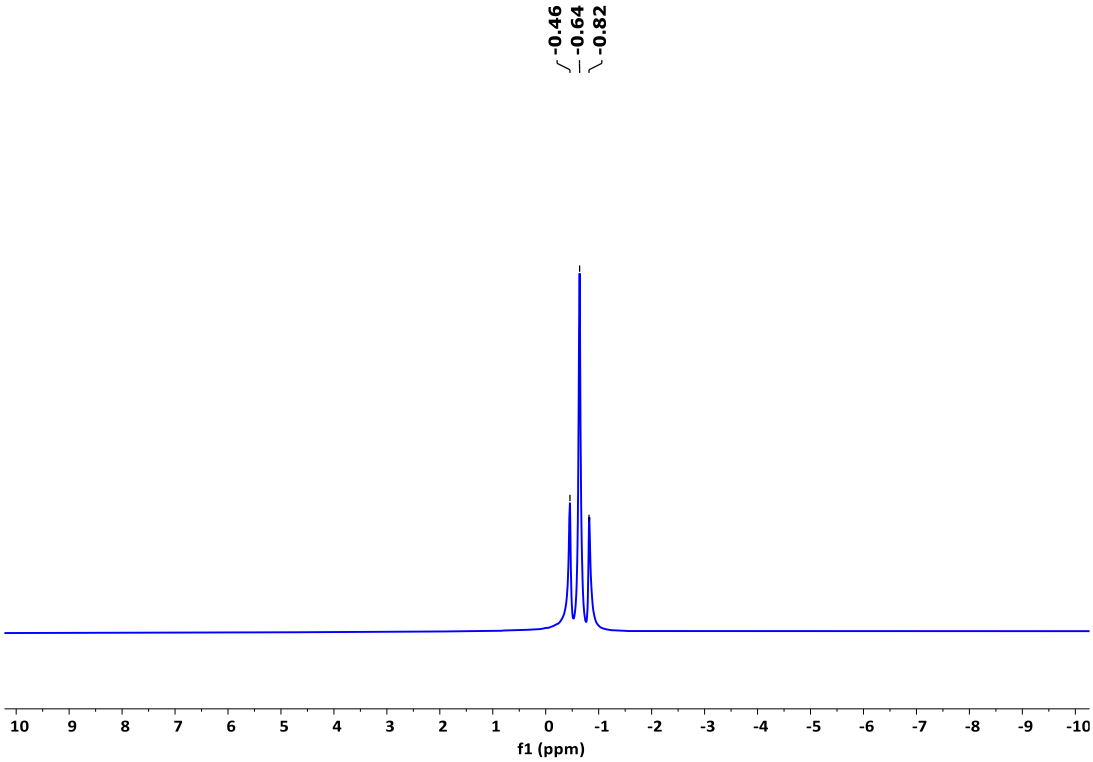

Figure S12. $^{11}B\{^{1}H\}$ NMR spectrum (160.4 MHz, RT) of compound **5a** in $CDCl_3$.

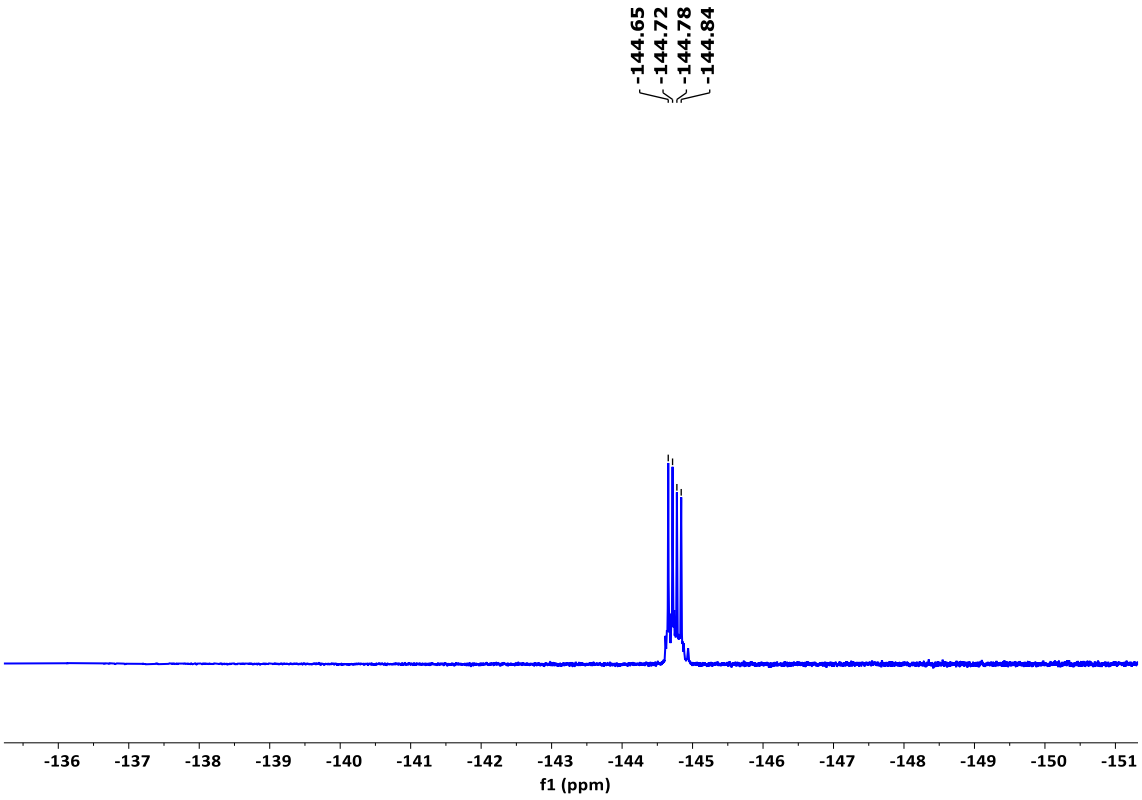

Figure S13. $^{19}F\{^{1}H\}$ NMR spectrum (471 MHz, RT) of compound **5a** in $CDCl_3$.

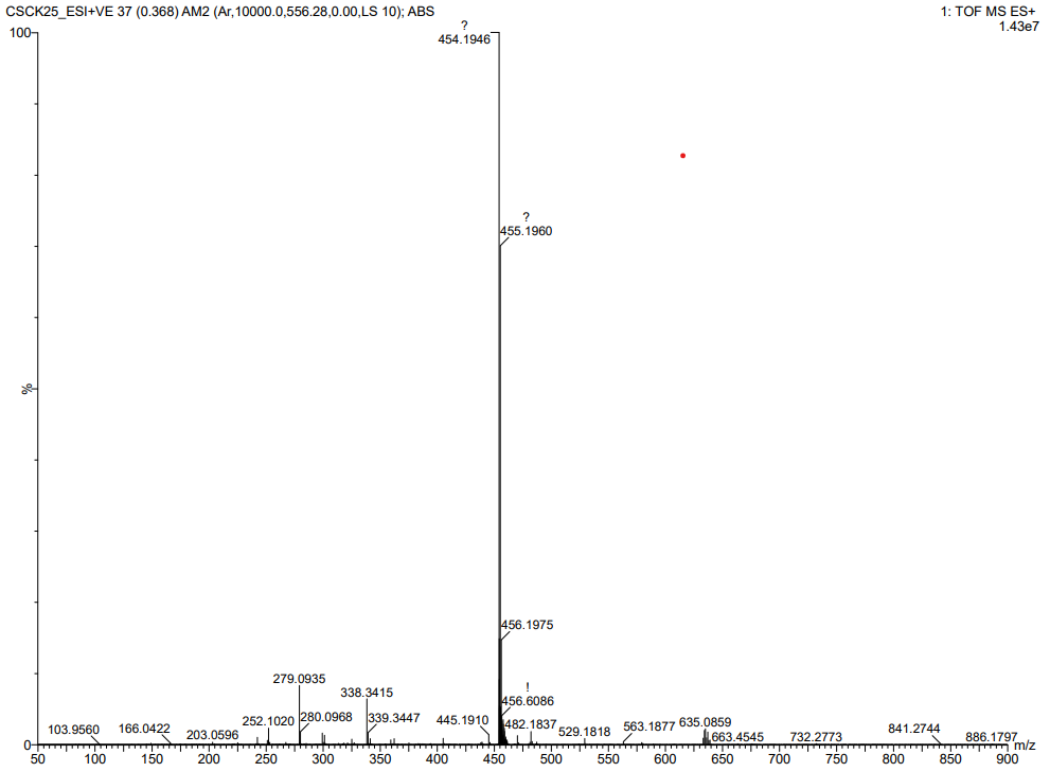

Figure S14. HRMS spectrum of compound **5a**.

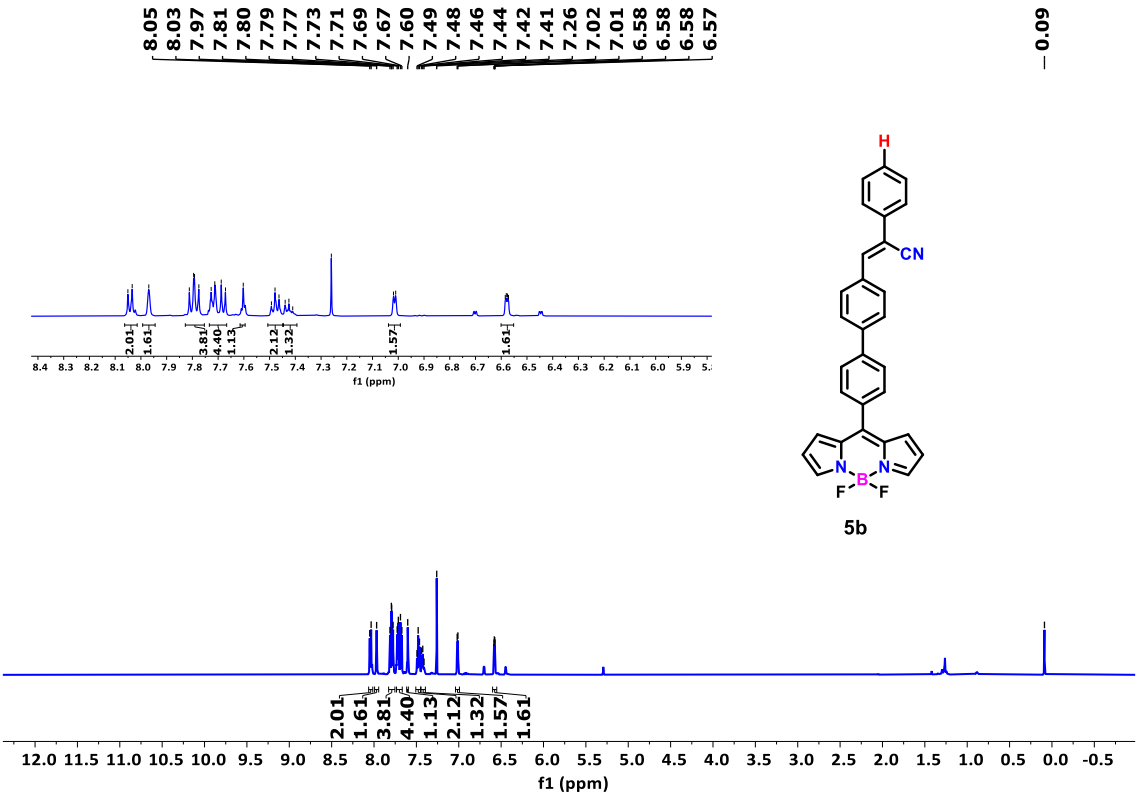

Figure S15. ^{1}H NMR spectrum (500 MHz, RT) of compound **5b** in $CDCl_3$.

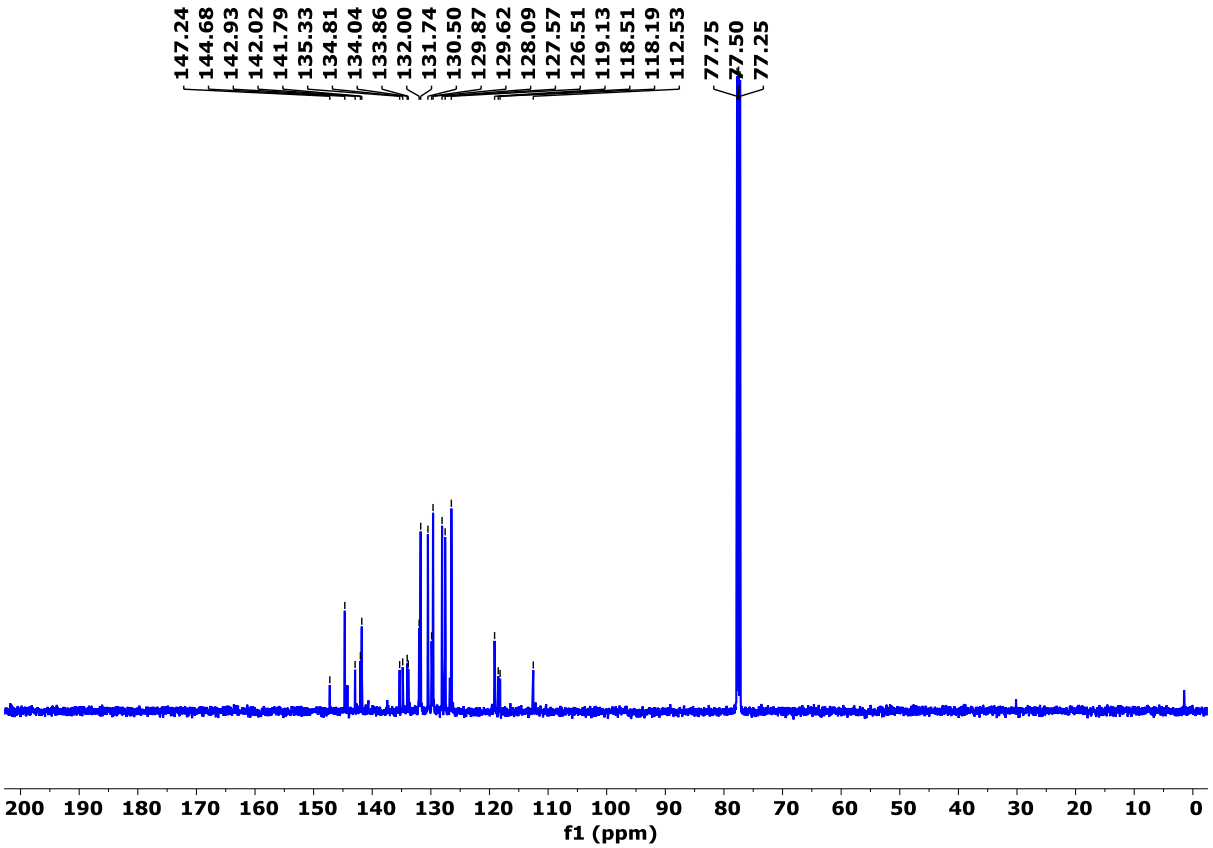

Figure S16. $^{13}C\{^{1}H\}$ NMR spectrum (126 MHz, RT) of compound **5b** in $CDCl_3$.

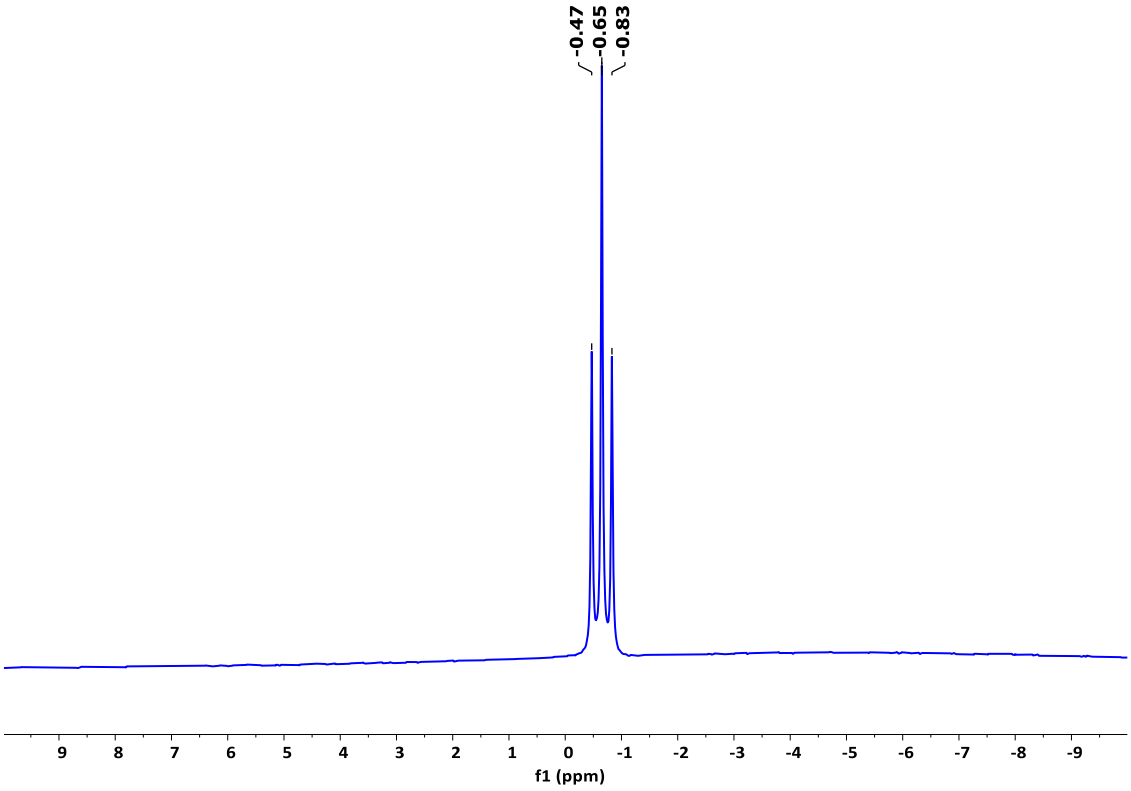

Figure S17. $^{11}B\{^{1}H\}$ NMR spectrum (160.4 MHz, RT) of compound **5b** in $CDCl_3$.

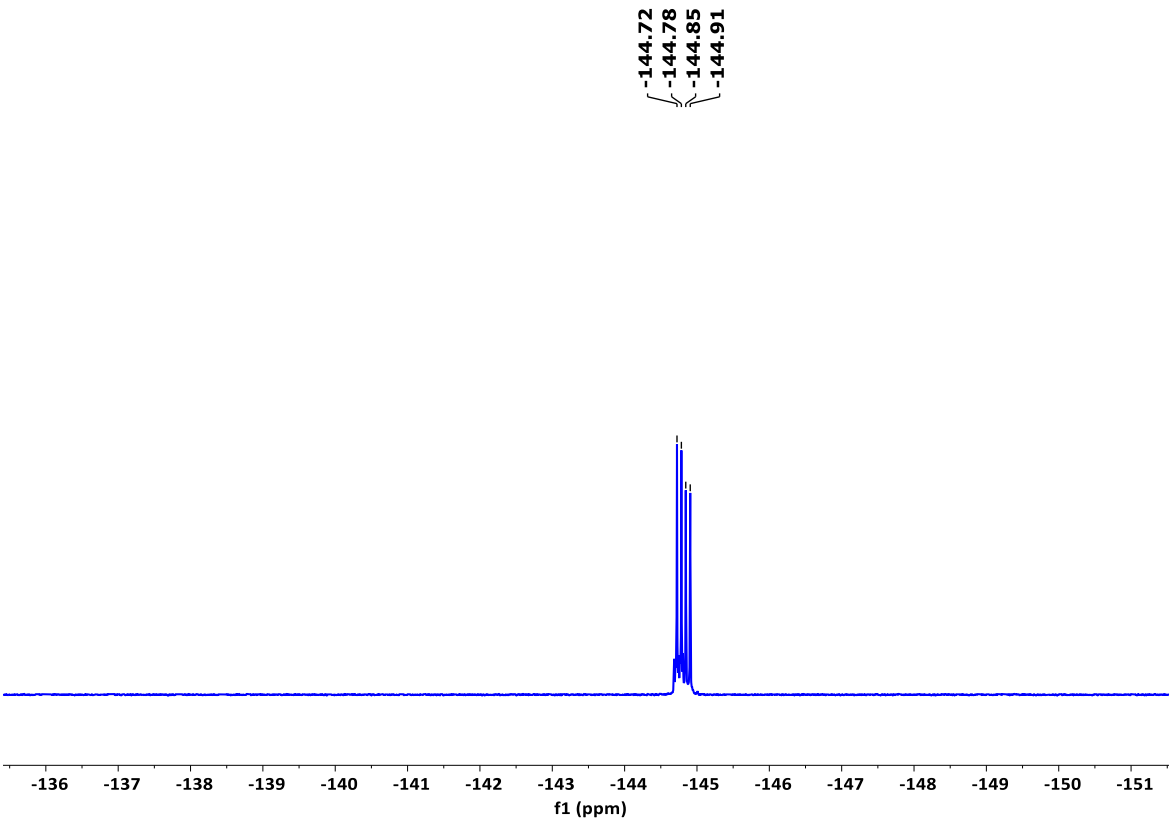

Figure S18. $^{19}F\{^{1}H\}$ NMR spectrum (471 MHz, RT) of compound **5b** in $CDCl_3$.

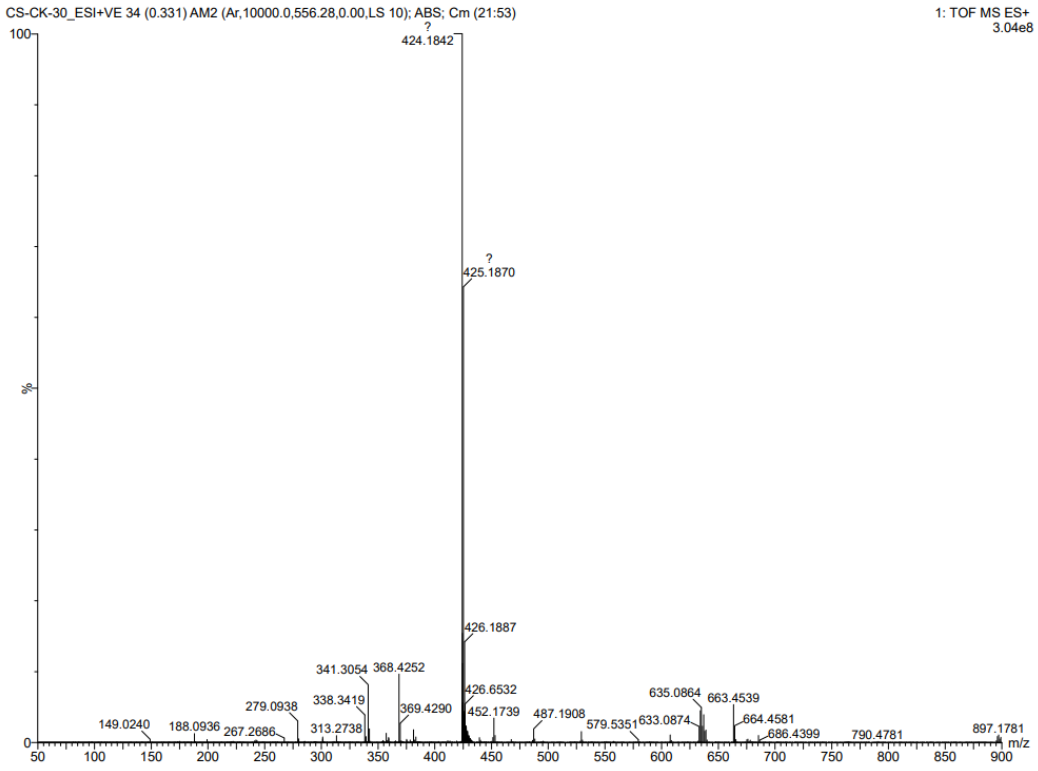

Figure S19. HRMS spectrum of compound **5b**.

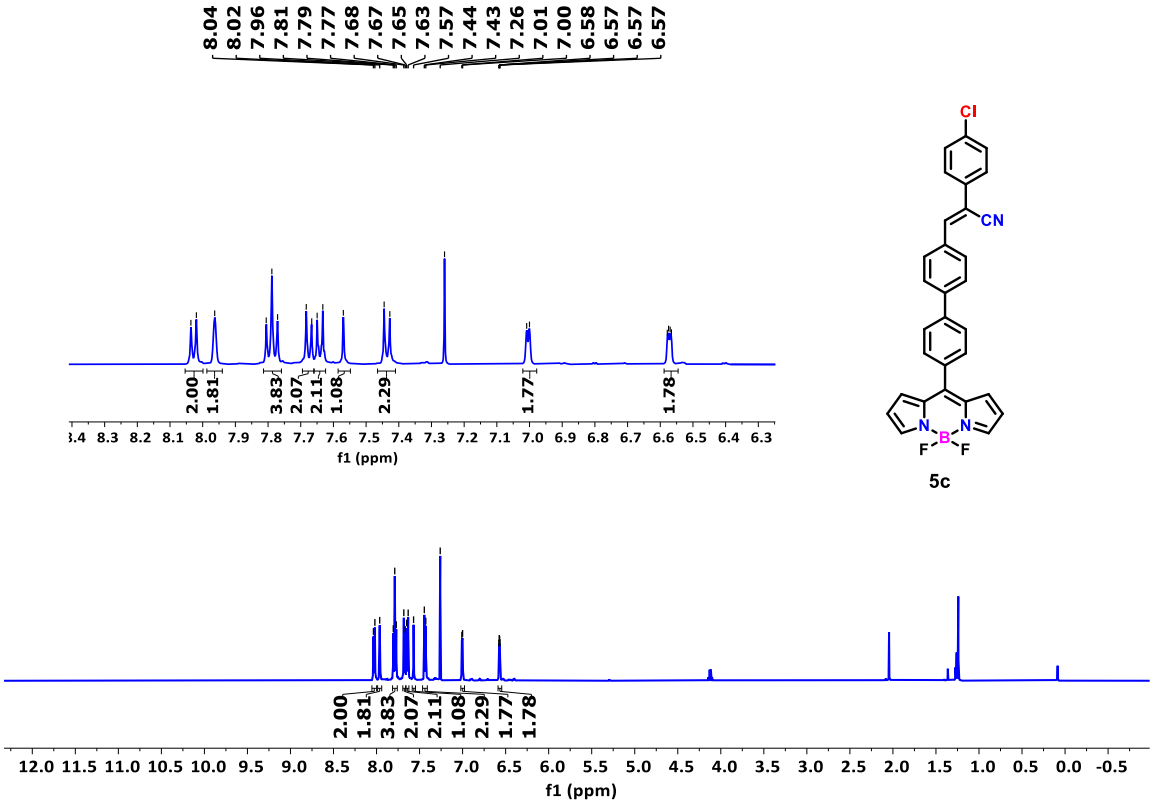

Figure S20. ^{1}H NMR spectrum (500 MHz, RT) of compound **5c** in $CDCl_3$.

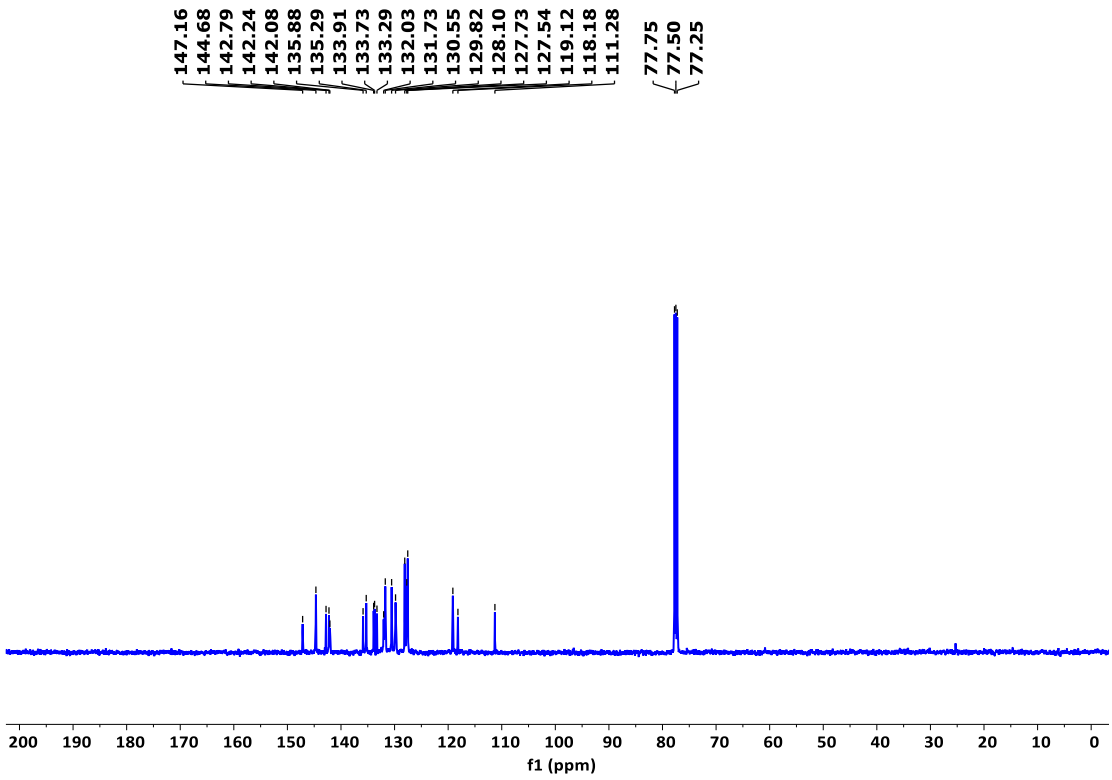

Figure S21. $^{13}C\{^{1}H\}$ NMR spectrum (126 MHz, RT) of compound **5c** in $CDCl_3$.

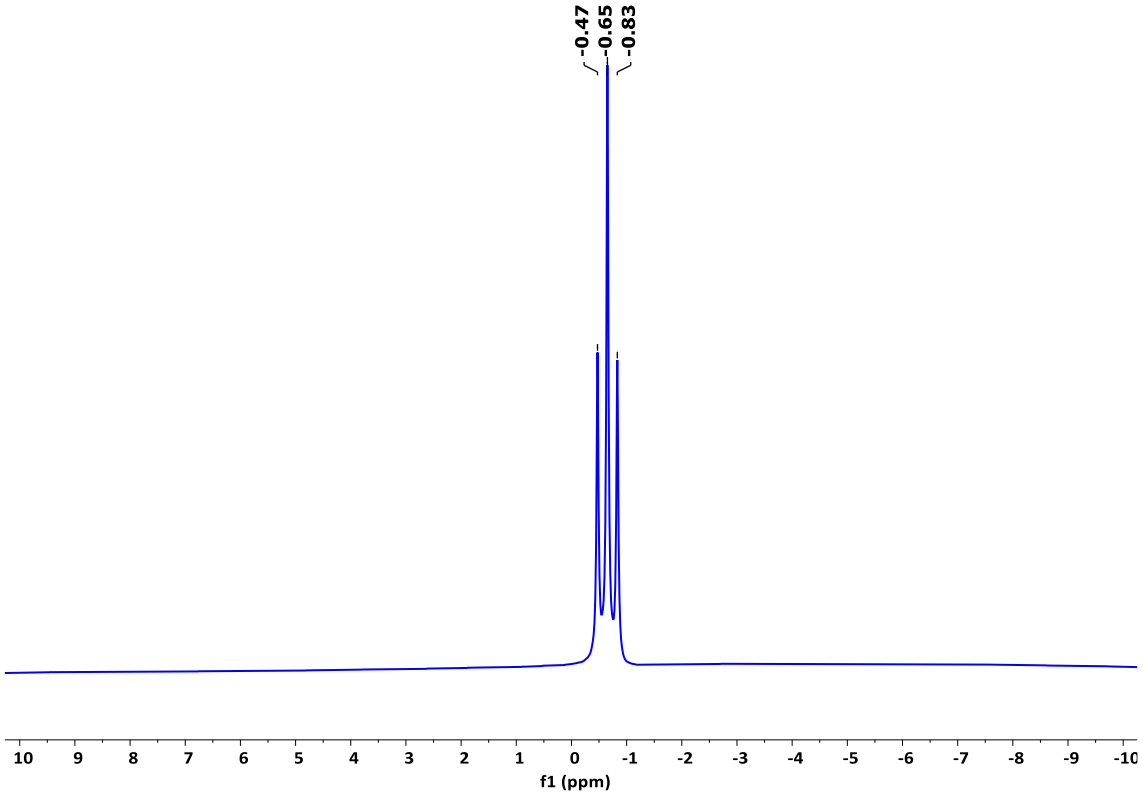

Figure S22. $^{11}B\{^{1}H\}$ NMR spectrum (160.4 MHz, RT) of compound **5c** in $CDCl_3$.

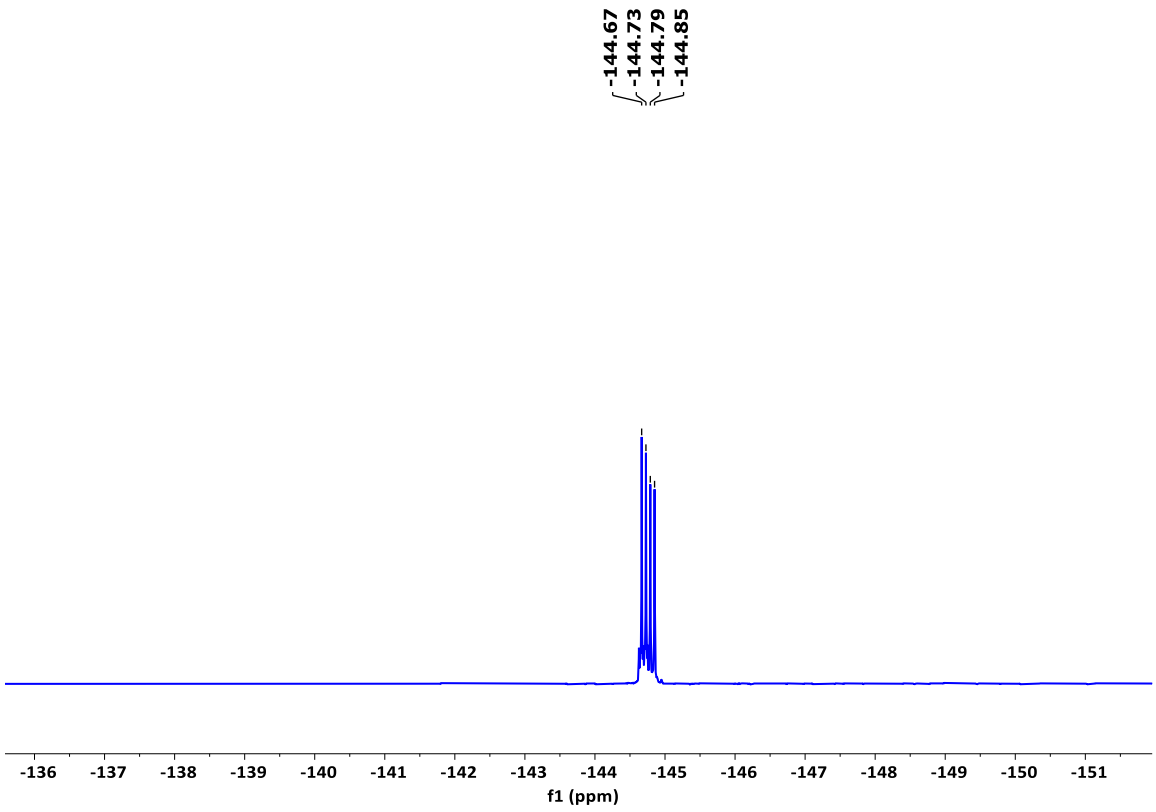

Figure S23. $^{19}F\{^{1}H\}$ NMR spectrum (471 MHz, RT) of compound **5c** in $CDCl_3$.

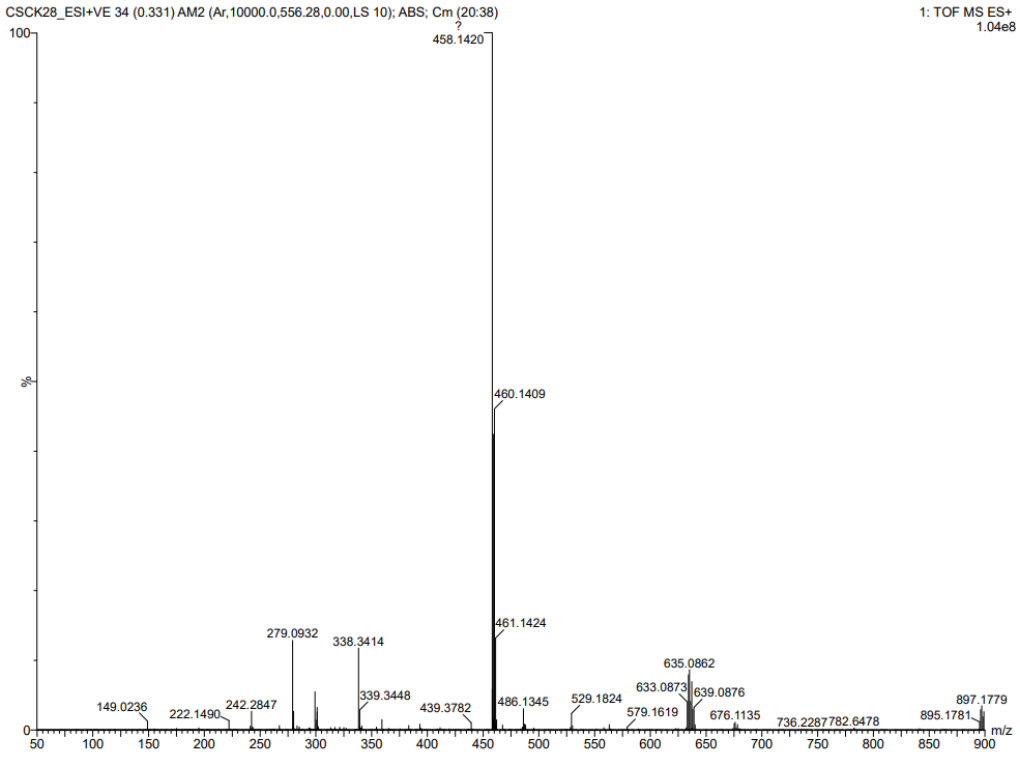

Figure S24. HRMS spectrum of compound **5c**.

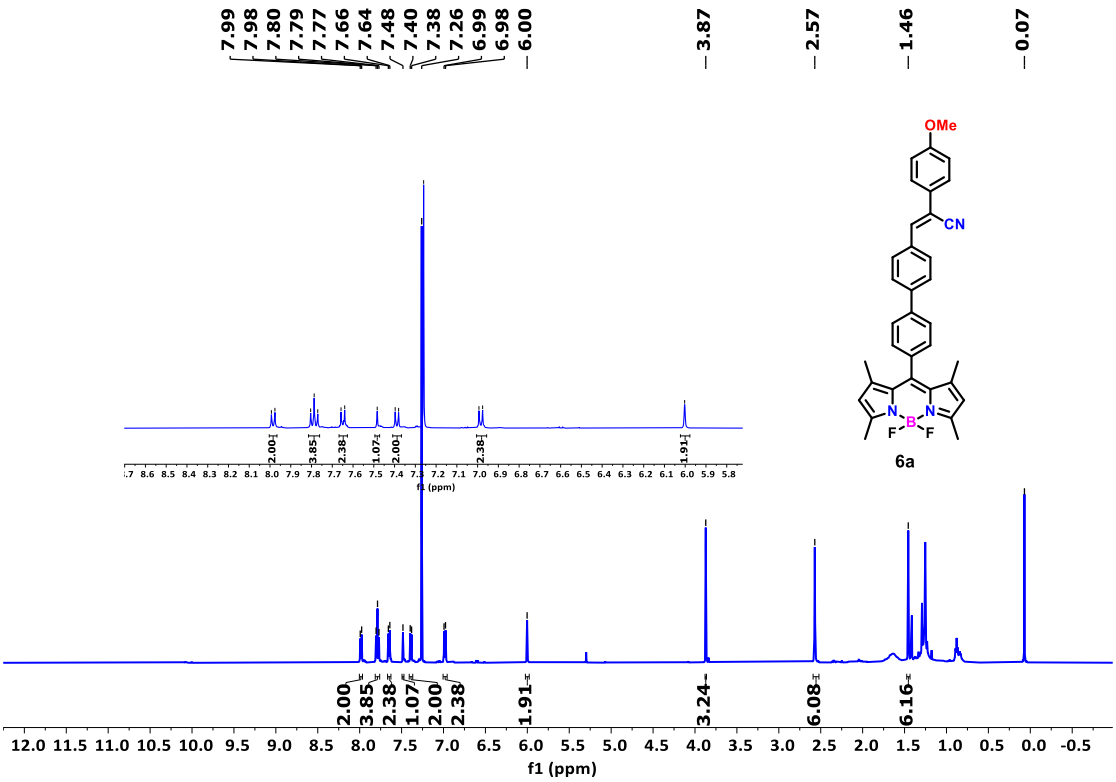

Figure S25. ^{1}H NMR spectrum (500 MHz, RT) of compound **6a** in $CDCl_3$.

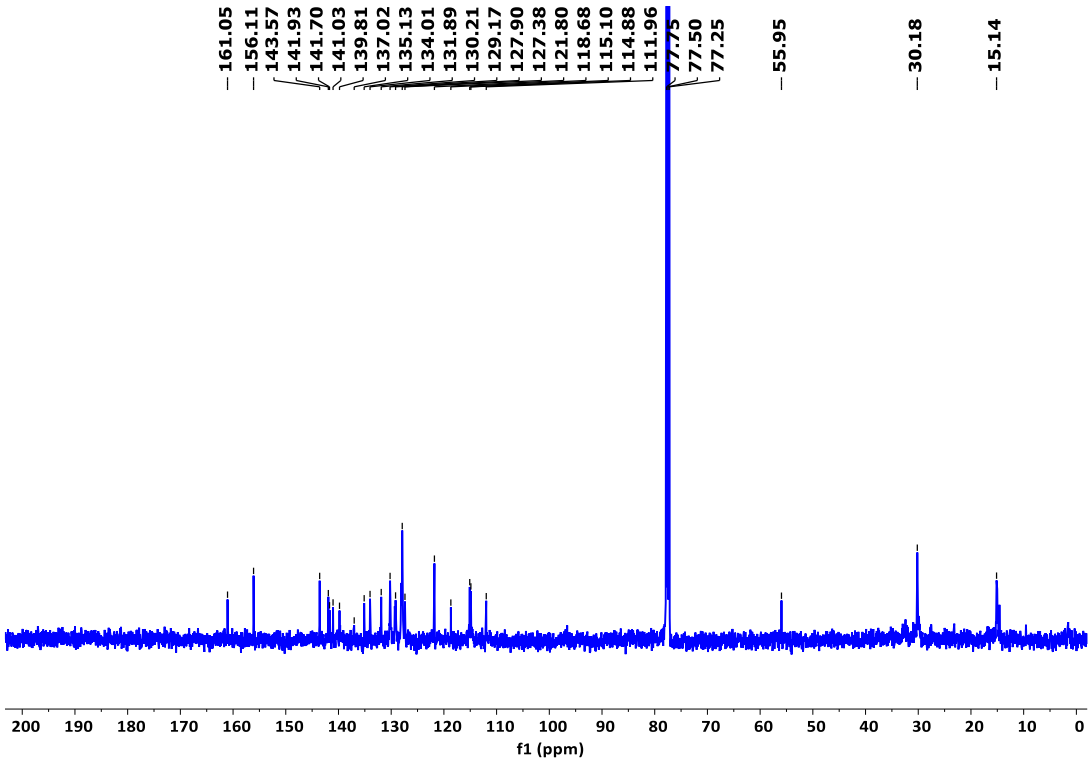

Figure S26. $^{13}C\{^{1}H\}$ NMR spectrum (126 MHz, RT) of compound **6a** in $CDCl_3$.

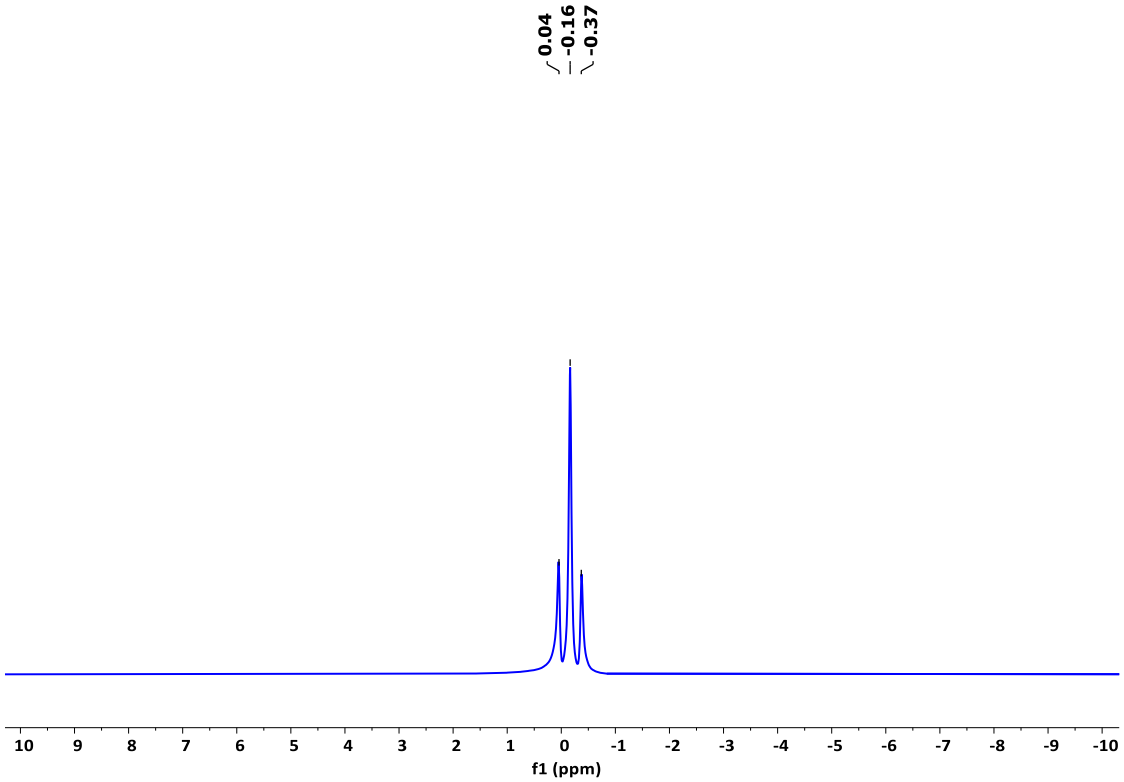

Figure S27. $^{11}B\{^{1}H\}$ NMR spectrum (160.4 MHz, RT) of compound **6a** in $CDCl_3$.

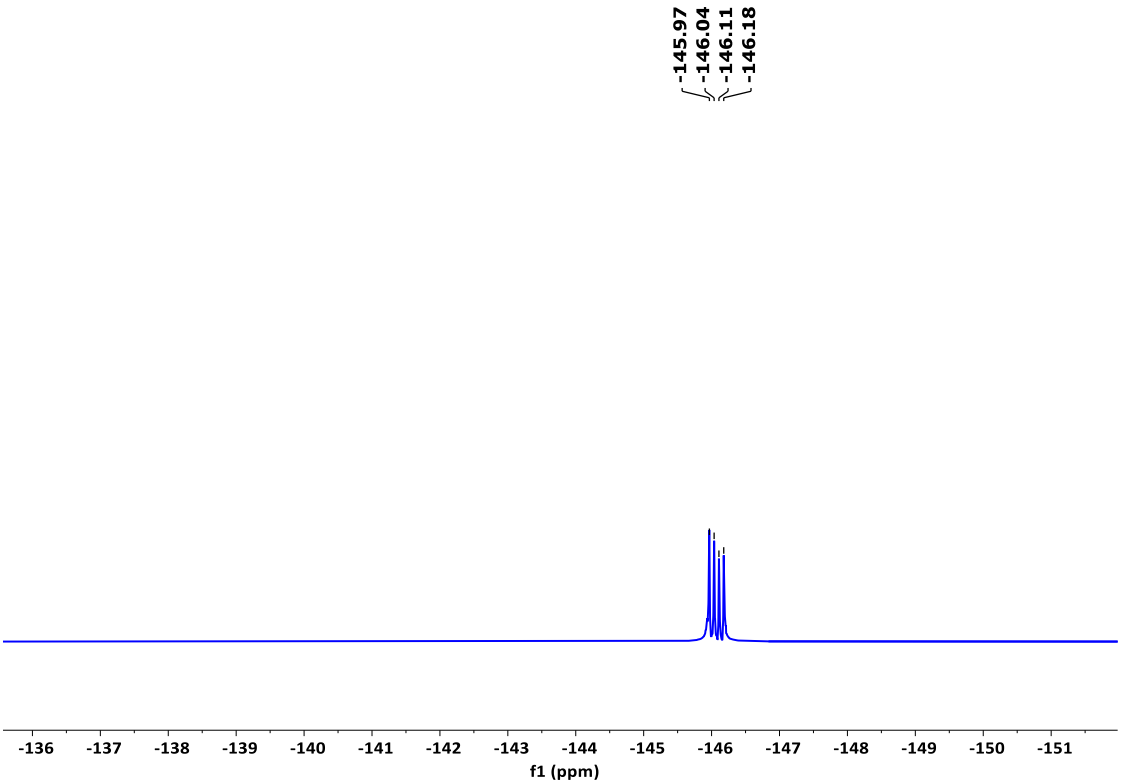

Figure S28. $^{19}F\{^{1}H\}$ NMR spectrum (471 MHz, RT) of compound **6a** in $CDCl_3$.

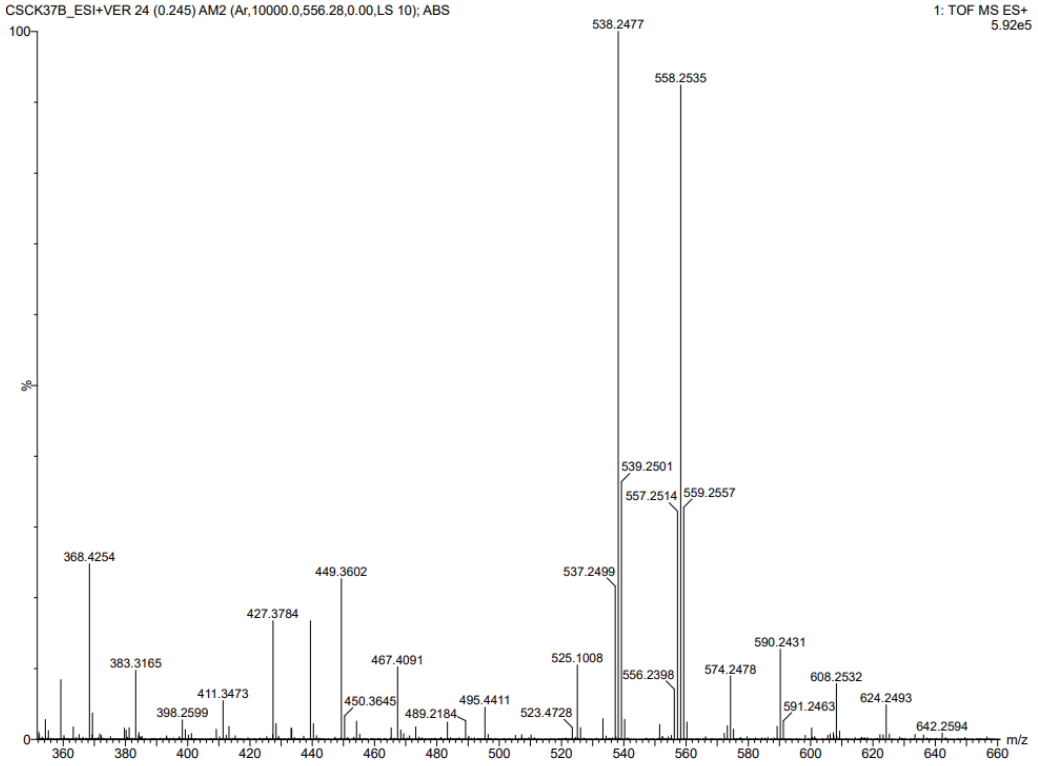

Figure S29. HRMS spectrum of compound **6a**.

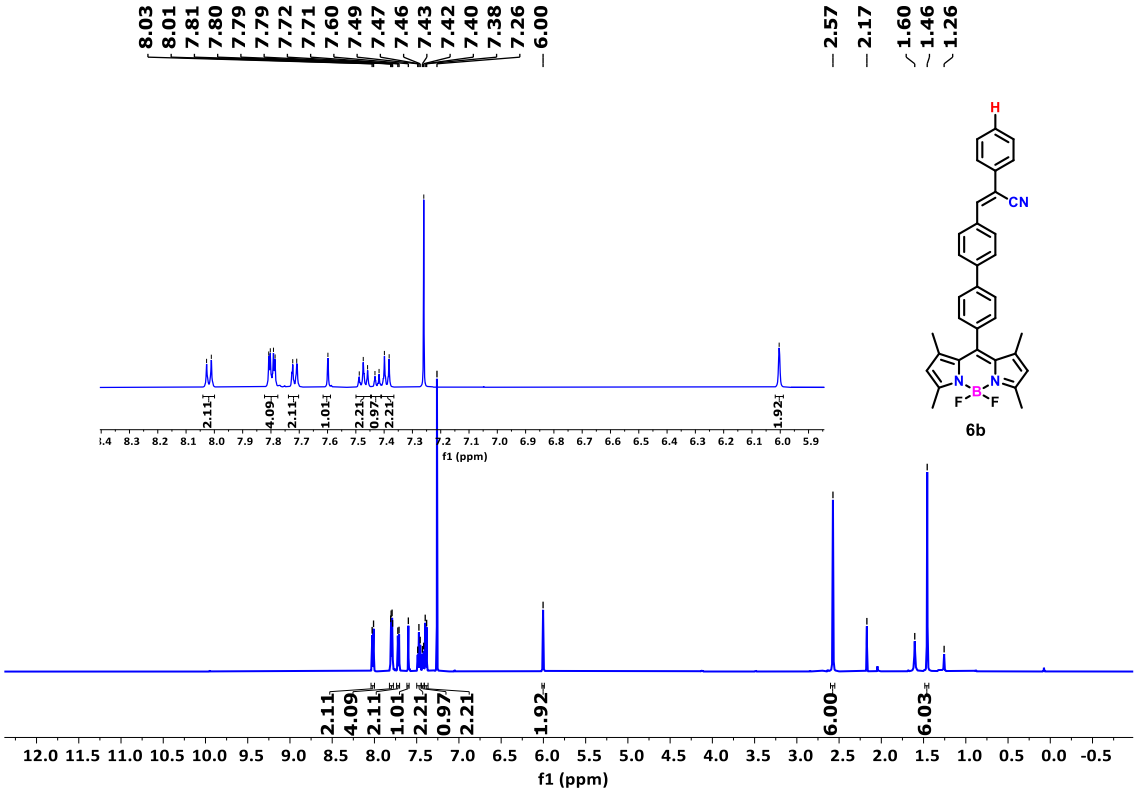

Figure S30. ^{1}H NMR spectrum (500 MHz, RT) of compound **6b** in $CDCl_3$.

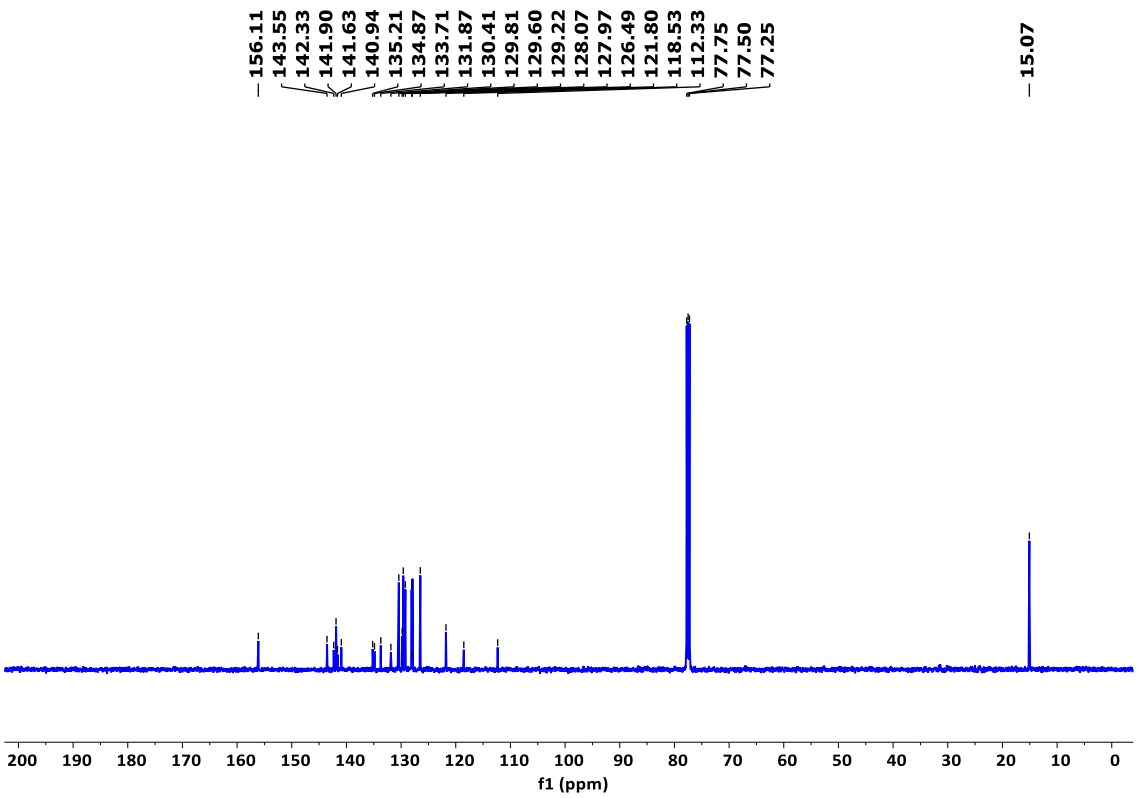

Figure S31. $^{13}C\{^{1}H\}$ NMR spectrum (126 MHz, RT) of compound **6b** in $CDCl_3$.

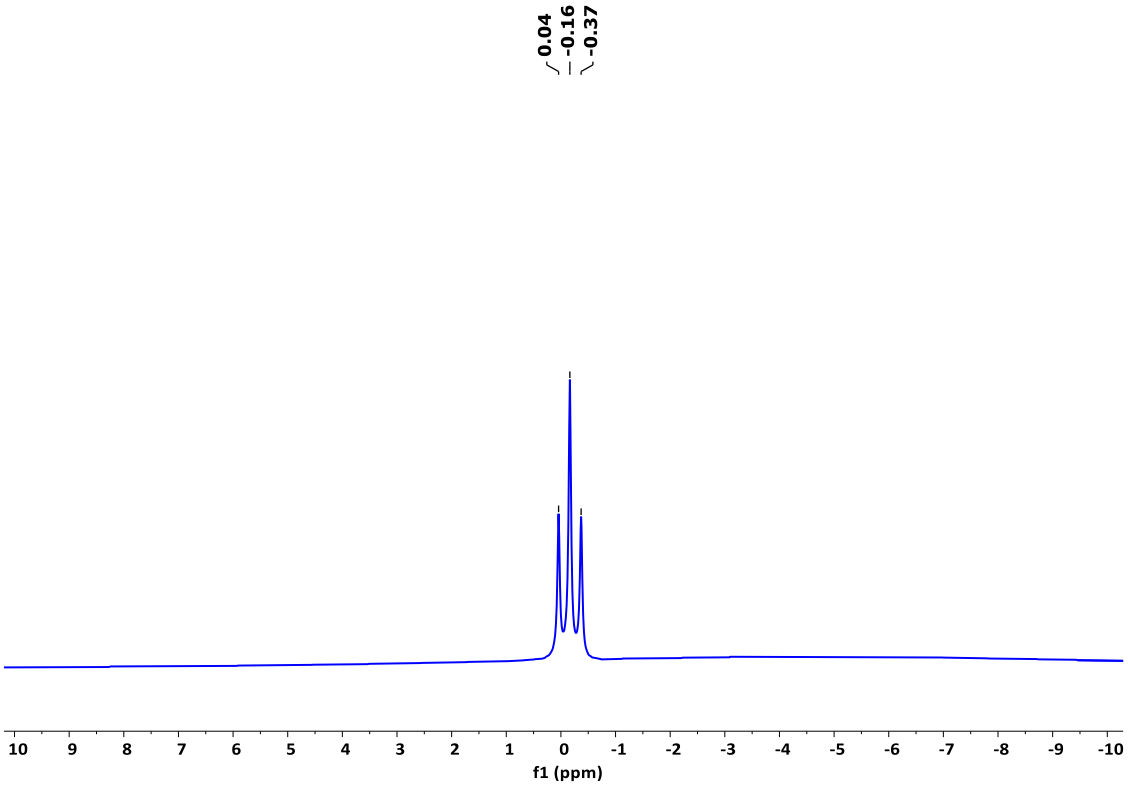

Figure S32. $^{11}B\{^{1}H\}$ NMR spectrum (160.4 MHz, RT) of compound **6b** in $CDCl_3$.

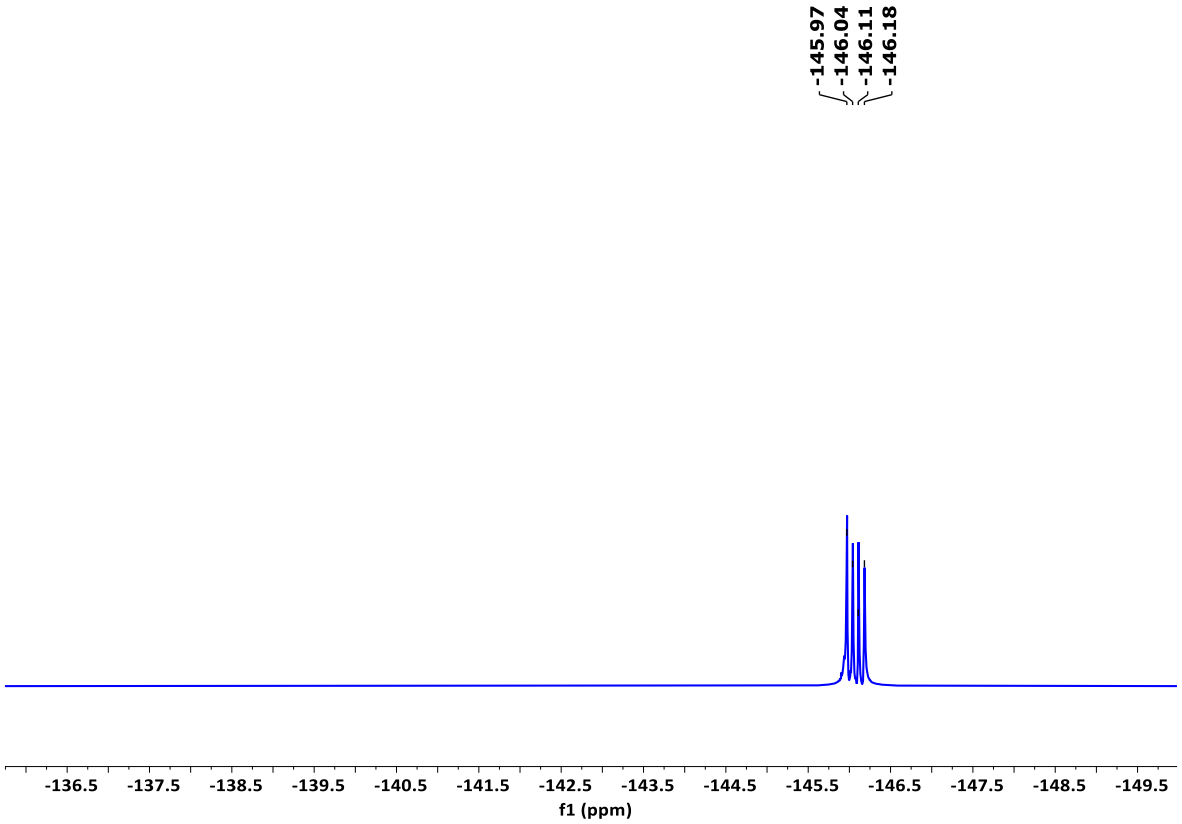

Figure S33. $^{19}F\{^{1}H\}$ NMR spectrum (471 MHz, RT) of compound **6b** in $CDCl_3$.

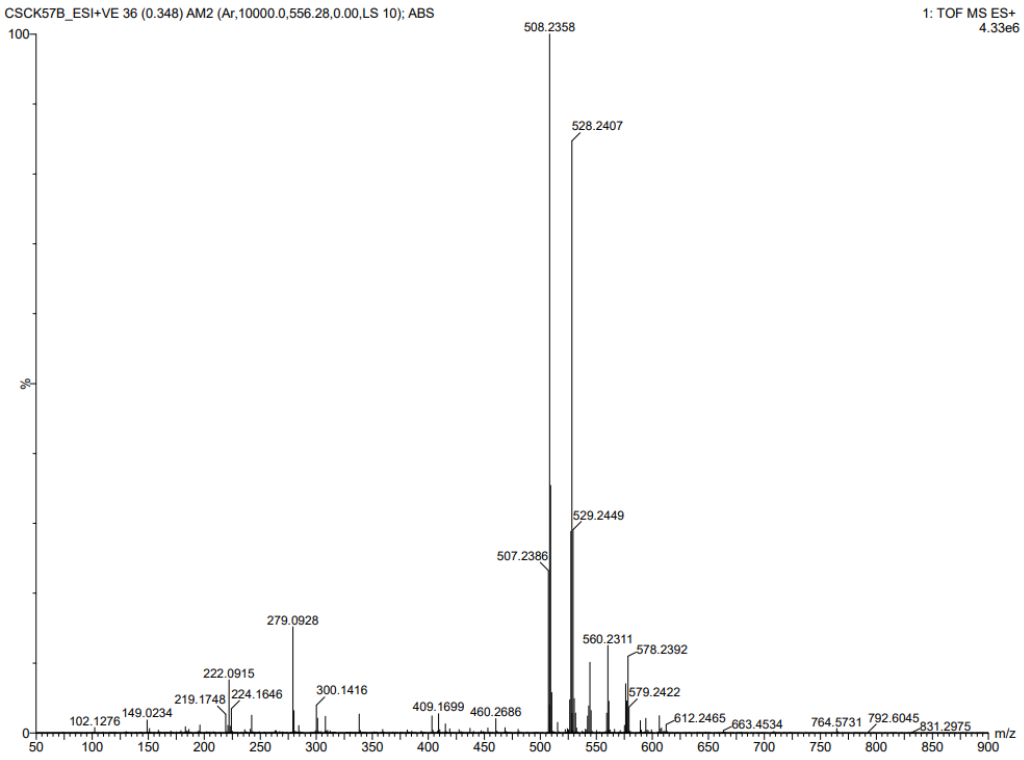

Figure S34. HRMS spectrum of compound **6b**.

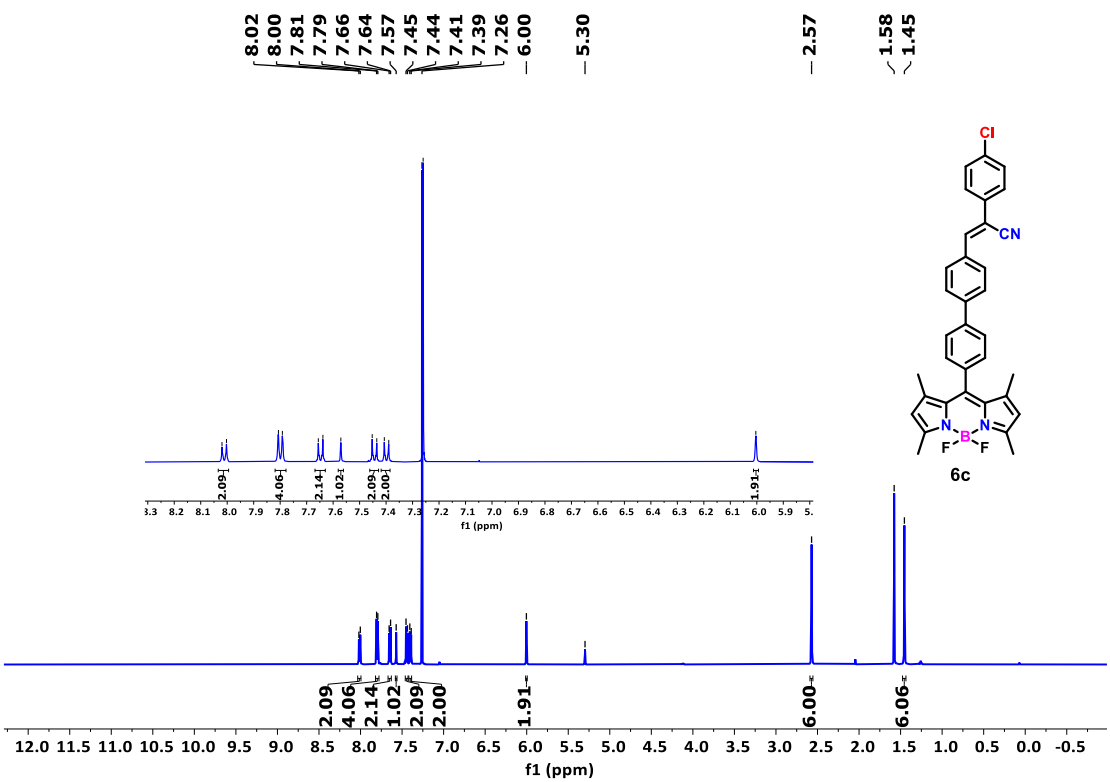

Figure S35. ^{1}H NMR spectrum (500 MHz, RT) of compound **6c** in $CDCl_3$.

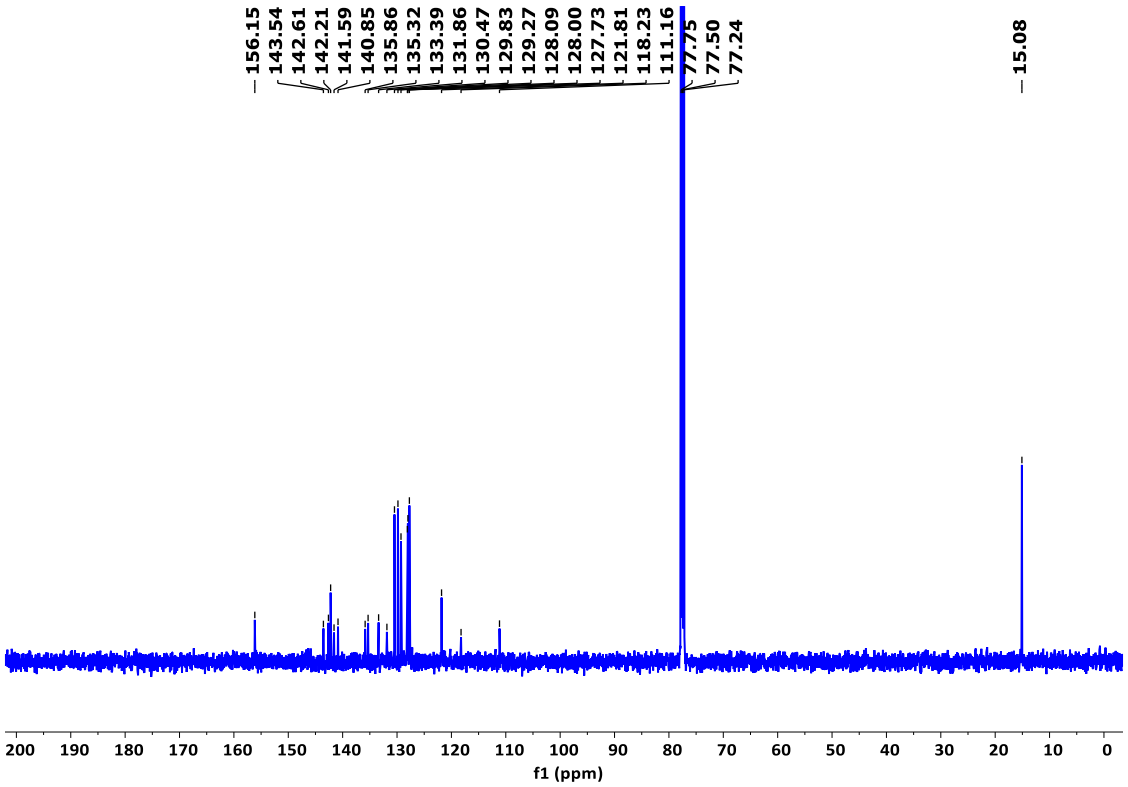

Figure S36. $^{13}C\{^{1}H\}$ NMR spectrum (126 MHz, RT) of compound **6c** in $CDCl_3$.

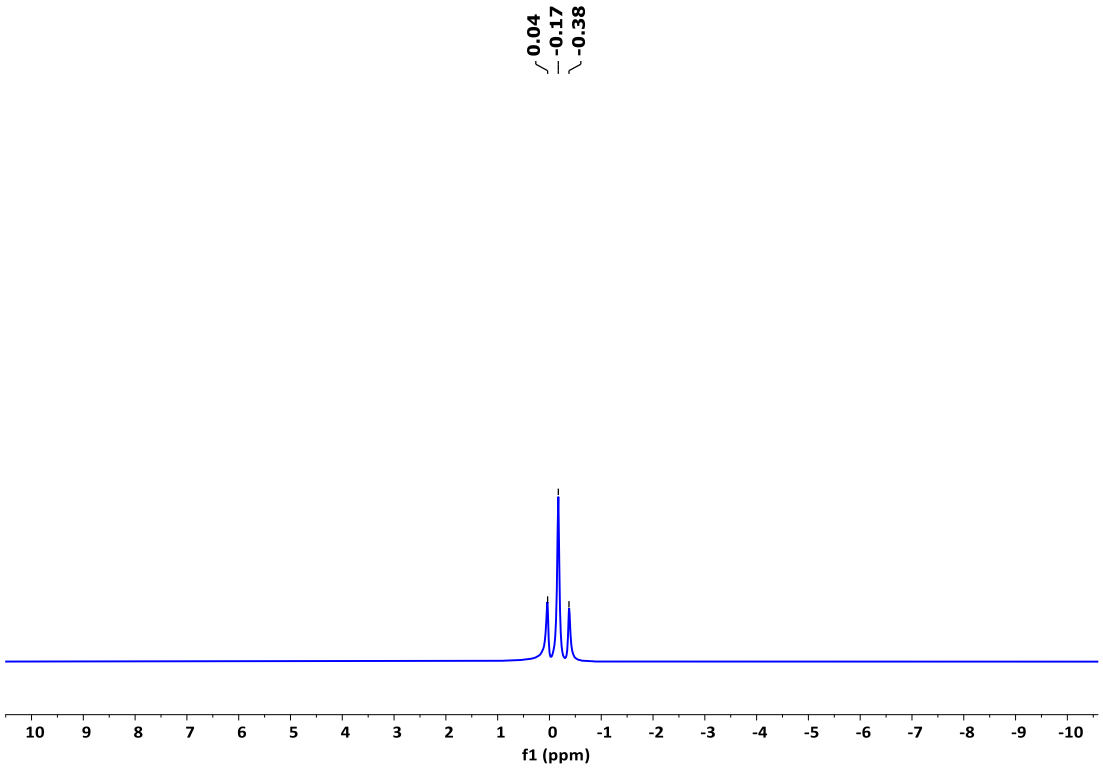

Figure S37. $^{11}B\{^{1}H\}$ NMR spectrum (160.4 MHz, RT) of compound **6c** in $CDCl_3$.

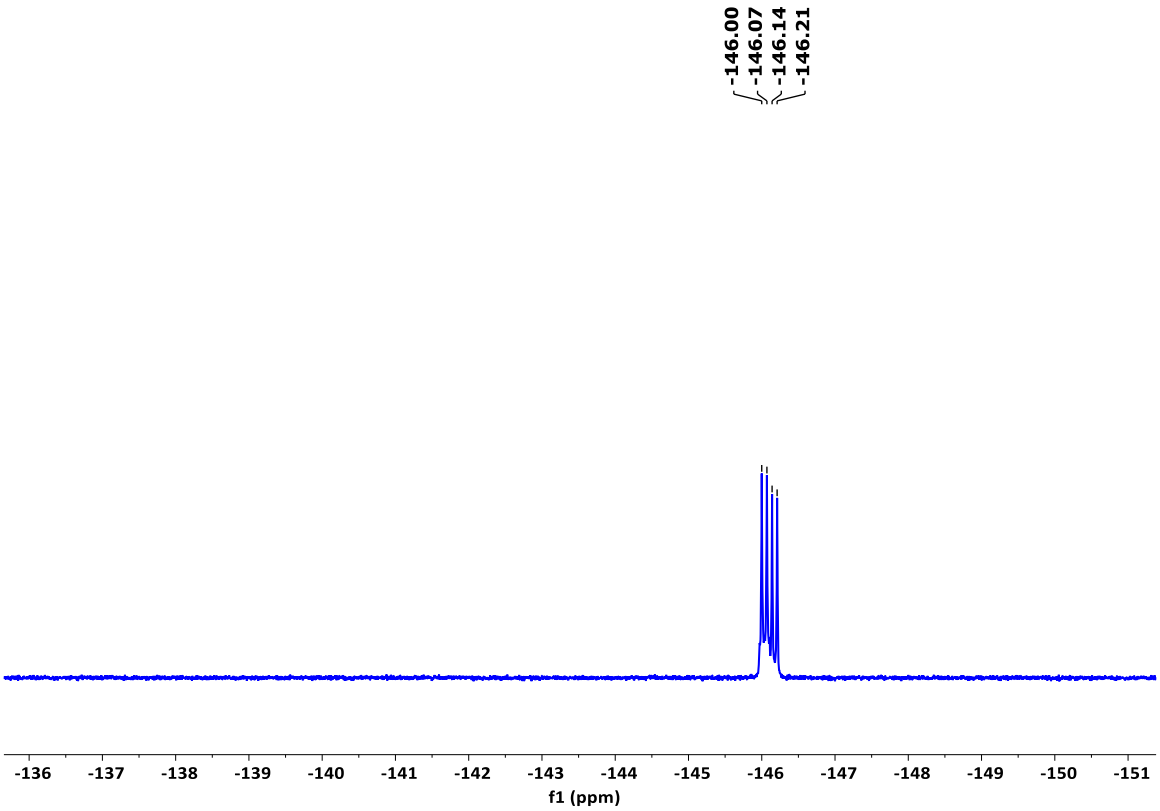

Figure S38. $^{19}F\{^{1}H\}$ NMR spectrum (471 MHz, RT) of compound **6c** in $CDCl_3$.

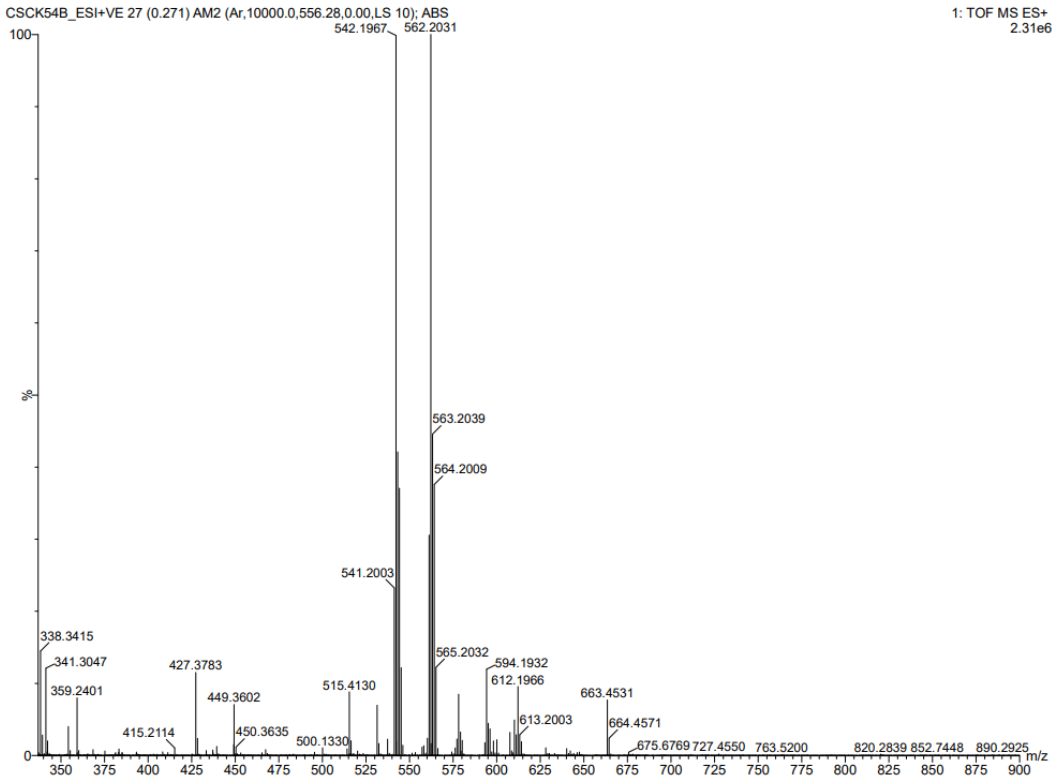

Figure S39. HRMS spectrum of compound **6c**.

4. Photophysical studies of the target molecules

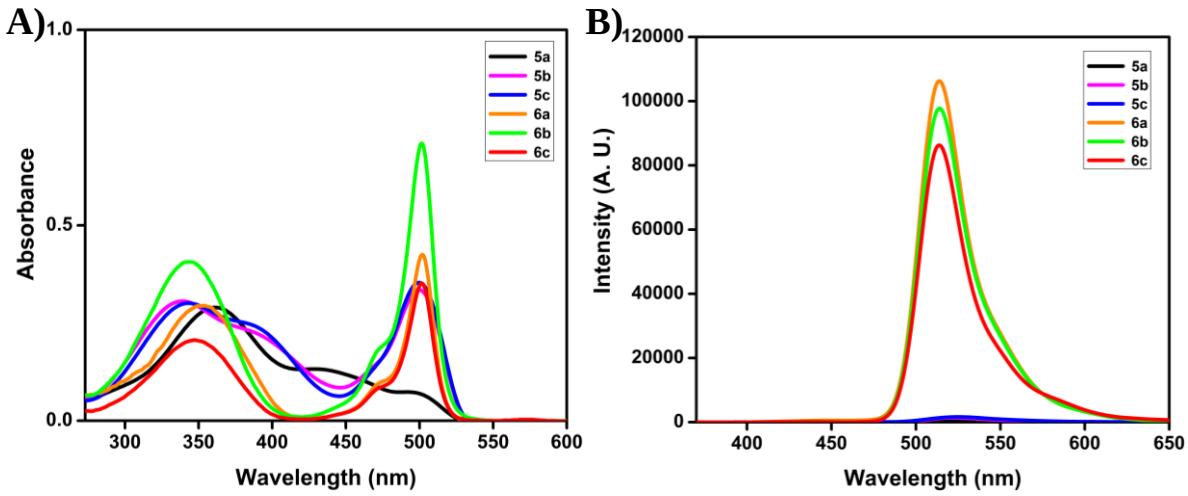

Figure S40. A) UV-Vis absorption (10 μM) and B) emission spectra of compounds **5a-c** and **6a-c** in DCM (2 μM, λ_{ex} = 350 nm).

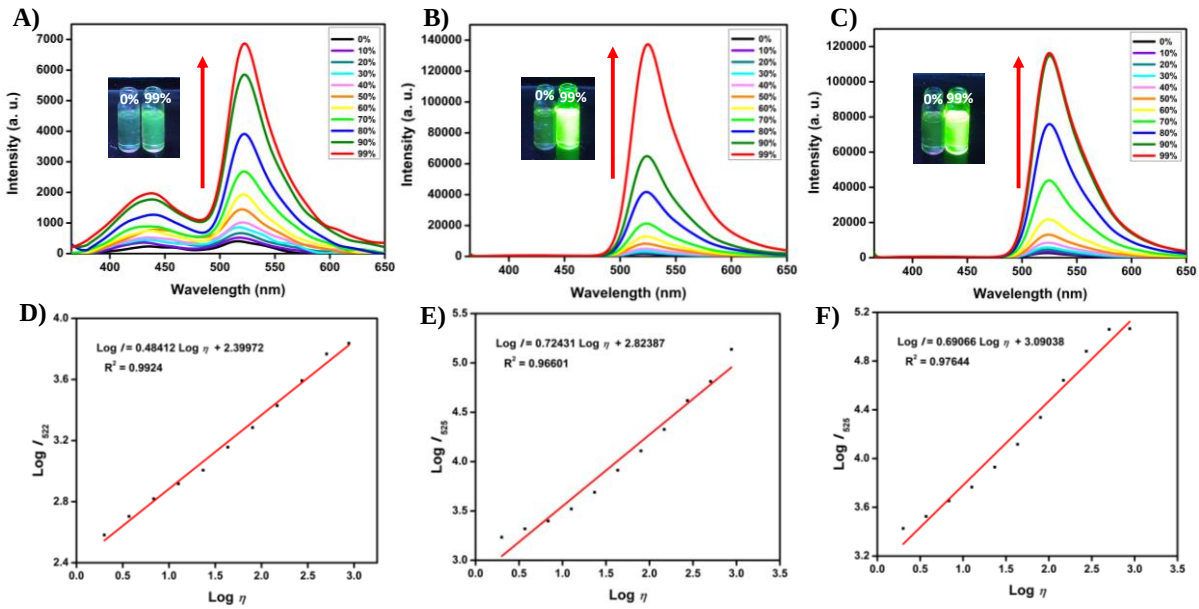

Figure S41. Emission spectra of compounds **5a** (A), **5b** (B), **5c** (C), in DMSO-Glycerol mixtures with increasing concentration of glycerol from 0% to 99% (10 μM, λ_{ex} = 350 nm). Inset photos taken under a UV 365 nm lamp are displayed on the top of the spectra. Linear relationship between Log *I* (fluorescence intensity) and Log η (viscosity) of compounds **5a** (D), **5b** (E), **5c** (F).

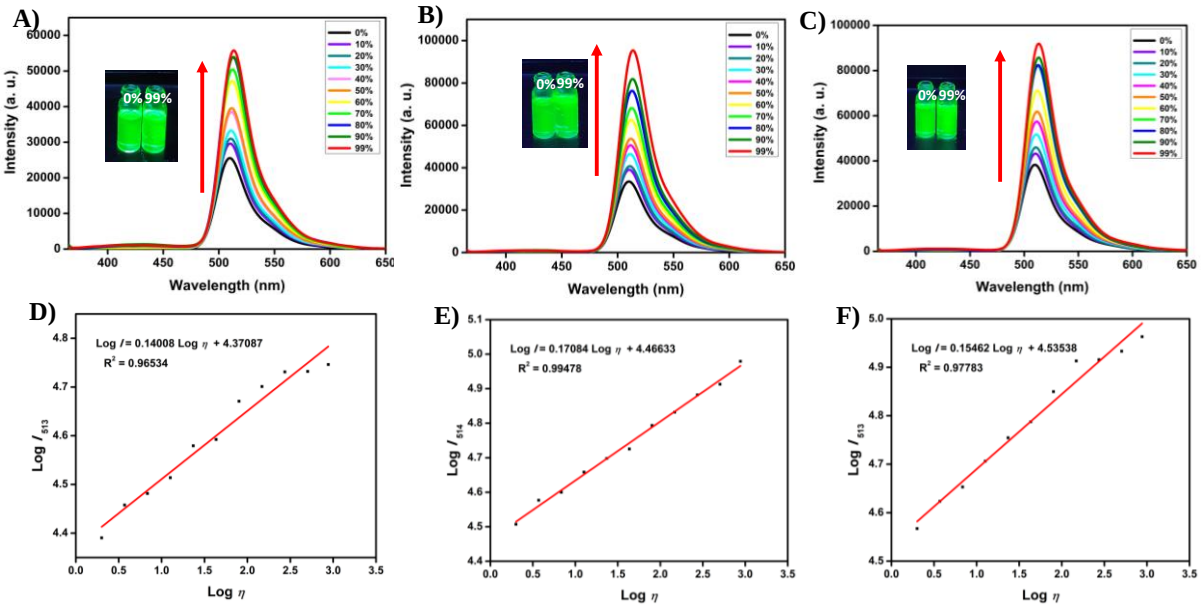

Figure S42. Emission spectra of compounds **6a** (A), **6b** (B), **6c** (C), in DMSO-Glycerol mixtures with increasing concentration of glycerol from 0% to 99% (1 μM, λ_{ex} = 350 nm). Inset photos taken under a UV 365 nm lamp are displayed on the top of the spectra. Linear relationship between Log *I* (fluorescence intensity) and Log η (viscosity) of compounds **6a** (D), **6b** (E), **6c** (F).

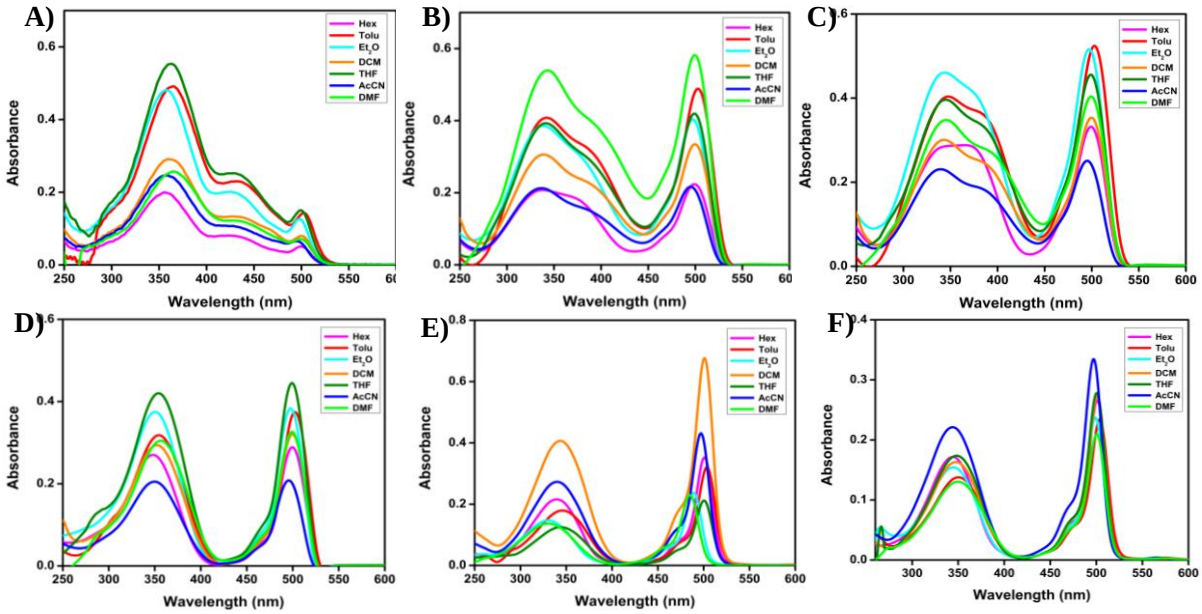

Figure S43. UV-Vis absorption spectra of compounds A) **5a**, B) **5b**, C) **5c**, D) **6a**, E) **6b**, F) **6c** in solvents of different polarity (10 μM).

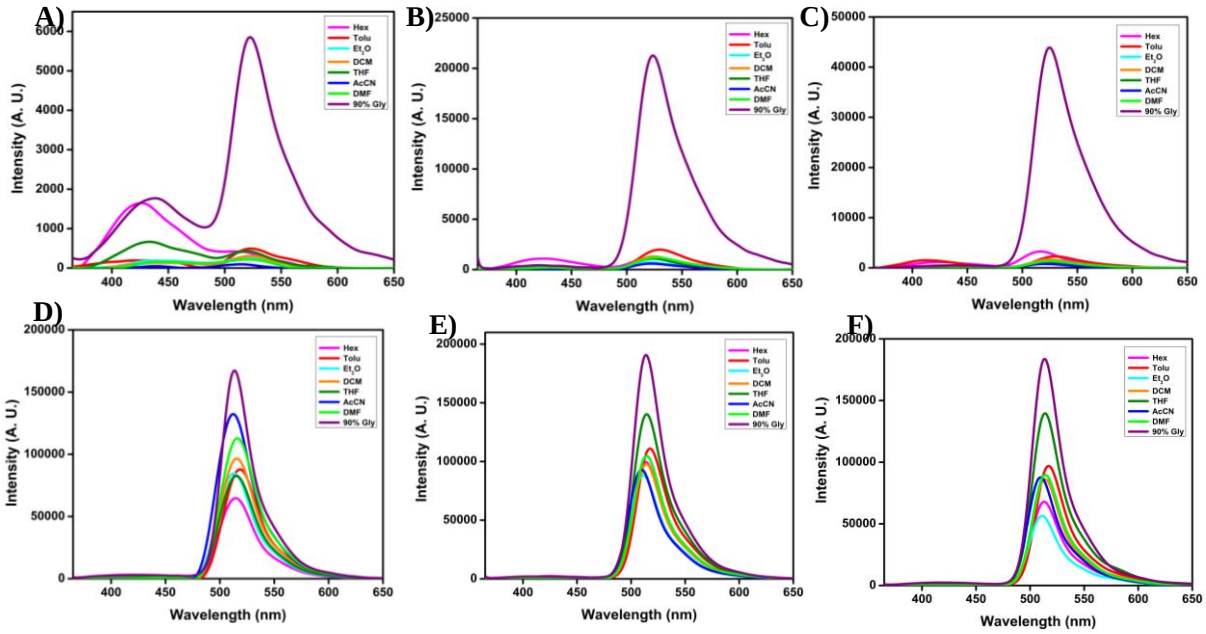

Figure S44. Emission spectra of compounds A) **5a**, B) **5b**, C) **5c**, D) **6a**, E) **6b**, F) **6c** in solvents of different polarity (2 μM, λ_{ex} = 350 nm).

Compounds	**Solvents**	λ_{max} (nm)	λ_{max} (nm)	**Δν** (cm^{-1})	**Φ**
5a	Hex	500	518	695	15
	Toluene	502	523	800	10
	Et_2O	498	518	775	08
	DCM	499	522	883	06
	THF	500	520	769	05
	AcCN	495	514	747	03
	DMF	500	521	806	03
5b	Hex	499	521	846	17
	Toluene	503	530	1013	13
	Et_2O	497	522	964	10
	DCM	500	524	916	07
	THF	499	524	956	05
	AcCN	495	522	1045	05
	DMF	500	527	1025	06
5c	Hex	499	517	698	21
	Toluene	503	530	1013	16
	Et_2O	497	522	964	14
	DCM	500	525	952	10
	THF	499	524	956	08
	AcCN	495	521	1008	07
	DMF	500	526	989	09
6a	Hex	499	514	585	58
	Toluene	502	518	615	51
	Et_2O	498	513	587	54
	DCM	499	515	623	50
	THF	499	515	623	56

	AcCN	496	512	630	48
	DMF	499	516	660	52
6b	Hex	501	513	467	62
	Toluene	503	517	538	52
	Et_2O	499	511	471	55
	DCM	501	514	505	50
	THF	500	514	545	62
	AcCN	497	510	513	52
	DMF	500	514	545	46
6c	Hex	501	513	467	68
	Toluene	503	517	538	60
	Et_2O	499	511	471	59
	DCM	501	514	505	54
	THF	500	514	545	69
	AcCN	497	510	513	48
	DMF	500	514	545	44

Table S1: Photophysical characteristics of compounds **5a-c** and **6a-c** in solvents of different polarity.

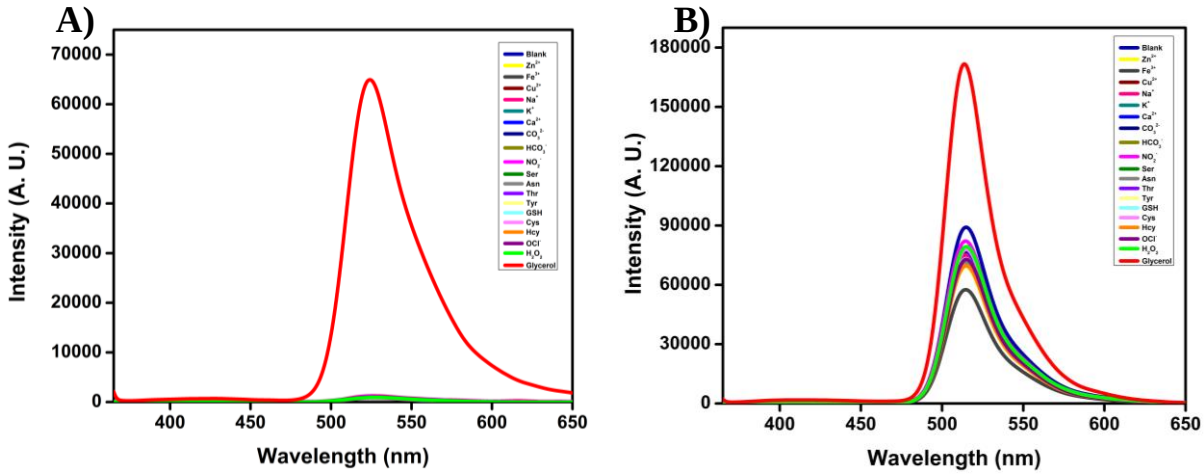

Figure S45. Fluorescence spectra of compounds (A) **5b** (2 μM, λ_{ex} = 350 nm) and (B) **6b** (2 μM, λ_{ex} = 350 nm), in DMSO with various analytes (100 μM) (Blank, $Zn(OAc)_2$, $FeCl_3$, $Cu(OAc)_2$, NaCl, KCl, $CaCl_2$, K_2CO_3, $NaHCO_3$, $NaNO_2$, Ser, Asn, Thr, Tyr, GSH, Cys, Hcy, OCl^-, H_2O_2, and Glycerol.

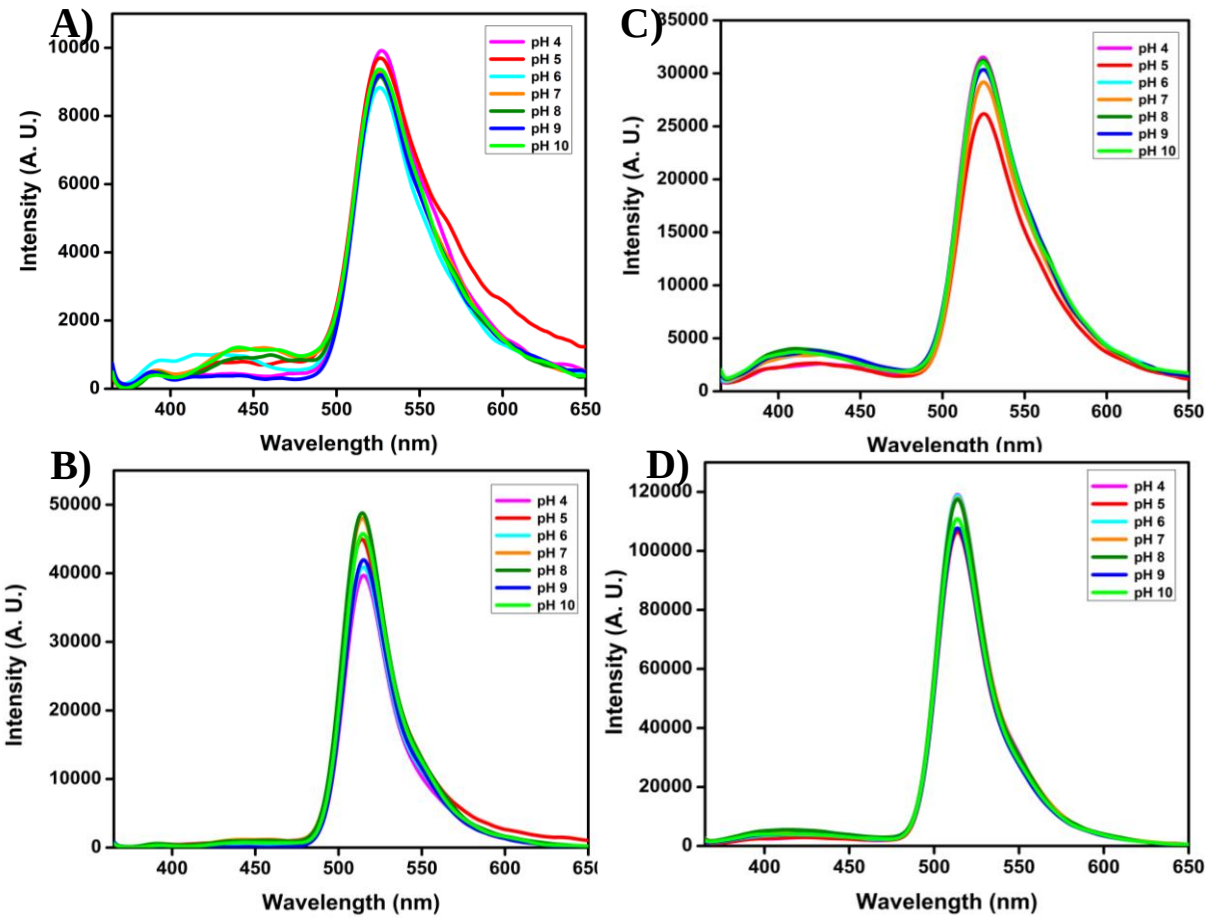

Figure S46. Fluorescence spectra of compounds **5b** (2 μM, λ_{ex} = 350 nm) at different pH values (4-10) with different viscous solutions DMSO (A) and DMSO:Glycerol= 1:1 (C). Fluorescence spectra of compounds **6b** (2 μM, λ_{ex} = 350 nm) at different pH values (4-10) with different viscous solutions DMSO (B) and DMSO:Glycerol= 1:1 (D).

5. DFT and TD-DFT Calculations

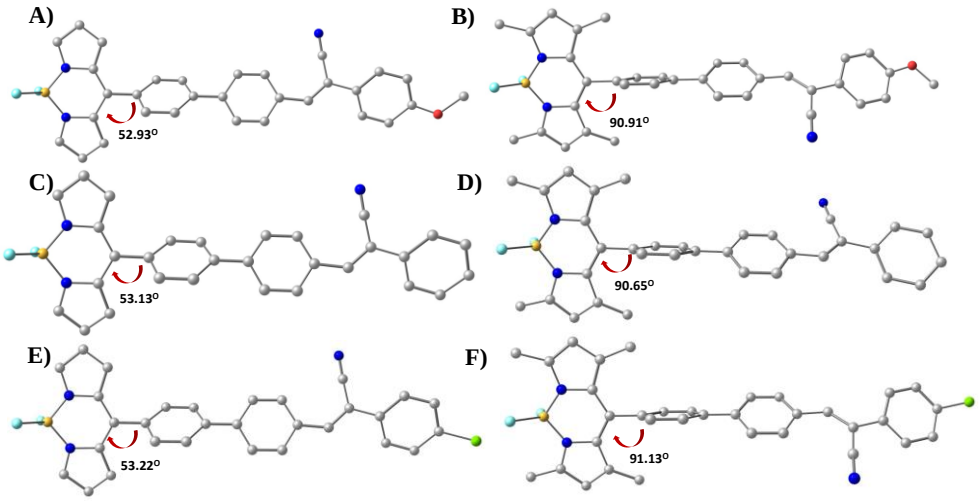

Figure S47. Optimized geometries of compounds **5a** (A), **5b** (C), **5c** (E), **6a** (B), **6b** (D), and **6c** (F).

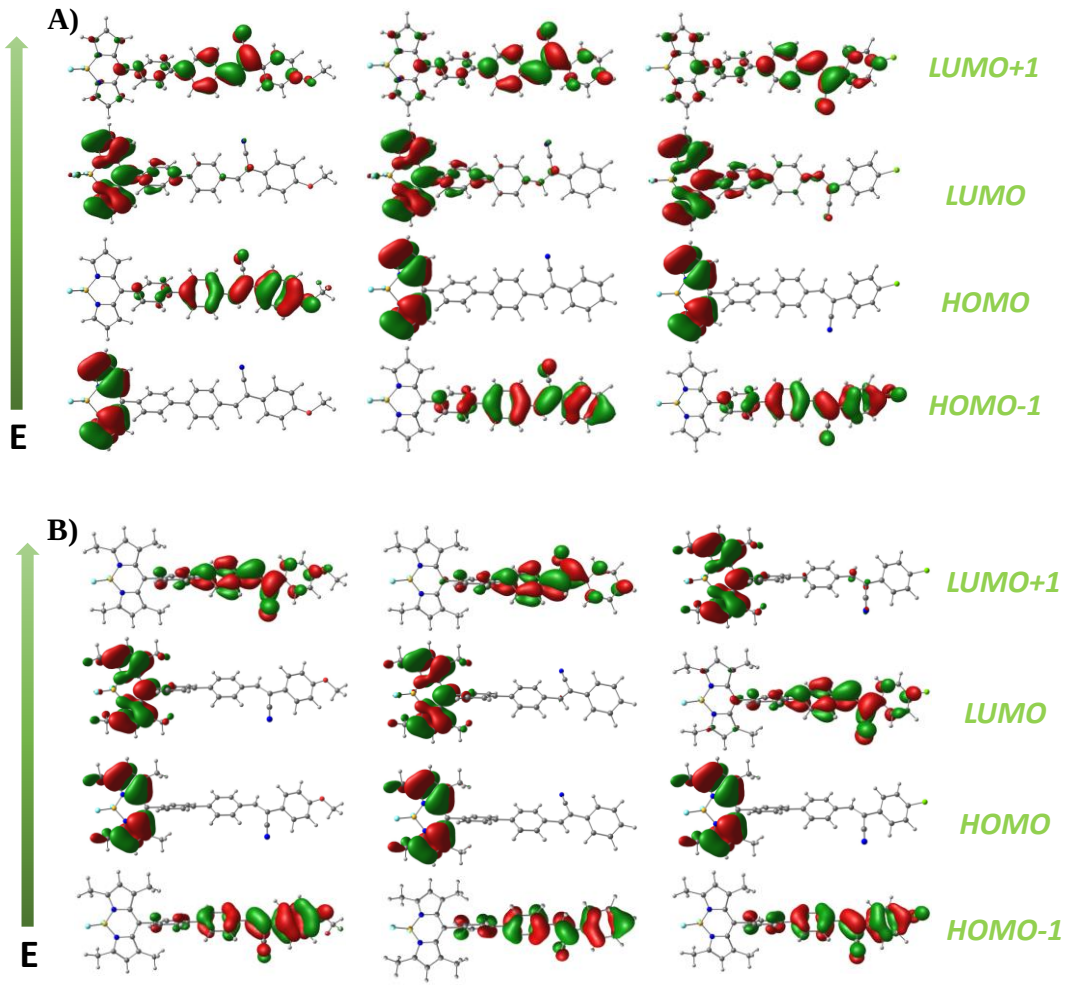

Figure S48: Frontier molecular orbitals (MOs) involved in the UV-vis absorptions (vertical excitation) of compounds A) **5a-c** and B) **6a-c**. Calculations were based on the optimized ground state geometry at the B3LYP/6-31G(d,p) level with Gaussian 09.

Compound	HOMO-1 (eV)	HOMO (eV)	LUMO (eV)	LUMO+1 (eV)	HOMO-LUMO (eV)
5a	-5.8935	-5.7718	-2.8624	-2.2256	2.91
5b	-6.1033	-5.9259	-2.9033	-2.3434	3.02
5c	-6.1908	-5.9616	-2.9517	-2.4829	3.01
6a	-5.7190	-5.3642	-2.3694	-2.2144	2.99
6b	-6.0415	-5.3935	-2.4013	-2.3366	2.99
6c	-6.1315	-5.4269	-2.4929	-2.4306	2.93

Table S2: DFT data of compounds **5a-c** and **6a-c**. Calculations were based on the optimized ground state geometry at the B3LYP/6-31G(d,p) level with Gaussian 09.

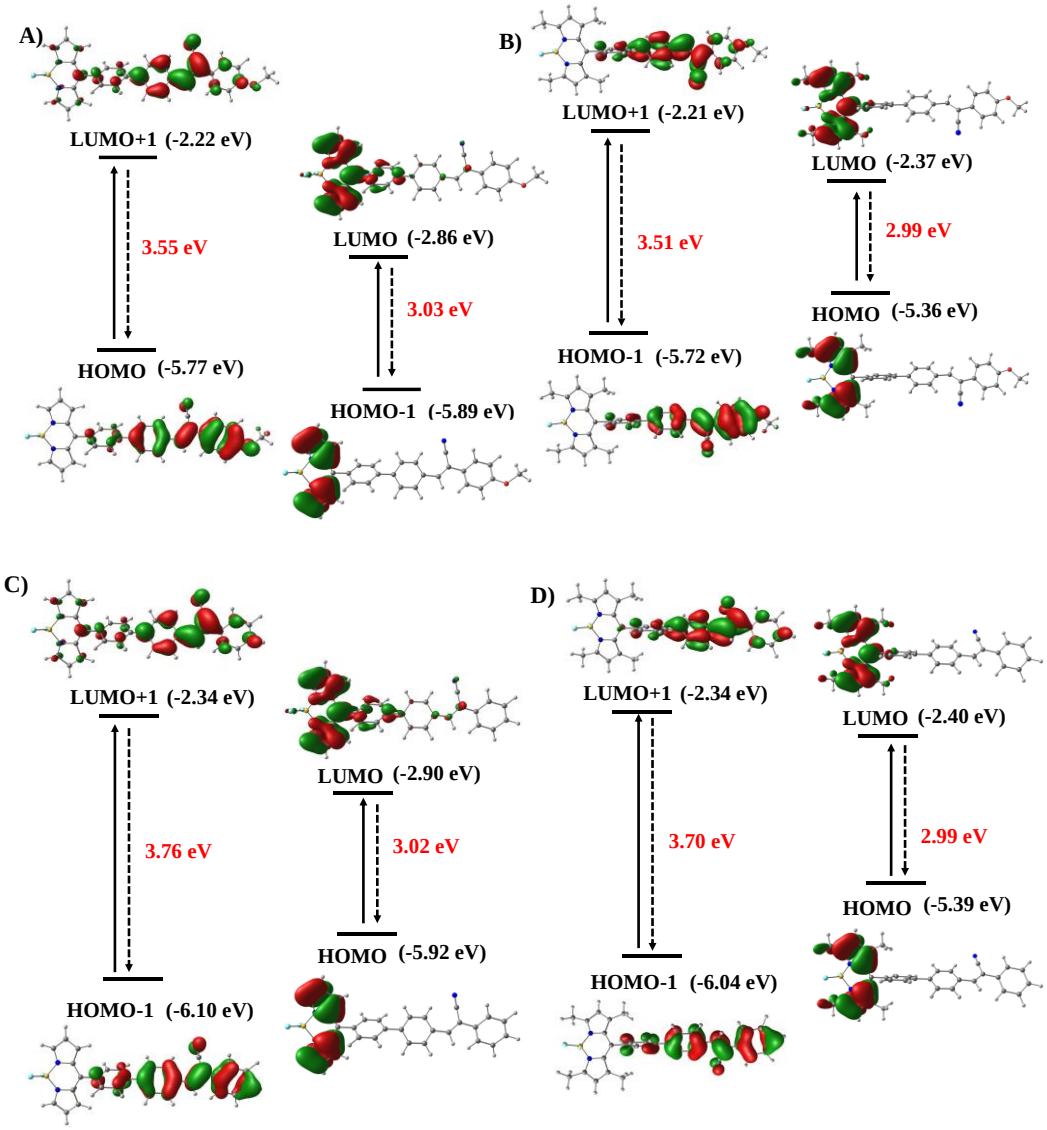

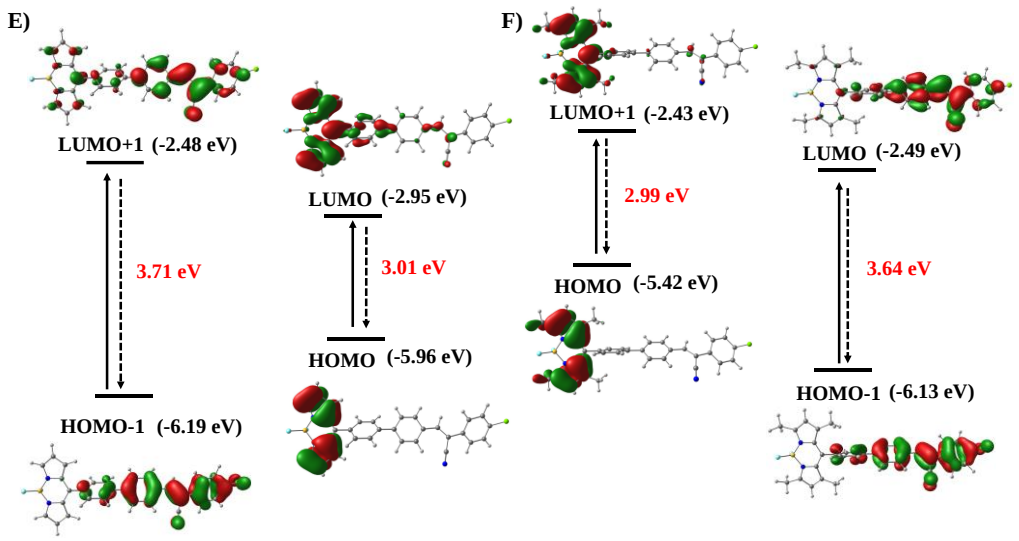

Figure S49: Important frontier molecular orbitals (MOs) and electronic transitions involved in the UV-vis absorptions (vertical excitation) of compounds **5a** (A), **5b** (C), **5c** (E), **6a** (B), **6b** (D), and **6c** (F)**.** Calculations were based on the optimized ground state geometry at the B3LYP/6-31G(d,p) level with Gaussian 09.

Compound	Electronic[a] transitions	TDDFT/6-31G(d,p)		
		Excitation energy	f[b]	Composition[c]
5a	$S_0 \rightarrow S_3$	3.28 eV (377 nm)	1.1914	H → L+1
	$S_0 \rightarrow S_1$	3.62 eV (473 nm)	0.3538	H → L
	$S_0 \rightarrow S_2$	3.01 eV (412 nm)	0.2503	H-1 → L
5b	$S_0 \rightarrow S_4$	3.50 eV (354 nm)	1.1512	H-1 → L+1
	$S_0 \rightarrow S_1$	2.86 eV (434 nm)	0.4564	H-1 → L
	$S_0 \rightarrow S_2$	2.99 eV (415 nm)	0.2268	H → L
5c	$S_0 \rightarrow S_4$	3.45 eV (360 nm)	1.1188	H-1 → L+1
	$S_0 \rightarrow S_1$	2.90 eV (428 nm)	0.5562	H-1 → L
	$S_0 \rightarrow S_2$	2.96 eV (419 nm)	0.1815	H → L
6a	$S_0 \rightarrow S_4$	3.45 eV (360 nm)	1.3696	H-1 → L+1
	$S_0 \rightarrow S_2$	3.03 eV (409 nm)	0.4609	H → L
6b	$S_0 \rightarrow S_5$	3.24 eV (383 nm)	1.4803	H-1 → L+1
	$S_0 \rightarrow S_2$	3.03 eV (409 nm)	0.4620	H → L
6c	$S_0 \rightarrow S_4$	3.38 eV (367 nm)	1.4759	H-1 → L
	$S_0 \rightarrow S_2$	3.03 eV (410 nm)	0.4621	H → L+1

Table S3: Selected Parameters for the UV−vis Absorptions (excitations) of the compounds **5a-c** and **6a-c**: the electronic excitation energies (eV), oscillator strengths (f), and the major configurations of the excited states. Calculations are based on the optimized ground-state geometries at the TDDFT/B3LYP/6-31G(d,p) level with Gaussian 09. (Conditions: [a]Only specific excited states were taken into account, [b]Oscillator strength, [c]H stands for HOMO and L stands for LUMO)

6. Cytotoxicity assay

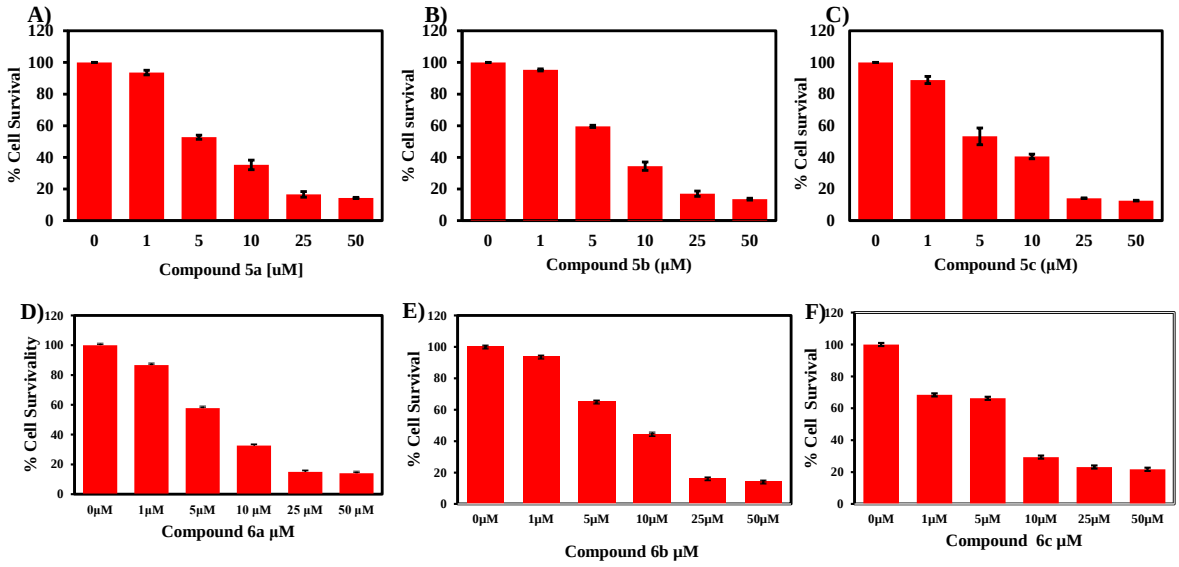

Figure S50. Cytotoxicity data of compounds A) **5a**, B) **5b**, C) **5c**, D) **6a**, E) **6b**, F) **6c** in HeLa cells.

7. Co-localization imaging

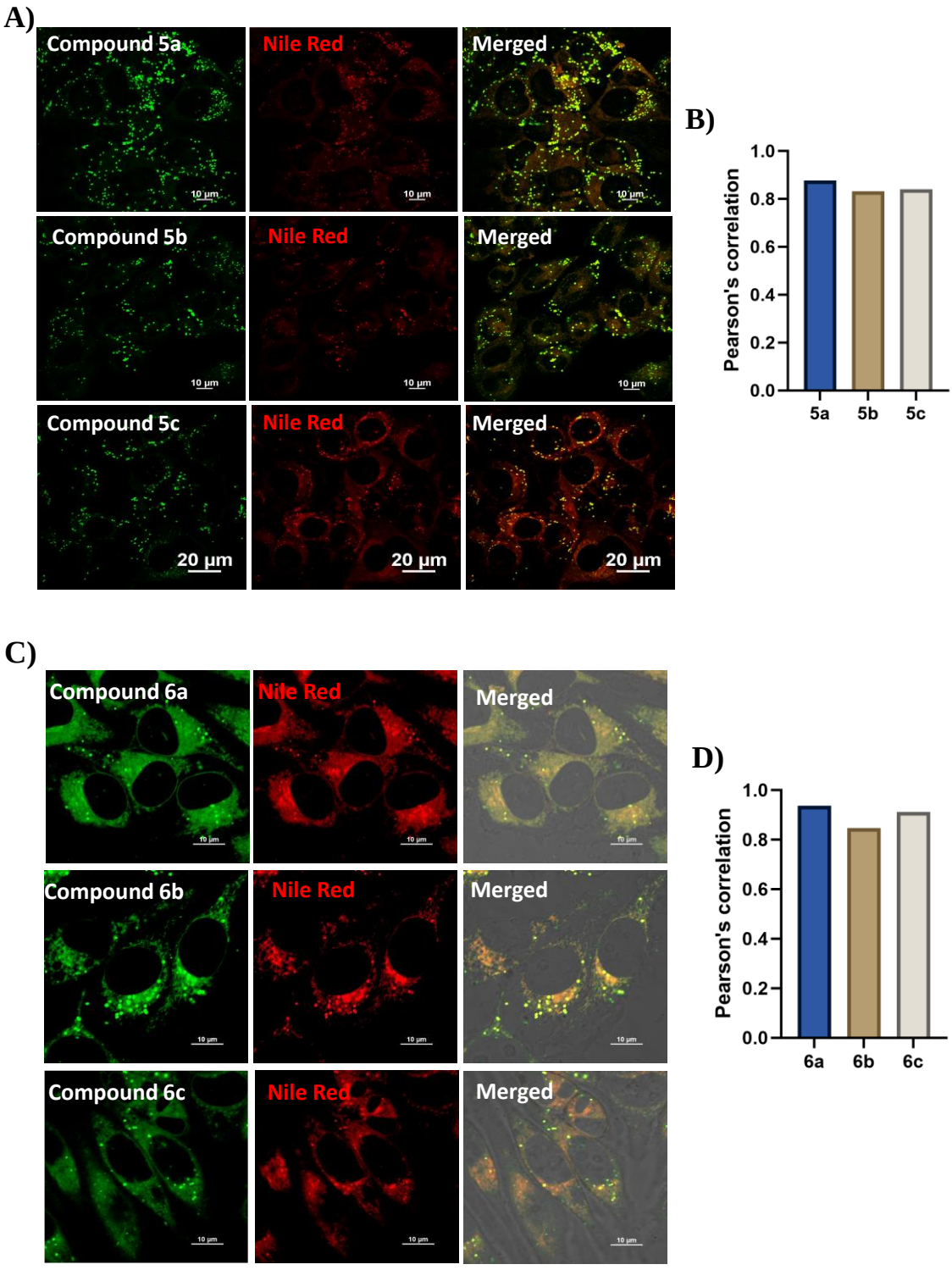

Figure S51. Confocal fluorescence microscopy images of intracellular co-localization in HeLa cells. Cells were incubated with compounds **5a-c** (A) and **6a-c** (C) (500 nM) (left), commercially available lipid droplet staining Nile Red (middle), and the merged images (right). Pearson's correlation of compounds **5a-c** (B) and **6a-c** (D).

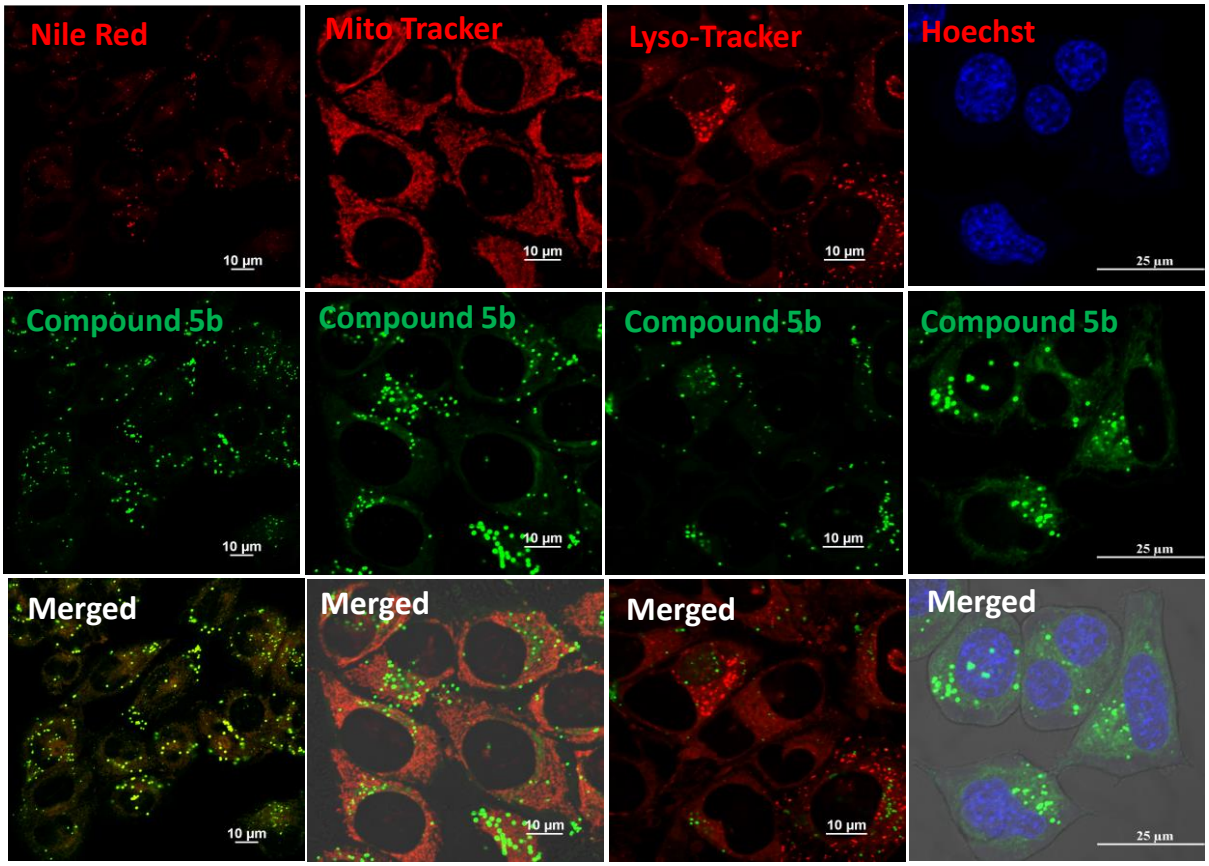

Figure S52. Confocal fluorescence microscopy images of intracellular co-localization in HeLa cells. Cells were incubated with compound **5b**, and commercially available fluorophores such as lipid droplet staining Nile Red, Mitochondria targeting Mito-Tracker, Lysosome targeting Lyso-Tracker, Nucleus-staining Hoechst. From top to bottom are commercial dyes, compound **5b**, and merged channel.

8. Photostability

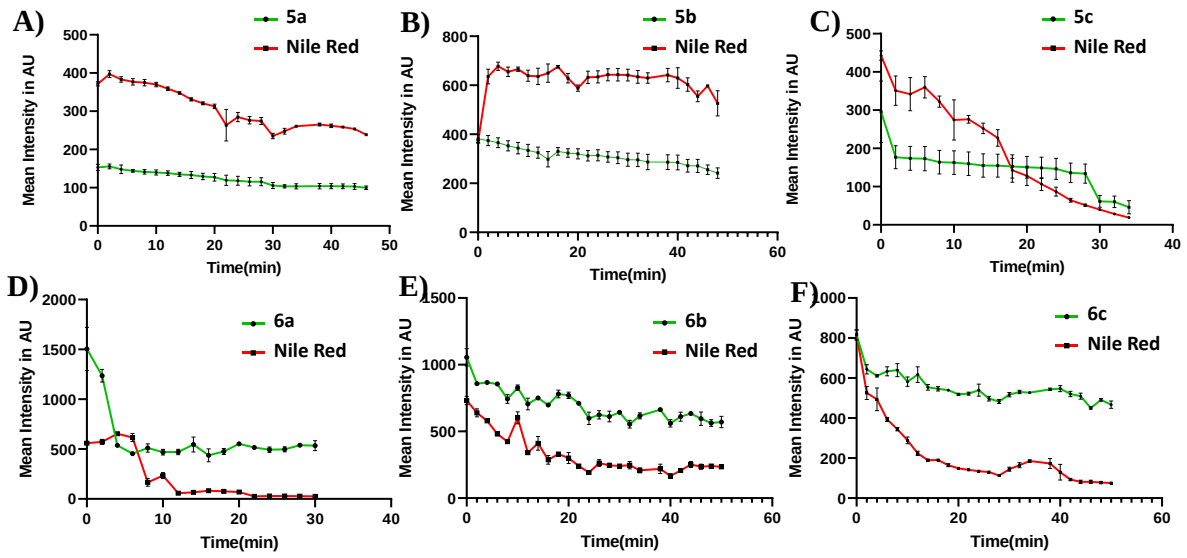

Figure S53. Photostability of probes. The mean fluorescence intensity of probes A) **5a**, B) **5b**, C) **5c**, D) **6a**, E) **6b**, and F) **6c** at different times under continuous irradiation with laser (488 nm).

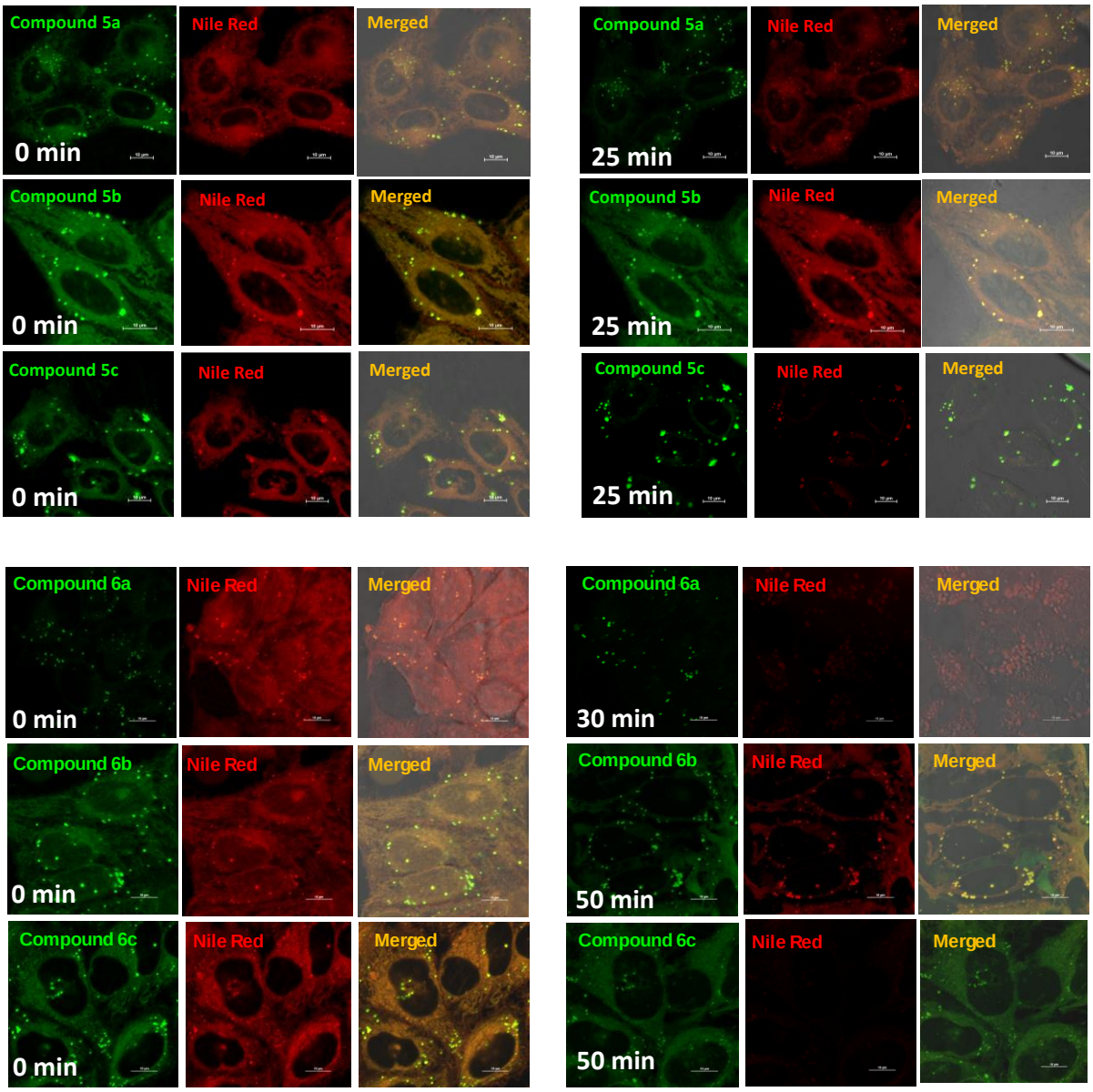

Figure S54. Photostability of probes. Confocal fluorescence microscopy images of HeLa cells incubated with compounds **5a-c** and **6a-c** (500 nM) (left), commercially available lipid droplet staining Nile Red (middle), and the merged images (right) under continuous irradiation with laser (488 nm).

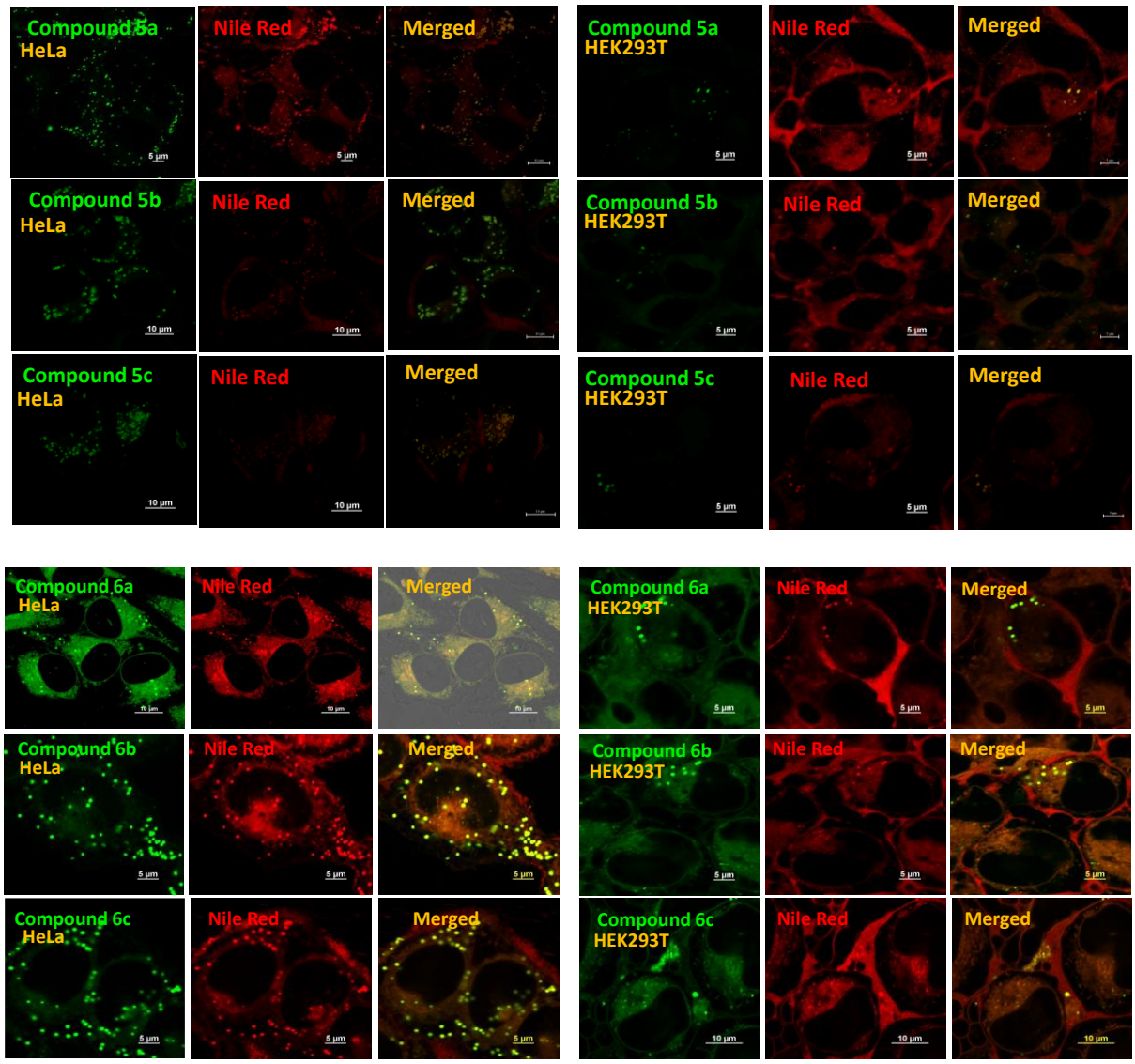

Figure S55. Confocal fluorescence microscopy images of different living cells incubated with compounds **5a-c** and **6a-c** (500 nM) (left), commercially available lipid droplet staining Nile Red (middle), and the merged images (right) including normal cells (HEK293T) and cancer cells (HeLa).

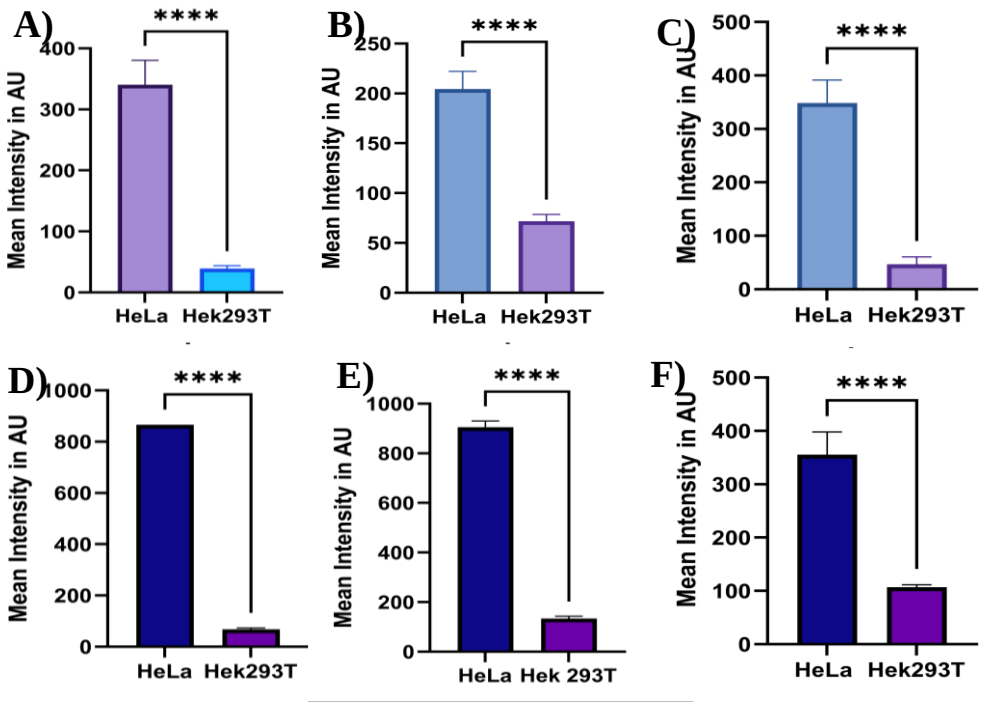

Figure S56. Quantitative changes in the fluorescence intensities of compounds **5a** (A), **5b** (B), **5c** (C), **6a** (D), **6b** (E), and **6c** (F) in cancer cells and normal cells.

9. DFT Calculations

Table S4: The coordinates of compounds **5a** (DFT/B3LYP/6-31G(d,p) level with Gaussian 09)

5	8.241344721	0.014930174	-0.154838733
6	7.628967367	2.530015817	-0.177087938
6	6.489134072	3.355865506	-0.247043628
6	5.385126818	2.515387775	-0.200878897
6	5.874383041	1.185631120	-0.085077898
6	5.199614150	-0.045742105	0.004784045
6	5.933152990	-1.243070453	0.099808900
6	5.508854862	-2.580371260	0.327734230
6	6.651933601	-3.363006588	0.420866628
6	7.750265535	-2.494741443	0.260215721
9	8.825439932	-0.040243665	-1.407271676
9	9.189363910	0.092185017	0.846585928
7	7.267151578	1.242422914	-0.082301369

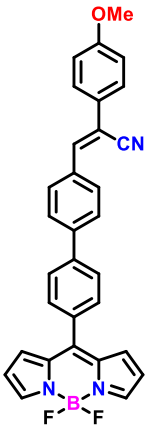

5a

7	7.325985293	-1.237207603	0.069069334
1	6.492383168	4.433329271	-0.327424087
1	4.344089503	2.797569363	-0.250679531
1	4.483262542	-2.901510215	0.433102361
1	6.707788683	-4.427389188	0.598080958
1	8.807941998	-2.718317026	0.282820448
1	8.674527100	2.804803200	-0.202104619
6	3.718897069	-0.084898541	0.016356595
6	3.015848152	-0.909028870	-0.878889008
6	2.979123558	0.697970482	0.919049529
6	1.625671430	-0.938079579	-0.877780874
1	3.566752905	-1.500254215	-1.602776412
6	1.589401124	0.655059785	0.925882298
1	3.501989691	1.315274402	1.641831910
6	0.880567352	-0.159112167	0.024875757
1	1.109391231	-1.549390789	-1.611128464
1	1.046168615	1.238830420	1.662149364
6	-0.600100034	-0.193618556	0.025128194
6	-1.301993059	-1.377462106	-0.259476270
6	-1.355189432	0.958624452	0.310157537
6	-2.689269768	-1.399760498	-0.259517100
1	-0.755105147	-2.294754116	-0.453822845
6	-2.743271396	0.941083337	0.309310891
1	-0.844641165	1.895464925	0.510042651
6	-3.451137122	-0.244706760	0.018975456
1	-3.204535709	-2.332647049	-0.472711808
1	-3.274166391	1.858077531	0.527850363
6	-4.902511394	-0.385640107	-0.015680191
6	-5.915323210	0.517166009	0.121316177

1	-5.227736995	-1.405604731	-0.204132143
6	-7.348979473	0.131738349	0.086557393
6	-8.330552363	1.052785442	-0.307311931
6	-7.774607953	-1.163816777	0.443061802
6	-9.677974220	0.702397130	-0.378383298
1	-8.039510327	2.064386712	-0.572213488
6	-9.109475238	-1.526118753	0.374788926
1	-7.054999815	-1.890219631	0.806638253
6	-10.076053838	-0.596905973	-0.043088642
1	-10.400196970	1.444998633	-0.694945007
1	-9.436070948	-2.520911793	0.658482197
6	-5.663670693	1.920032440	0.285596661
7	-5.510964321	3.067986494	0.411550995
8	-11.358266981	-1.050843219	-0.074488052
6	-12.383236428	-0.150925336	-0.473760413
1	-13.314056721	-0.717196206	-0.427059662
1	-12.449340667	0.710409942	0.202341617
1	-12.228538550	0.206749984	-1.499248895

Table S5: The coordinates of compounds **5b** (DFT/B3LYP/6-31G(d,p) level with Gaussian 09)

5	7.453059272	0.062394559	-0.119609452
6	6.817168932	2.572026553	-0.129170257
6	5.670048232	3.387379895	-0.205239544
6	4.573866588	2.536137429	-0.175114090
6	5.074892401	1.210361097	-0.062989518
6	4.411515786	-0.027844557	0.014379638
6	5.155296132	-1.218479977	0.111795863
6	4.741587021	-2.560575438	0.331318012
6	5.891139174	-3.332351329	0.433926805
6	6.982670863	-2.452954533	0.287146681

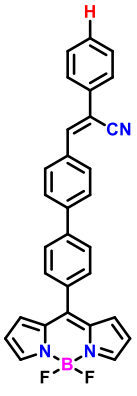

5b

9	8.042191403	0.017804691	-1.370000897
9	8.396058262	0.144287221	0.885942020
7	6.466965938	1.280509341	-0.046070258
7	6.548227560	-1.199082218	0.095313816
1	5.663720701	4.465324407	-0.278586728
1	3.530657635	2.808647789	-0.232822343
1	3.718129264	-2.892011150	0.425088817
1	5.955550153	-4.396652928	0.608673303
1	8.042175898	-2.666425884	0.319656201
1	7.860196817	2.857113689	-0.141967606
6	2.930956098	-0.081486630	0.011458225
6	2.244794455	-0.905759422	-0.896517956
6	2.175411898	0.686998490	0.913348502
6	0.854978431	-0.949357780	-0.907955614
1	2.808411522	-1.485940362	-1.619531508
6	0.786139995	0.630075105	0.907192053
1	2.685583133	1.304249116	1.645159118
6	0.094341228	-0.184896047	-0.006064312
1	0.351480028	-1.560630572	-1.650141470
1	0.230233606	1.202825846	1.642657247
6	-1.386001053	-0.235585435	-0.018136970
6	-2.072075218	-1.426048833	-0.313463887
6	-2.155416788	0.907325417	0.266536955
6	-3.459036961	-1.463932177	-0.322931179
1	-1.513399846	-2.335991385	-0.508491220
6	-3.543114214	0.874188046	0.256526338
1	-1.656341305	1.848650567	0.473826624
6	-4.234627718	-0.318751502	-0.042938771
1	-3.962629299	-2.401326217	-0.543951925

1	-4.086333170	1.783973359	0.475056581
6	-5.684210867	-0.476151753	-0.083470403
6	-6.707203625	0.412752676	0.060143820
1	-5.998197076	-1.497532138	-0.283458461
6	-8.136999540	0.001288107	0.010223615
6	-9.121582867	0.902937638	-0.428751799
6	-8.537156655	-1.289441932	0.397866085
6	-10.457491202	0.515388910	-0.506457131
1	-8.835780055	1.909766480	-0.716475276
6	-9.872782516	-1.674532006	0.316320160
1	-7.805662985	-1.986421504	0.794157512
6	-10.839106740	-0.775715442	-0.139931481
1	-11.200956556	1.225752857	-0.855284750
1	-10.161483049	-2.674456620	0.626368911
6	-6.477971925	1.816335855	0.242919595
7	-6.340056639	2.964280781	0.384995779
1	-11.881032719	-1.075653239	-0.196847880

Table S6: The coordinates of compounds **5c** (DFT/B3LYP/6-31G(d,p) level with Gaussian 09)

5	8.226487964	-0.037841806	-0.131456687
6	7.644360498	2.484565772	-0.162630615
6	6.514873730	3.324013475	-0.241816872
6	5.400687804	2.497048349	-0.201241842
6	5.873253460	1.161601599	-0.079875002
6	5.183744865	-0.061352790	0.008435947
6	5.901509778	-1.267225674	0.111497433
6	5.459298101	-2.598880795	0.339401835
6	6.592010998	-3.394907425	0.442837097
6	7.702044417	-2.540242008	0.288163969
9	8.816156946	-0.103757287	-1.380508437

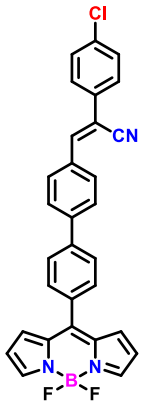

5c

9	9.169353972	0.030826521	0.875074423
7	7.266563398	1.201702053	-0.067918240
7	7.294478609	-1.278264015	0.090907200
1	6.531680611	4.401193348	-0.324121292
1	4.363512652	2.791903975	-0.258197966
1	4.429179818	-2.907545127	0.437821488
1	6.633805100	-4.459437845	0.622935747
1	8.756718963	-2.776714144	0.318676533
1	8.693264102	2.746867801	-0.180899056
6	3.702161309	-0.082871460	0.010851656
6	2.995122591	-0.896601714	-0.890540549
6	2.966847254	0.706111620	0.911607149
6	1.604643350	-0.910789713	-0.896432933
1	3.543358990	-1.492513268	-1.612564821
6	1.576627838	0.679061090	0.910853669
1	3.492864299	1.316015684	1.638327524
6	0.864228444	-0.125739289	0.004540181
1	1.085534618	-1.515047709	-1.633646274
1	1.036193010	1.267355677	1.645587661
6	-0.616862131	-0.145340471	-0.001142131
6	-1.328880417	-1.322610487	-0.288187682
6	-1.360926815	1.014834585	0.281740144
6	-2.716236439	-1.331639108	-0.291697493
1	-0.790000698	-2.244698589	-0.481499828
6	-2.748881622	1.010716163	0.277941974
1	-0.841420364	1.946354504	0.482756372
6	-3.466247313	-0.168972760	-0.013561231
1	-3.240052636	-2.259339484	-0.506529890
1	-3.271761413	1.932613311	0.495324222

6	-4.918316426	-0.295902386	-0.047381761
6	-5.921360117	0.616486150	0.093024834
1	-5.253972740	-1.312011135	-0.239120694
6	-7.359027861	0.237159495	0.051898823
6	-8.328770253	1.161487318	-0.372307273
6	-7.788969506	-1.045331631	0.434022929
6	-9.674600927	0.813465867	-0.444446549
1	-8.027608707	2.164617931	-0.656381469
6	-9.130716466	-1.406684120	0.363590551
1	-7.075251852	-1.765560473	0.820108100
6	-10.067284789	-0.473556908	-0.081231520
1	-10.411847971	1.533410107	-0.781012723
1	-9.451465137	-2.396781707	0.667232396
6	-5.662394265	2.016456599	0.261564129
7	-5.503183246	3.163084244	0.391039977
17	-11.762436160	-0.920994647	-0.166098958

Table S7: The coordinates of compounds **6a** (DFT/B3LYP/6-31G(d,p) level with Gaussian 09)

6	4.483239089	-0.033199908	-0.041034952
6	5.199521623	-1.227382279	0.144631135
6	5.146328234	1.193227152	-0.211027334
6	4.659061770	2.529138811	-0.410768860
6	5.786325566	3.335576236	-0.512350373
6	6.931531650	2.523602612	-0.379156146
6	4.770627718	-2.584054556	0.336549431
6	5.931726487	-3.337179431	0.464801491
6	7.040468026	-2.473006446	0.355054415
5	7.508066612	0.037350938	-0.008368198
7	6.599115256	-1.215342184	0.163968470

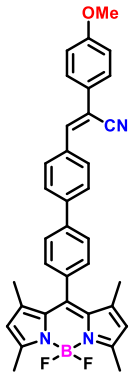

6a

7	6.545218711	1.246357352	-0.199650221
1	5.796312146	4.406302226	-0.666820120
1	5.987992422	-4.406050242	0.622289135
6	2.989071069	-0.068496286	-0.056460350
6	2.289584065	-0.241748765	-1.257642777
6	2.258562752	0.072179716	1.130527671
6	0.897191508	-0.272594954	-1.270608741
1	2.841632032	-0.343136593	-2.187352656
6	0.866307851	0.040833481	1.115829513
1	2.786750705	0.198545898	2.070963523
6	0.156019133	-0.131752653	-0.084731989
1	0.377142568	-0.379964037	-2.217504366
1	0.323293295	0.125744568	2.051934600
6	-1.325623924	-0.163253467	-0.099507001
6	-2.028550374	-1.001992686	-0.981018937
6	-2.080013882	0.644897195	0.770325401
6	-3.416023513	-1.024933049	-0.987948412
1	-1.481800021	-1.662608161	-1.646713121
6	-3.468209640	0.626352295	0.765546438
1	-1.568752236	1.321731672	1.447877309
6	-4.177146162	-0.211064263	-0.121801956
1	-3.931654862	-1.692278960	-1.673638474
1	-3.998153423	1.273353076	1.452025784
6	-5.628590475	-0.315344551	-0.220766220
6	-6.640595238	0.371976459	0.381696648
1	-5.954827879	-1.077006440	-0.924466812
6	-8.074752738	0.061068701	0.152976587
6	-8.499149081	-1.225556966	-0.235882694
6	-9.058273000	1.046960926	0.318252704

6	-9.834981321	-1.499240894	-0.478249641
1	-7.777823287	-2.031733057	-0.322004575
6	-10.406717492	0.784719202	0.080088111
1	-8.768221054	2.044422421	0.633217915
6	-10.803788974	-0.493832737	-0.327618549
1	-10.160576833	-2.492612304	-0.768100756
1	-11.130118137	1.579578795	0.214246717
6	-6.387817373	1.471446684	1.267869810
7	-6.234862499	2.376065492	1.985740585
6	3.247092783	3.027456687	-0.501375773
1	2.701246594	2.573755491	-1.334225462
1	2.672803767	2.810883214	0.404541338
1	3.247897122	4.110672731	-0.649123200
6	8.367593289	2.930155908	-0.416288427
1	8.864167928	2.660055183	0.520652516
1	8.894078402	2.397329500	-1.213930641
1	8.458526314	4.006051584	-0.577339591
6	3.381709924	-3.147522411	0.397447957
1	2.796546749	-2.717383849	1.215945340
1	2.818668443	-2.960334527	-0.522068879
1	3.429977139	-4.229103933	0.549494173
6	8.492724658	-2.812349347	0.426627178
1	9.000166269	-2.512352732	-0.495252598
1	8.973277185	-2.262032933	1.241287612
1	8.629532693	-3.884026009	0.583377461
9	8.318230048	-0.110956982	-1.132909482
9	8.287246984	0.222933717	1.132170406
8	-12.087047984	-0.865377795	-0.586902285
6	-13.114428203	0.104470937	-0.433474808

1	-12.970911523	0.954841888	-1.111600577
1	-14.045969659	-0.403278774	-0.686006780
1	-13.170900570	0.472202576	0.598531029

Table S8: The coordinates of compounds **6b** (DFT/B3LYP/6-31G(d,p) level with Gaussian 09)

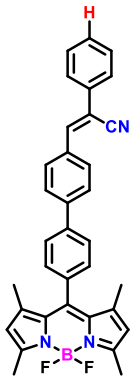

6b

6	-3.744033311	0.027037301	-0.032477135
6	-4.402767184	-1.203789869	-0.186374618
6	-4.463892396	1.219388099	0.150979410
6	-4.039513488	2.579496562	0.328395357
6	-5.202769586	3.328171199	0.462343609
6	-6.308510108	2.458039223	0.370124888
6	-3.911291703	-2.538823141	-0.382112983
6	-5.035665905	-3.351182006	-0.465870985
6	-6.183303225	-2.543637119	-0.326120087
5	-6.767811829	-0.057535577	0.032991042
7	-5.801185128	-1.263400352	-0.159657987
7	-5.863127759	1.201003364	0.184445177
1	-5.262539040	4.397929557	0.612298829
1	-5.042257384	-4.422998906	-0.612721292
6	-2.250250367	0.069205234	-0.062979968
6	-1.563628440	0.241803835	-1.271651448
6	-1.507483359	-0.064368135	1.117207729
6	-0.171601489	0.279273507	-1.298569610
1	-2.125390911	0.337593357	-2.196082149
6	-0.115613009	-0.026660548	1.088670941
1	-2.025809182	-0.190199975	2.063154539
6	0.581573877	0.145625820	-0.119512026
1	0.338479694	0.386037660	-2.250941494
1	0.436948381	-0.105975785	2.019663270
6	2.062879954	0.184828523	-0.148705818

6	2.752279389	1.025677512	-1.038870742
6	2.829518656	-0.617727484	0.715821764
6	4.139453253	1.056533784	-1.058778253
1	2.195272809	1.681437129	-1.700702207
6	4.217405856	-0.591173650	0.698245030
1	2.328080990	-1.296116519	1.399020496
6	4.912216594	0.249153754	-0.197244331
1	4.645159649	1.725076439	-1.750619391
1	4.758094631	-1.233768945	1.380532789
6	6.362064274	0.363001887	-0.307878745
6	7.382937624	-0.313854222	0.289637028
1	6.678805962	1.122443689	-1.018412691
6	8.813609751	0.009128033	0.034531032
6	9.214726847	1.309497046	-0.318373615
6	9.798210435	-0.987910544	0.142241211
6	10.551202196	1.593306113	-0.587155999
1	8.483232276	2.110480098	-0.353583115
6	11.134974026	-0.699976085	-0.124425651
1	9.511615286	-1.994522726	0.430050903
6	11.517528590	0.589522881	-0.495577439
1	10.840566793	2.605855664	-0.852501071
1	11.878332380	-1.487176346	-0.041981048
6	7.150514986	-1.408052626	1.186562392
7	7.010461718	-2.307105647	1.913998618
1	12.560031160	0.814204456	-0.699430001
6	-2.652766227	3.149952213	0.371521047
1	-2.055666569	2.724606266	1.183849422
1	-2.099867867	2.963817450	-0.554408320
1	-2.704616500	4.231611958	0.521756051

6	-7.761538333	2.791324214	0.453115467
1	-8.275352932	2.487856927	-0.464134559
1	-8.232923923	2.240131027	1.272466312
1	-7.901628697	3.862657689	0.609234792
6	-2.498056553	-3.031247718	-0.484638073
1	-1.962150705	-2.578193907	-1.324257403
1	-1.916105077	-2.809252041	0.415099738
1	-2.495513137	-4.114959495	-0.628581497
6	-7.617680334	-2.957205713	-0.345562056
1	-8.107373816	-2.677045212	0.591995505
1	-8.153511246	-2.437313953	-1.145568174
1	-7.704941768	-4.035481824	-0.491948766
9	-7.532412469	-0.237487364	1.184242024
9	-7.591736626	0.077411296	-1.082998611

Table S9: The coordinates of compounds **6c** (DFT/B3LYP/6-31G(d,p) level with Gaussian 09)

6	4.468588621	-0.043705822	-0.041718259
6	5.171429921	-1.244639199	0.151245508
6	5.144696267	1.173748021	-0.223872998
6	4.671915195	2.513694741	-0.432161071
6	5.807817518	3.306189256	-0.544736140
6	6.944285457	2.482106897	-0.409675690
6	4.727926707	-2.595036905	0.354635400
6	5.880782435	-3.360081429	0.485326252
6	6.998918192	-2.509207826	0.365785687
5	7.493895827	-0.007493382	-0.020224228
7	6.571063464	-1.248247595	0.166215771
7	6.544075371	1.210947155	-0.218175633
1	5.829482246	4.375488425	-0.707578050

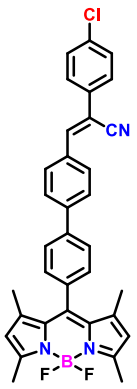

6c

1	5.925592847	-4.428290430	0.650692173
6	2.974024252	-0.062127053	-0.052835495
6	2.269813114	-0.230929184	-1.251931515
6	2.248252268	0.089752390	1.135668622
6	0.877240399	-0.247385264	-1.261400068
1	2.818508938	-0.340644766	-2.182616366
6	0.855727031	0.073794049	1.124639812
1	2.780248799	0.212914841	2.074319131
6	0.141196192	-0.095131679	-0.073822658
1	0.353828033	-0.351932806	-2.206744144
1	0.316204714	0.167368061	2.061939675
6	-1.340679673	-0.111887154	-0.084917984
6	-2.053282689	-0.946094646	-0.963216954
6	-2.084703276	0.705965927	0.785224688
6	-3.440748172	-0.955864766	-0.966856651
1	-1.514219028	-1.613046436	-1.628650163
6	-3.472770751	0.700507242	0.784179605
1	-1.564966857	1.379358773	1.459541921
6	-4.190658565	-0.133011056	-0.099600890
1	-3.964576635	-1.619470854	-1.649907118
1	-3.995229766	1.354174497	1.470136933
6	-5.642564406	-0.225017446	-0.192541860
6	-6.645645176	0.469493755	0.415700065
1	-5.978342187	-0.981548828	-0.897459928
6	-8.083308634	0.168456414	0.180719286
6	-8.511707093	-1.120447611	-0.180980514
6	-9.054791755	1.174539374	0.317987187
6	-9.853510357	-1.390598862	-0.430976320
1	-7.796825195	-1.934344515	-0.241105409

6	-10.400763084	0.916498450	0.073857037
1	-8.754828954	2.174720142	0.613593583
6	-10.791703466	-0.366074910	-0.306293915
1	-10.172974503	-2.390269355	-0.702837617
1	-11.139287456	1.703453654	0.175902694
6	-6.386677314	1.563848282	1.304709437
7	-6.227975998	2.465129621	2.025446887
6	3.265448778	3.027794037	-0.520562078
1	2.712281707	2.578124416	-1.350835203
1	2.691143145	2.820807134	0.387591106
1	3.278323248	4.110427764	-0.671740526
6	8.384660419	2.871798992	-0.457593604
1	8.886690241	2.588815526	0.472495212
1	8.897286962	2.338778377	-1.264227107
1	8.486893125	3.947586171	-0.612296728
6	3.333018495	-3.142645350	0.423595765
1	2.756877717	-2.704467754	1.244303446
1	2.767508708	-2.951443666	-0.493576509
1	3.369891539	-4.224327335	0.577943928
6	8.447414015	-2.864069454	0.436670439
1	8.958287552	-2.565035687	-0.483517321
1	8.933289166	-2.322554591	1.254168527
1	8.572978992	-3.937733574	0.589033033
9	8.297397504	-0.174473499	-1.146624840
9	8.279204072	0.178397394	1.115800932
17	-12.487114398	-0.702644287	-0.614114283

10.References

1) H. Park, J. D. MaEachon II and J. A. Pollock, Synthesis and characterization of hydrogen peroxide activated estrogen receptor beta ligands, *Bioorg*. *Med*. *Chem*., 2019, **27**, 2075-2082.
2) M. S. Alam, Y. -J. Nam and D. -U. Lee, Synthesis and evaluation of (Z)-2,3-diphenylacrylonitrile analogs as anti-cancer and anti-microbial agents, *Eur*. *J*. *Med*. *Chem*., 2013, **69**, 790-797.
3) S. Lieber, F. Scheer, W. Meissner, S. Naruhn, T. Adhikary, S. Müller-Brüsselbach, W. E. Diederich and R. Müller, (Z)-2-(2-Bromophenyl)-3-{[4-(1-methyl-piperazine)amino]phenyl}-acrylonitrile (DG172): an orally bioavailable PPARβ/δ-selective ligand with inverse agonistic properties. *J*. *Med*. *Chem*., 2012, **55**, 2858−2868.
4) R. S. Szabadai, J. Roth-Barton, K. P. Ghiggino, J. M. White and D. J. D. Wilson, Solvatochromism in diketopyrrolopyrrole derivatives: experimental and computational studies, *Aust. J. Chem.*, 2014, **67**, 1330-1337.
5) (a) A. Afrin and P. C. A. Swamy, Tailoring emission color shifts in mechanofluorochromic-active AIE systems of carbazole-based d−π−a conjugates: impact of π spacer unit variants, *J. Org. Chem*., 2024, **89**, 7946-7961; (b) A. Afrin and P. C. A. Swamy, Aggregation induced emission and reversible mechanofluorochromism active carbazole-anthracene conjugated cyanostilbenes with different terminal substitutions, *New J. Chem.,* 2023, **47**, 18919-18932.
6) (a) P. R. Aswathy, S. Sharma, N. P. Tripathi and S. Sengupta, Regioisomeric BODIPY benzodithiophene dyads and triads with tunable red emission as ratiometric temperature and viscosity sensors, *Chem. Eur. J.*, 2019, **25**, 14870-14880; (b) N. Kaur, N. V. Steerteghem, P. Singla, P. Kaur, K. Clays and K. Singh, Second-order nonlinear polarizability of ferrocene–BODIPY donor–acceptor adducts. Quantifying charge redistribution in the excited state, *Dalton Trans.*, 2017, **46**, 1124-1133.
7) M. Wang, Y. Zhang, T. Wang, C. Wang, D. Xue and J. Xiao, Story of an age-old reagent: an electrophilic chlorination of arenes and heterocycles by 1-chloro-1,2-benziodoxol-3-one, *Org. Lett.*, 2016, **18**, 1976-1979.